INVESTIGATION FOR GROUNDWATER AT THE PERMANENT SITE OF THE FEDERAL POLYTECHNIC NASARAWA, NASARAWA STATE, NIGERIA.

BY

OGA, FIDELIS ADZE

M.SC/SCI/07041/95/96

B.SC. (HONS) PHYSICS

THESIS SUBMITTED TO THE POSTGRADUATE SCHOOL, AHMADU BELLO UNIVERSITY, ZARIA, IN PARTIAL FULFILLMENT OF THE REQUIREMENTS FOR THE AWARD OF THE DEGREE OF MASTER OF SCIENCE, APPLIED GEOPHYSICS.

DEPARTMENT OF PHYSICS

FACULTYY OF SCIENCE

AHMADU BELLO UNIVERSITY,

ZARIA-NIGERIA

JANUARY, 2007

DECLARATION

I hereby declare that, this thesis titled investigation for groundwater at the permanent site of the Federal Polytechnic Nasarawa, Nasarawa State, Nigeria is an original work carried out by the author (Oga, F. Adze) under the supervision of Prof. I. B. Osazuwa and Dr. M. N. Umego. To the best of my knowledge no part thereof has been submitted elsewhere for the award of any degree. The works of others have been duly referenced and acknowledged.



O. F. ADZE

AUTHOR.

January, 2007

CERTIFICATION

This thesis entitled: Investigation for groundwater at the permanent site of the Federal Polytechnic Nasarawa, Nasarawa State, Nigeria, by Oga Fidelis Adze, meets the regulations governing the award of the degree of Master of Science, Applied Geophysics of Ahmadu Bello University and is approved for its contribution to knowledge and literary presentation.

Prof. I. B. Osazuwa
Chairman, Supervisory Committee

19/01/2007
Date

Dr. M. N. Umego
Member, Supervisory Committee

Date

Prof. N. Hariharan
Head of Department

19/01/2007
Date

Prof. J. U. Umoh
Dean, Postgraduate School

Date

DEDICATION

This thesis is dedicated to my late sister (Miss Gloria Oga) whose death came at the verge of my departure for this programme.

Table of contents

	Page
Title page	i
Declaration	ii
Certification	iii
Dedication	iv
Table of contents	v
Acknowledgements	ix
List of figures	xi
List of table	xiii
Abbreviations and symbols	xiv
Abstract	xv
Chapter one Introduction	1
1.1 General introduction	1
1.2 Statement of the problem	3
1.3 Objectives of the research	4
1.4 Significance of the research	4
1.5 Location and accessibility of Nasarawa	5
1.6 Drainage	5
1.7 Choice of the method	7
Chapter two Geology	11
2.1 Regional geology	11

2.2 Local geology of the area..... 12

2.3 Previous geophysical work in the area..... 15

2.4 Hydrogeology..... 15

2.5 Hydrology..... 19

Chapter three Electrical resistivity survey..... 22

3.1 Introduction..... 22

3.2 Theory of electrical resistivity method..... 23

3.3 The concept of apparent resistivity..... 26

3.4 Electrode configurations..... 29

3.4.1 The schlumberger configuration..... 30

3.4.2 Wenner spread..... 31

3.5 Resistivity sounding..... 31

3.6 Horizontal profiling..... 34

3.7 Instrumentation..... 35

3.7.1 Abem terrameter sas system..... 37

3.7.2 Digital terrameter sas 300..... 38

3.7.3 Transmitter designed for deep penetration..... 39

3.7.4 Microprocessor monitors and controls measurements 40

3.8 Data collection..... 41

3.9 Field problems encountered..... 42

Chapter four Interpretation 43

4.1 Introduction..... 43

4.2 Outline of the Zohdy method..... 46

4.3 Initial data presentation..... 48

4.3.1 Iterative procedure..... 48

4.3.1a. Depth determination..... 49

4.3.1b. Resistivity determination..... 50

4.4 Ambiguity in the relation between the resistivity curve and the sub surface layer distribution..... 52

4.5 Options and characteristics..... 53

4.6 Interpretation of azimuthally soundings..... 57

Chapter five Results 58

5.1 Analysis of results..... 58

5.2 Iso – resistivity contour maps..... 60

5.2.1 Resistivity map of the surface layer..... 61

5.2.2 Iso – Resistivity map at 5m depth..... 61

5.2.3 Iso – Resistivity map at 10m, 15m, etc. Depth..... 64

5.3 Geologic sections..... 64

5.3.1 General introduction..... 64

5.3.2 Subsurface geologic section along profiles AB..... 69

5.3.3 Subsurface geologic section along profiles CD, EF, GH, IJ, and GLI..... 72

5.4 Map of aquifer layer..... 72

5.4.1 Depth of aquifer..... 72

5.4.2 Aquifer layer thickness map..... 78

5.5 Depth to basement map..... 78

5.6 Azimuthal sounding..... 82

Chapter six Conclusion and recommendations 87

6.1 Conclusion..... 87

6.2 Recommendations and future work 89

References 91

Appendix A: Interpreted model layers..... A1

Appendix B: Iso - resistivity contour maps..... A41

Appendix C: Iso - resistivity contour data..... A49

Appendix D: Depth to aquifer contour data..... A52

Appendix E: Aquifer thickness data..... A54

Appendix F: Depth to basement data..... A56

Acknowledgements

This project would not have come to a logical and successful completion without the contribution of a host of individuals.

I wish to express my profound thanks and appreciation to my major supervisor, Professor I. B. Osazuwa, who has relentlessly supervised, and edited this work to achieve this standard. He has also sponsored and provided me with financial grant and provided computational facilities that make this project work a success. Also I wish to thank my co - Supervisor, Dr. M. N. Umego for his assistance and proof reading the draft and making corrections and suggestions.

I am grateful to Mr. Kola Lawal for his willingness to assist in this work at any time during the course of this project.

My thanks extends to my lecturers and staff of the department who assisted me in one way or the other in this work. (Prof. S. B. Ojo, Dr. P. N. Sule, Dr. R. Kangkolo,).

I am equally grateful to Dr. Garba of the department of geology for his contribution and provision of the geological map of the immediate south of the survey area.

I am indebted to Prof. K. Schoeneich, for his contribution towards my understanding of the basement terrain.

Not to forget my parents who brought me up, I must say God bless you all (Late Mr. James Oga and Mrs. Oga).

IBRAHIM LIBRARY

Finally, I thank the International Program in the Physical Sciences Uppsala University Sweden for the financial assistance for this project.

List of figures

Fig No. Title Page

1.1 Map of Nasarawa Local Government Area showing the survey area..... 6

1.2 Topographic map of some parts of Federal Polytechnic Nasarawa showing the sounding points..... 10

2.1 A geological sketch map of Nigeria..... 13

2.2 A geological sketch map of the immediate south of the survey area..... 14

3.4 General electrode configuration..... 28

3.5 Schlumberger and Wenner electrode spread..... 32

3.6 Increase in electrode spread increases depth of current penetration..... 33

3.7 Field resistivity equipment set up..... 36

5.1 Apparent resistivity field curve..... 58

5.2 Interpreted layer model (n – layer) of fig. 5.1..... 59

5.3 Iso - resistivity contour map at the surface..... 63

5.4 Iso – resistivity contour map 5m depth..... 64

5.5 - 5.15 Iso – resistivity contour maps at 10m – 60m depth..... 65

5.16 Iso – resistivity contour map at 5m depth showing the profiles chosen..... 70

KASHIM IBRAHIM LIBRARY

5.17 - 22 Geologic section equivalent to geoelectric contour section along profiles AB..... 71

5.17 - 22 Geologic section equivalent to geoelectric contour section along profiles CD, EF, GH, IL, and GL..... 73

5.23 Depth to aquifer contour map..... 79

5.24 Aquifer thickness contour map..... 80

5.25 Map of depth to fresh basement..... 81

5.26 - 5.27 Patterns of resistivity anisotropy map..... 82

List of table

Table No.	Title	Page
5.1	Resistivity ranges used for this survey work	51

Abbreviations and symbols

T.R.P.	Town Regional Planning
VES	Vertical Electrical Sounding
WHO	World Health Organization
ρ	Resistivity
σ	Conductivity
π	Pii
m	Meter
E	East
W	West
N	North
S	South
et al.	and others

KASHIM IBRA

ABSTRACT

A geophysical survey was carried out in the Federal Polytechnic Nasarawa and the process of electrode layout employed was the Schlumberger array which was applied in the vertical mode. The maximum current electrode separation was 300m. Fourty - six vertical electrical sounding surveys were carried out, with six of these being radially sounded in three directions oriented at 60° to each other (azimuthal sounding). Data analysis using zohdy software was applied.

Analysis showed that the area comprised of four subsurface layers. The first which is the top layer is lateritic while the second layer is strongly weathered. The second layer constitutes the aquifer zones in the area having relatively low resistivity range of 30 - 200m. The depth to basement varies at different locations and areas of shallow basement or high resistivities can serve as good locations for the erection of buildings. The variation in the depth to the basement indicates that the basement profile is not a smooth continuous surface but an undulating surface. The average depth to basement was found to be 33 meters and this suggests that the depth to basement in the survey area is generally shallow.

Analysis of the azimuthal sounding surveys showed that the subsurface of the survey area is generally anisotropic. It is therefore recommended to carry out azimuthal sounding surveys at any desired survey area in order to select the preferred direction of sounding prior to any main resistivity survey.

Fractures were found to occur at depths ranging from 5 meters to 50 meters depending on the sounding location. The pattern of anisotropy associated to fractures was found to be neither circular nor elliptical. The general trend of fractures in the area could not be ascertained or generalized since the data coverage was limited and more azimuthal sounding surveys are required to cover the entire survey area. The sounding points in which fractures occur are recommendable locations for groundwater bore holes.

CHAPTER ONE

INTRODUCTION

1.1 GENERAL INTRODUCTION

Water is indispensable to life as it sustains life. Without it, almost all metabolic processes in living organisms will come to a standstill. The role of water in industries, agricultural projects and a growing community such as ours is too numerous to enumerate. Potable water is a precious resource and Mankind, through the ages, has been faced with the problem of providing suitable water in sufficient quantity for use. In most rural areas of Nigeria, potable water is a luxury. The people have no access to treated pipe borne water, and therefore have had to rely on dry river channels, streams and shallow hand-dug wells for their water supply. In order to adequately supply water to her citizens, the Federal Government of Nigeria has set up the Federal Ministry of Water Resources, and the various State Governments have their State water boards. Population explosion and increased industrial developmental activities have led to the increase in the demand for groundwater either as supplement to supplies from surface sources, or, in some cases, as a main source of supplies itself. The location of suitable and productive reservoirs of groundwater is on the increase in many countries of

the world of which Nigeria is not an exception. In Nigeria, the exploitation of groundwater by boreholes was introduced as early as 1936 (Wright and Burgess, 1992). There are three main sources of water namely: rain water, surface water, and groundwater. Among these sources, groundwater is considered to be more lasting and economical. In the case of rainwater, it falls under a well-defined period of rainy season and cannot, in these areas, be favourably harnessed for industrial projects as it cannot be relied upon since there will be scarcity of water during the dry season. In the case of surface water, dams are constructed across streams so as to allow for the effective use of the surface water. Due to high losses of the water as a result of evaporation, a large catchment area is required (Weinbenga, 1955). In some parts of the world, there is the absence of perennial surface water and this is a limiting factor to the use of dams.

Groundwater may ooze out as seepage or tapped from shallow hand-dug wells which are sunk to the water table in the weathered basement. The availability of water in sufficient quantity from wells or wildcat test drilling cannot be guaranteed since nothing is known about the thickness of the water bearing or saturated beds. During the dry season the groundwater yield may fall and may progressively dry up. Thus the location of suitable subsurface

aquiferous zones for potable water is not an easy task, and the use of geophysical exploration in groundwater search helps to reduce the risk involved in wildcat test drilling.

In this research work, a geophysical investigation was carried out within the precinct of the Federal Polytechnic Nasarawa mainly to locate the aquiferous zones.

1.2 STATEMENT OF THE PROBLEM

The Nasarawa Polytechnic community and the entire environs are faced with the problem of acute water shortage to an increasing degree that led to the closure of the institution in November 1997. The supply of pipe borne water in the area is irregular and unreliable. Most of the water available in the rivers dries up during the dry season and as a result, water borne diseases like *typhoid*, and *diarrhea* are common. It is therefore pertinent that an alternative source of water be sought to augument the supplies from rural water schemes and shallow hand-dug wells. To locate the positions of thick saturated sediments is not an easy task and the cost of drilling is very high to risk wildcat drilling, hence the necessity for this project.

1.3 OBJECTIVES OF THE RESEARCH

It is in a view to solving the aforementioned problems that this research is being embarked upon. The objectives of the research are stated as follows.

(i) To locate suitable and favorable aquifers for potable groundwater and to determine their thicknesses.

(ii) To investigate the subsurface anisotropy.

(iii) To investigate the subsurface lithological units and their boundaries.

(iv) To determine the overburden thicknesses and depth to basement.

(v) To study the basement profile in the area.

(vi) Provide recommendations on the bases of the results as to locations of water boreholes.

1.4 SIGNIFICANCE OF THE RESEARCH

The study has provided detailed information necessary for the sitting of high yielding water boreholes. Thus it is a vital guide in planning developmental programs. The significance of this study is obvious as no geophysical investigation of such a magnitude has earlier been carried out in the survey area and even in Nasarawa Local Government Area as a whole.

KASHIM IBRAHIM LIBRARY

1.5 LOCATION AND ACCESSIBILITY OF NASARAWA

Nasarawa is about forty kilometers (40 Km) South-West of Keffi and is situated roughly between longitudes 7° 25' and 8° 10' East, and latitudes 8° 00' and 8° 45' North (Fig. 1.1). The Federal Polytechnic Nasarawa is sited within this area. The Area is served by a fairly good network of roads and footpaths. A tarred road passes through Nasarawa and Toto Local Government Area.

Untarred roads link Nasarawa town (Local Government Headquarters) with nearby villages like Gudigi Sabo in the North-West and Loko on the river Benue to the South. Nasarawa town is also linked with Ogapa and Udegi-Mbeki which are mining villages for columbite, and tantalite to the South-East.

1.6 **DRAINAGE** The survey area has two distinct seasons, namely: the rainy and dry seasons. The rainy season lasts from late April to September. The dry season begins in October and lasts till March.

The hydrological system of the area is mainly based on the tributaries of Kurafe and Haderi river systems. These two relatively big rivers, although not navigable, serve as the main drainage system for the area as well as major sources of rural water supply. The two rivers converge at a point one

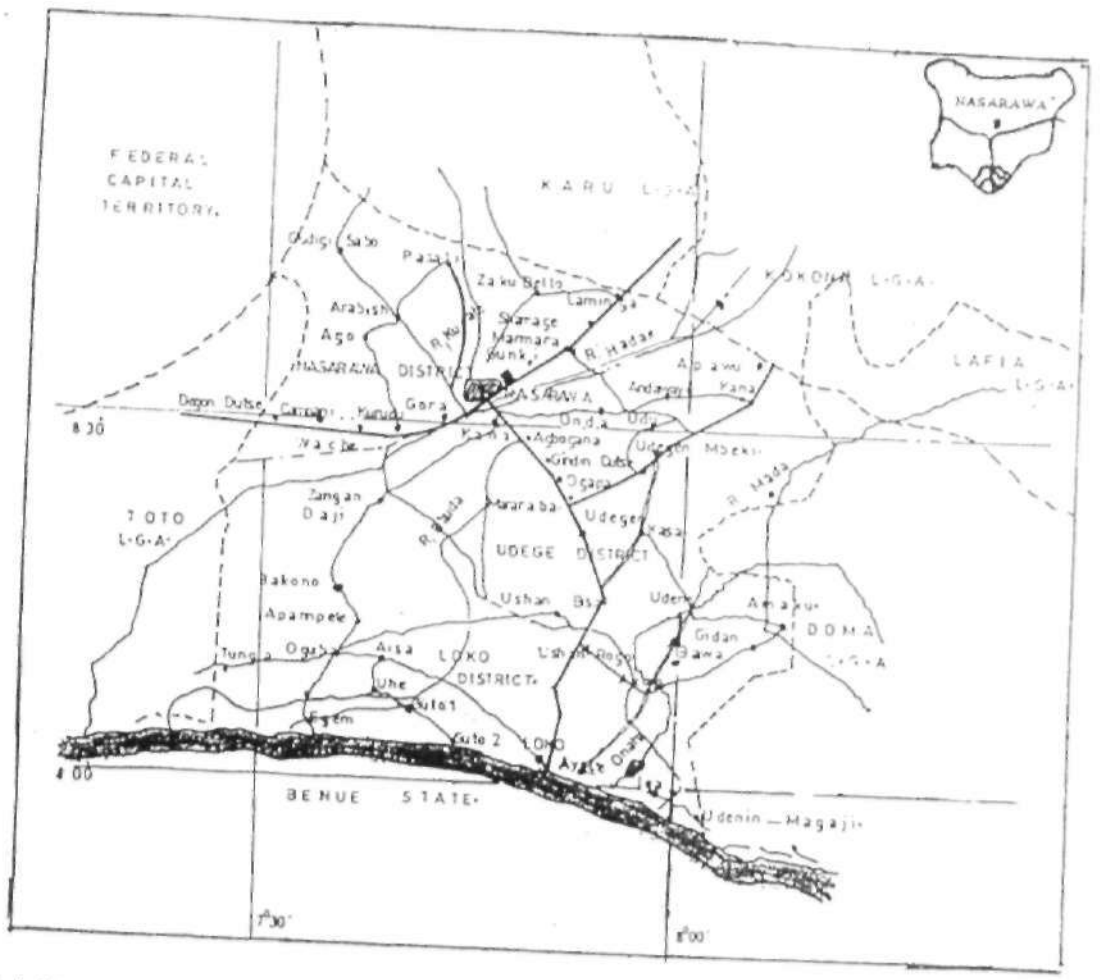
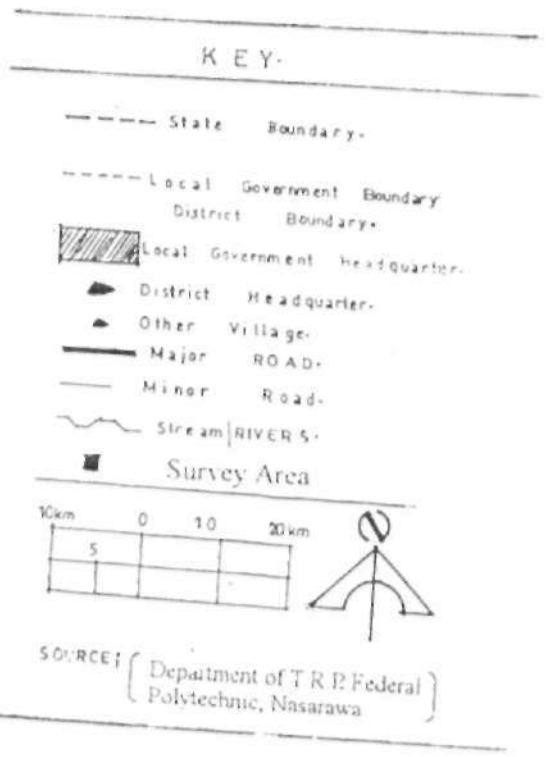


Fig. 1.1 Map of Nasarawa Local Government Area showing the survey area



kilometer south of Nasarawa before finally flowing down to join the Benue River. They are however, not navigable at all at any time of the year, but each has a bridge at Nasarawa which helps to facilitate easier and quicker transportation. During the dry season, most places in these rivers dry up. There are no perennial streams but these major rivers can carry substantial floodwater for short periods during the height of the rainy season.

1.7 CHOICE OF THE METHOD

There are several methods available for geophysical exploration. These are electrical, seismic, electromagnetic, gravity, and magnetic methods. The choice of the method to be used depends on the problem at hand. For groundwater search, the method to be employed is based on the fact that certain physical properties of rock change considerably depending on the amount of water contained in them. These physical properties are: electrical conductivity, elasticity, magnetic susceptibility, and gravitation of the earth. The measurement of these parameters can be made in a variety of ways leading to a variety of results. All these varying techniques are possible due to the large variation in the conductivity of the earth.

For groundwater exploration, the seismic, resistivity, and electromagnetic methods can be used. However the seismic and electrical methods are most commonly used due to the fact that they have a high resolving power in relation to the particular problems encountered in prospecting for groundwater. The problems include the location of saturated sediments and the delineation of the water table (Kollert, 1969). The method of geophysical prospecting employed in this work is the electrical resistivity method. The seismic method was not used because as at the time of the survey, no functional seismic exploration equipment was available in the department. Resistivity methods of geophysical prospecting have been incorporated into groundwater development programs in many areas to an increasing degree to improve the efficiency of citing high yielding water boreholes. The electrical resistivity technique had the widest application because it has contributed to a much high percentage of successful water wells as compared to the expenses encountered in wild-cat test drilling (Worthington, 1977). Knowledge of the geology of the survey area is essential prior to the application of any geophysical technique. Dc-resistivity methods have been successfully used by a number of investigators to detect bedrock fractures. Most of these investigations

have used collinear arrays (Wenner or Schlumberger) rotated about a fixed center point to measure azimuthal variations in apparent resistivity that are related to sets of similarly oriented, steeply dipping fractures (Lane, et. al., 1995) Fig. 1.2 shows the topography in some parts of the survey area and the locations of the vertical electrical soundings.

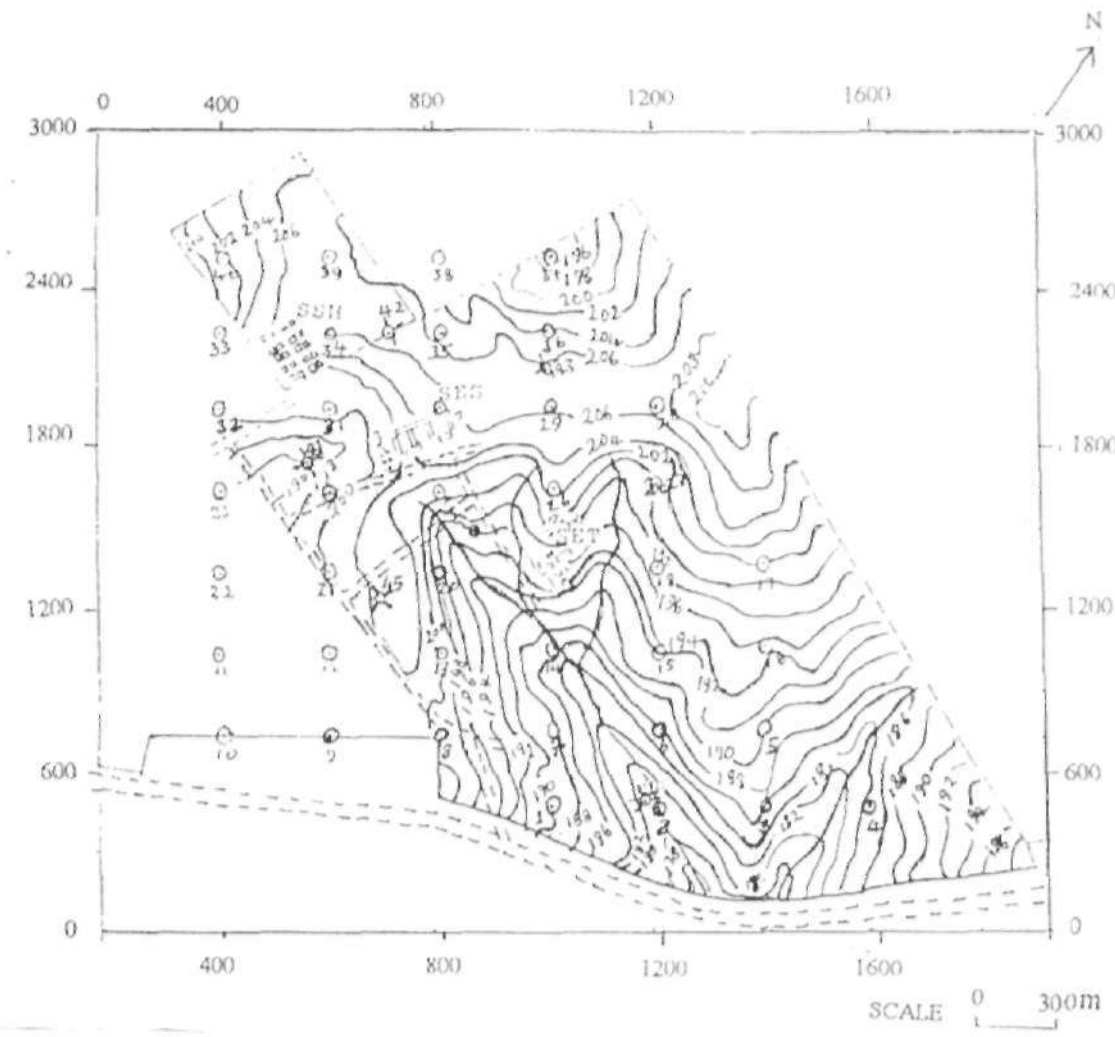


Fig. 1.2.Topographic map of some parts of Federal Polytechnic Nasarawa.

(Showing VES point).

(Source: Department of Town and Regional Planning, Fed. Poly. Nasarawa.

LEGEND

200 Elevation Contour

θ Sounding point

SES School of Env. Studies

SET School of Engineering Tech

SSH Senior staff Housing

Stream

Road

Radial sounding Point

CHAPTER TWO

GEOLOGY

2.1 REGIONAL GEOLOGY

The survey area which is located between longitude 7° 45' and 7° 50' East and latitude 8° 30' and 8° 40' North has the Federal Polytechnic sited within it. The survey area is part of the Nigerian basement complex which is believed to be Precambrian in age and covers half of the total area of Nigeria. The basement complex constitutes the oldest exposed rock in Nigeria. It comprises of the remnants of an ancient sedimentary series the metasediments which have been transformed into anatetic migmatites and granites. The metasediments include quartzofelspathic, biotite and hornblende gneiss, schists, quartzites, marble and calc-silicate rocks. Mineral assembleges correspond to those of the amphibolite facies. The migmatite gneiss complex of the basement complex is the host rock of the Nigerian basement complex. It is also the oldest of all rock lithologies, comprising of migmatites, gneiss, amphibolites in granitic mix up. The lithology is found mainly in Kano, Malumfashi, Zaria, Kaduna axis, Ibadan, Iwo Ilesha, Ife axis, Obudu, Oban axis in the Eastern part of Nigeria. The granites of the basement complex are referred to as the older granites. They are the

unmetamophoused component of the basement complex that intruded the migmatic gneiss complex and the schist belt during the Pan African Orogeny (Oyawoye, 1964). Lithologically, it is characterised by granites, granadiorites, syenites and gabbros. Three phases in the older granites are distinguished; Basic and intrusive rocks, fine grained granite or migmatites, and syntectonic to late tectonic granites. The older granites which are associated with pegmatites are of the common occurrence and being resistant, give rise to picturesque smoothly domed inselbergs. Fig.2.1 shows the basement complex of Nigeria.

2.2 LOCAL GEOLOGY OF THE AREA At the time of this survey, no geological map of the survey area was available. The only geological map available was that of the immediate south of the survey area (Fig.2.2). The area is composed of younger granites (Mesozoic), older granites and pegmatitic granites (Pan-African, and Late Precambrian to Early Paleozoic), mica gneiss (Precambrian) and Ta-Na-Sn- bearing pegmatites of uncertain age. From core samples obtained in the survey area, mica gneisses were found to be predominant in the area and it is most probable that the mica gneiss in the immediate south of the survey area on Fig.2.2 extend to the survey area. The major rock type in the survey area is found to be mica gneiss.

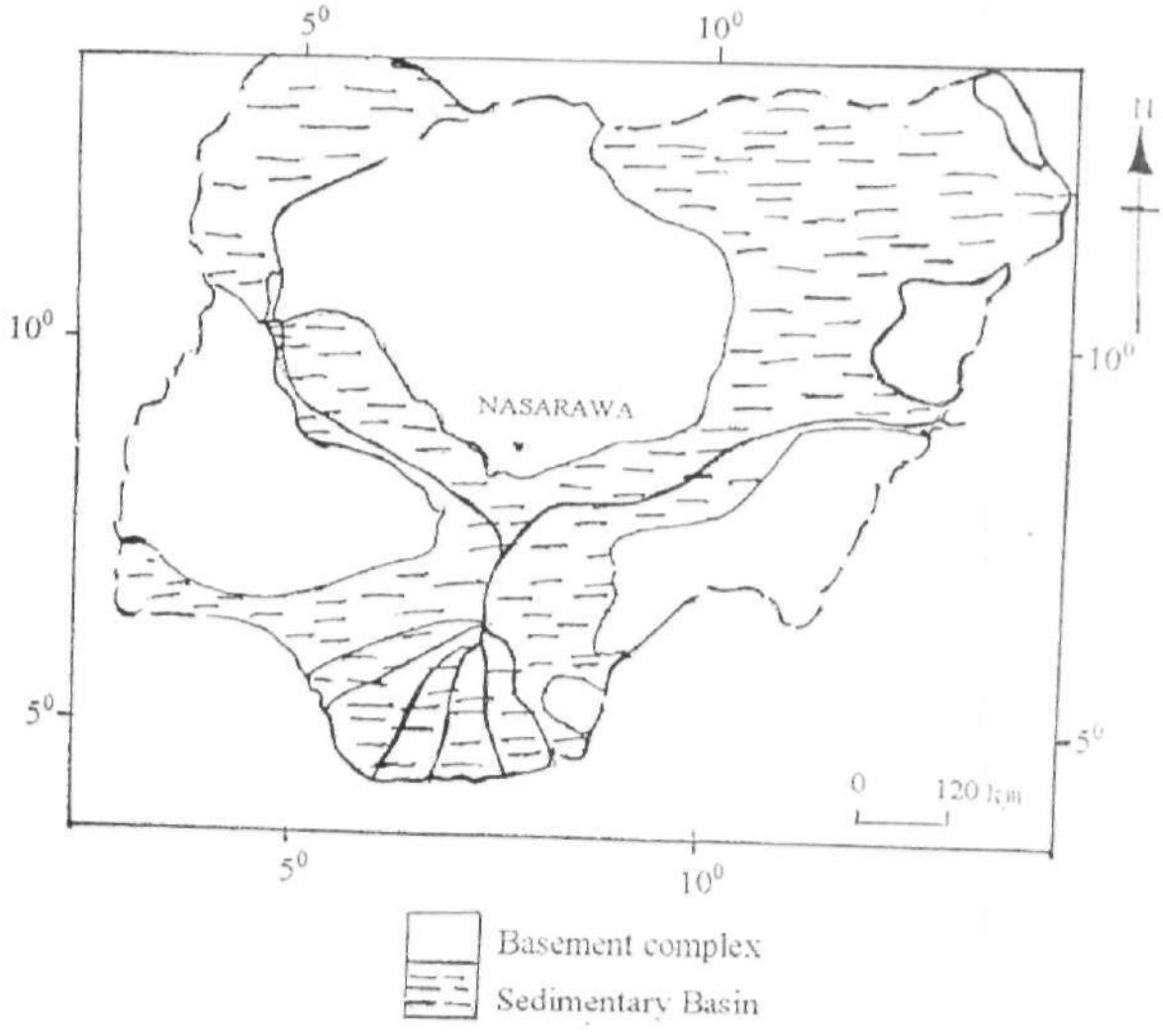


Fig. 2.1. A geological sketch map of Nigeria.

(Source: Geological survey Kaduna).

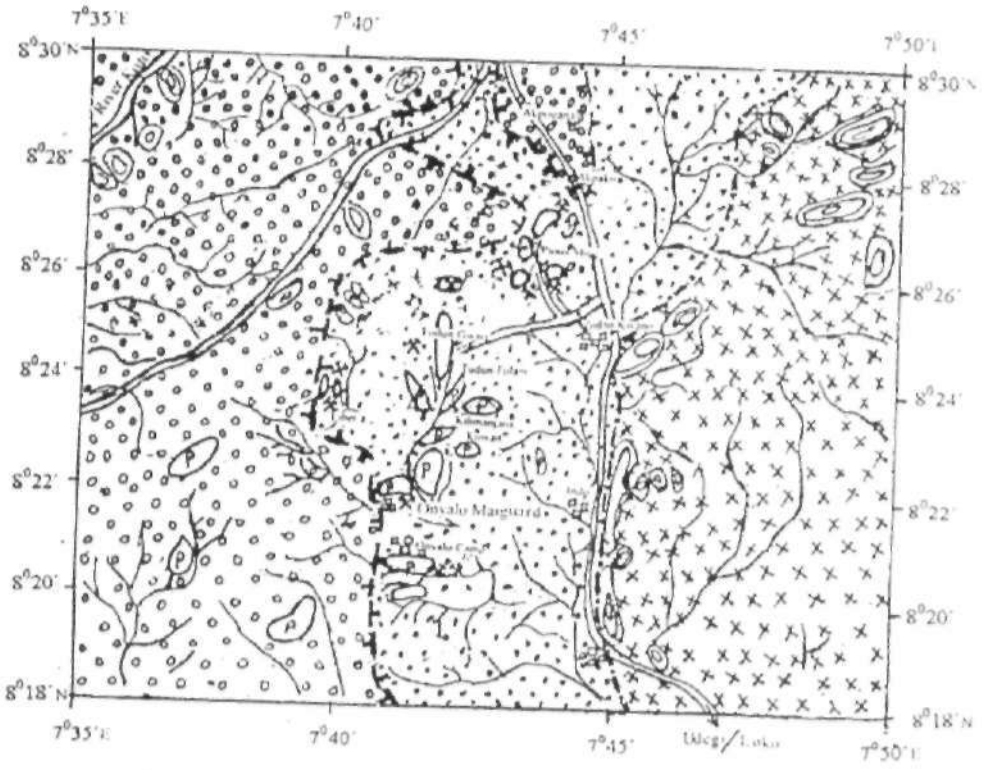


Fig. 2.2 A Geological map of the immediate South of the survey area (Source: Quilos International Nig. Ltd., Nasarawa)

LEGEND

- Younger Granites (Mesozoic)
- Older Granites and Pegmatic Granites (Pan-African, Late Precambrian – Early Palaeozoic)
- Mica Gneiss (Precambrian)
- P = Ta – Nb – Sn – bearing pegmatites (Uncertain age)
- Geological Boundary (Certain)
- Geological Boundary (Inferred, gradational)
- Mine camps and workings in mineralized pegmatites
- Hill ranges, inselbergs, and tors
- Rivers and Streams
- Major roads
- Settlements

2.3 PREVIOUS GEOPHYSICAL WORK IN THE AREA

Despite the fact that Nasarawa Local Government Area is the heart of mining activities in Nasarawa State, only one geophysical report on groundwater is available in the area. (Ibisam, 1997). The survey comprised of four vertical electrical soundings and four profiling. The area coverage was about 200 m x 100 m. The aim of the survey was primarily to unravel the subsurface to aid the citing of water boreholes for the student Hostel in the temporary site of the polytechnic. The thickness of the overburden was estimated at approximately 8.5m to 15 m. Two water borehole sites were recommended. Two aquifer types were identified namely: the weathered overburden aquifer and the fractured aquifer. Fractures were observed to occur between the depths of 17.5 m to 32 m. The static head water levels range from 3.5 m to 7 m as at December 1997. However, due to the limited extent of the data coverage it is not sufficient to generalize these findings in the entire survey area and it's environ.

2.4 HYDROGEOLOGY

The survey area falls under the hydro geological province of the crystalline basement area and underlain by rocks which covers about 50% of the

country's landmass. Over 97% of the crystalline rocks belong to the basement complex (Oyawoye, 1964). The complex is a heterogeneous mixture of crystalline rocks, which include metasediments and granites or gneisses. Groundwater availability in the basement complex is very unpredictable. The crystalline basement rocks by their nature are generally known to be non-porous and impermeable or impervious with no storage capacity when they are fresh and unfractured or unweathered.

The presence of water in rocks depends on the availability of space within the interstices or pores between the composite mineral grains and voids such as crevices, joints, fissures, fracture planes, and solution cavities (Preez and Barker, 1965). For rocks of the crystalline basement to store certain amount of water, they have to be porous and permeable, they should also have interconnected porosity. Porosity and permeability are developed in crystalline basement rocks through secondary structural features such as fracturing, fissuring, jointing and weathering. These may impose secondary aquifer characteristics on these rocks. (i.e. Groundwater occurs either within the weathered bedrock or in the jointed and fractured system in the bedrock). Fractured crystalline aquifers are made up of faults, fractures, joints and folds. Fractures may be caused by tectonic stresses in the rocks. The

occurrence of groundwater in this aquifer is controlled by the extent and volume of fissures or joints in the fresh rock. On the contrary, the occurrence of groundwater in overburden or weathered basement is controlled by the degree and depth of weathering as well as the thickness of the overburden.

Weathering of the crystalline basement rocks may be in the form of physical breaking of the rocks into loose materials or chemical decomposition of the mineral constituents of the rocks. Recoverable groundwater often occurs in the weathered mantle covering the basement. Laterite often develops in the weathered profile and can be locally important as a source of groundwater when its characteristic honey comb structure is well developed. The gneisses and the granites weather to clayey products which often reduce the permeability and the groundwater potential of the weathered materials. Groundwater in the basement is essentially unconfined and the water table is restricted to sub-basins, which may be locally hydrologically isolated.

The occurrence of groundwater is influenced by two main factors: the first being the hydrological and meteorological factors such as stream flow, rainfall, infiltration, evaporation and evapotranspiration or vegetation cover and the second is the geological factors such as lithology, texture and

LIBRARY

structure of the rock (Davis and Dewiest, 1966). Though these factors are interdependent, rainfall and geology are the dominant factors as the former is the source while the latter is the reservoir. In basement aquifers, the most significant climatic variables in determining runoff and groundwater recharge are rainfall and potential evaporation. Both are affected by the seasonal movement of the sun; the pattern of the seasonal rainfall in particular being derived from the movement of large scale zones of high and low pressure caused by the migration of the sun. An increase in the amount of rainfall recharges the groundwater potential of an area. Since evaporation is a major component of the hydrogeological balance of the area of interest a high input of solar radiation leads to potential evaporation. All groundwater originates as rainfall which on falling on the earth's surface is dissipated by either downward percolation, surface-runoff or evapotranspiration (Akpoborie, 1972). The survey area is characterised by an erratic annual rainfall, which falls during a well defined period of rainy season normally between the months of May and September each year. There are no perennial streams in the area but one of the two major rivers which runs south wards at a distance of about one kilometer (1 km) due west of survey area, can carry substantial amount of floodwater for short periods during the height of the wet season.

The two main types of aquifers in the study area are the weathered overburden aquifer and the fractured - crystalline aquifers. The groundwater head levels range from 3.5 m to 7.5 m (Ibisam, 1997).

2.5 HYDROLOGY

Within the survey area, the most important water reservoirs occur in the weathered basement lenses at relatively shallow depths beneath a clay layer of variable thickness. The source of the groundwater aquifers are due to the accumulations of the limited rainfalls that occur during the rainy season over the past years.

At a constant temperature, water resistivity (Rw) decreases with increasing salinity (Todd, 1959), whereas at a constant salinity, water resistivity decreases with increasing temperature. This follows that the water has a negative temperature coefficient of resistivity and the greater the salt content or salinity, the lower the resistivity or the greater the electrical conductivity and conversely.

The resistivity of porous rocks varies with the mobility, concentration and the degree of dissociation of the ions, with the latter depending on the dielectric constant of the solvent. It also varies with the volume, and the

arrangement of the pores and more importantly with the resistivity and amount of the pore fluid. This implies that the electrical conductivity of most porous rocks is almost completely dependent on their water content.

Archie's law gives the empirical relationship for the dependence (Telford, et al., 1976).

$$\rho_e = a\phi^{-m}S^{-n}\rho_w$$

Where, ρ_e = Resistivity of porous rocks

ϕ = Fractional pore volume (porosity)

S = Fraction of the pores filled with water

ρ_w = Resistivity of water

$n = 2, \quad 0.5 \leq a \leq 2.5$

and

$1.3 \leq m \leq 2.5$

The resistivity of water varies considerably from 0.05 - 3 x 10^3 ohm-m, (Telford, et. al., 1976) depending on the amount and resistivity of dissolved chlorides, sulphates and other minerals. Therefore it follows, from the light of this discussion, that the resistivity of water is a function of temperature, type and concentration of ions present and hence a measure of the water salinity and quality (Preez and Barber, 1965). Though no water samples were

IBRAHIM LIBRARY

collected from the survey area and subsequently tested for water quality. previous analyses carried out by Rusafiya in selected wells in Nasarawa town and its environs and the results available from Nasarawa Water Board provides indication that groundwater in Nasarawa area is good for direct consumption and there was no history of contamination or the presence of bacteria/chemical constituents above the WHO standard (Ibisam, 1997).

CHAPTER THREE

ELECTRICAL RESISTIVITY SURVEY

3.1 INTRODUCTION

The electrical resistivity method is classified under the artificial energy source of the electrical methods of exploration. The basis of the method is that when current is driven into the earth via electrodes, any subsurface variation in resistivity will alter the current flow, which will in turn affect the distribution of the electrical potential. The degree to which the potential at the surface is affected depends upon the size, location, shape and conductivity of the materials within the ground (Vingoe, 1972). From measurements of the electrical potential it is usually possible to obtain information about the subsurface resistivities. The principle of the direct commutated or low frequency alternating current is that current is driven into the earth by means of point electrodes or long line contacts and the resulting potential established in the earth is then measured in the vicinity of the current flow. Two electrodes were used in this work to introduce the current into the ground and the resulting potential difference between a second pair of electrodes placed between, and collinear with the current electrodes was being measured. The

product of the resistance obtained and a geometrical factor gives the apparent resistance.

3.2. THEORY OF ELECTRICAL RESISTIVITY METHOD

There are two basic equations governing the electrical methods (Telford et al., 1976).

Consider a direct current or an alternating current whose frequency is low enough to make displacement current negligible in a medium which is assumed to be homogeneous, and isotropic (Keller and Frischknecht, 1970).

The relationship between current density $\underline{J}$ and electrical field intensity $\underline{E}$ is given by Ohm's law,

$$\underline{J} = \sigma \underline{E} \qquad \ldots (1)$$

Where σ = conductivity of the medium

But the electrical field intensity $\underline{E}$ is the gradient of a scalar potential U given by

$$\underline{E} = -\nabla U \qquad \ldots (2)$$

$$\therefore \underline{J} = -\sigma \nabla U \qquad \ldots (3)$$

The divergence condition states that all the current flowing into a chunk of material must leave the other side provided there is no other current source

KASHIM IBRAHIM LIBRARY

or sink within the chunk. The divergence of a current density vector must be zero elsewhere except at the current source and this is the principle of current conservation (Keller and Frisecknecht, 1970).

$$\nabla.\underline{J} = 0 \qquad \ldots (4)$$

From equations, (3) and (4)

$$\nabla.\underline{J} = -\nabla.(\sigma\nabla U) = 0$$

or

$$-\nabla\sigma.\nabla U - \sigma\nabla^2 U = 0 \qquad \ldots (5)$$

Since σ is constant, $\nabla\sigma = 0$ which implies that the first term of the equation (5) vanishes, and we have

$$-\sigma\nabla^2 U = 0$$

or $$\nabla^2 U = 0 \qquad \ldots (6)$$

Equation (6) is Laplace's equation

In spherical polar coordinates, Laplace's equation is

$$\frac{1}{r^2}\frac{\delta}{\delta r}\left(r^2\frac{\delta U}{\delta r}\right) + \frac{1}{r^2\sin\theta}\frac{\delta}{\delta\theta}\left(\sin\theta\frac{\delta U}{\delta\theta}\right) + \frac{1}{r^2\sin^2\theta}\frac{\delta^2 U}{\delta\phi^2} = 0 \qquad \ldots (7)$$

Considering a single current source and assuming there is complete symmetry of current flow with respect to the θ and ϕ directions, the derivatives with respect to these directions is zero.

Thus,

$$\frac{\delta}{\delta r}\left(r^2 \frac{\delta U}{\delta r}\right) = \frac{d}{dr}\left(r^2 \frac{dU}{dr}\right) = 0 \qquad \ldots(8)$$

Integrating equation (8) gives

$$r^2 \frac{dU}{dr} = a$$

or

$$\frac{dU}{dr} = \frac{a}{r^2}$$

$$\therefore dU = \frac{a}{r^2} dr$$

$$U = \int \frac{a}{r^2} dr$$

$$U = -\frac{a}{r} + b \qquad \ldots(9)$$

Where a and b are constants of integration and r is the distance from the single current electrode.

For very large distances the potential is assumed to be zero. i.e.

$U = 0$ when $r \rightarrow \infty \Rightarrow b = 0$

$$\therefore \quad U = -\frac{a}{r} \qquad \ldots(10)$$

The current flows radially outward in all directions from the point current electrode and the total current crossing a sphere of radius r is,

$I = 4\pi r^2 \underline{J}$ By substituting $\underline{J}$ implies that

$$I = -4\pi r^2 \sigma \left(\frac{dU}{dr}\right) = -4\pi\sigma a$$

$$I = \frac{-4\pi a}{\rho} \qquad \ldots (11)$$

Since $\sigma = \frac{1}{\rho}$

Where, ρ = resistivity of the medium

$$\therefore a = \frac{-\rho I}{4\pi}$$

Hence from equation (10)

$$U = \frac{\rho I}{4\pi r} \quad \text{or } \rho = 4\pi r \left(\frac{U}{I}\right) \qquad \ldots (12)$$

U is the potential in a homogeneous isotropic medium.

3.3 THE CONCEPT OF APPARENT RESISTIVITY

The concept of apparent resistivity is one of the basis of the earth resistivity method. It is important to understand what is actually measured by an array

of current and potential electrodes. In real earth, the measured resistivity is not the same as the true resistivity since the earth is not homogeneous.

Suppose that C_1 and C_2 are the current electrodes in which C_1 and C_2 are positive and negative respectively and P_1, P_2 are the potential probes. Figure 3.4.

IF ΔU is the potential difference between P_1 and P_2, then,

$$\Delta U = \frac{I\rho}{2\pi}\left\{\left(\frac{1}{r_1} - \frac{1}{r_2}\right) - \left(\frac{1}{r_3} - \frac{1}{r_4}\right)\right\} \quad \ldots(13)$$

$$\rho = \frac{\Delta U}{I}\left\{\frac{2\pi}{\left(\frac{1}{r_1} - \frac{1}{r_2}\right) - \left(\frac{24}{r_3} - \frac{1}{r_4}\right)}\right\}$$

$$\rho = K\frac{\Delta U}{I} \quad \ldots(14)$$

Where $K = \dfrac{2\pi}{\left\{\left(\frac{1}{r_1} - \frac{1}{r_2}\right) - \left(\frac{1}{r_3} - \frac{1}{r_4}\right)\right\}}$

k is called a geometrical factor which depends on the type of electrode array used.

This resistivity (ρ) will be constant for different electrode separation over a homogeneous isotropic media. In practice the earth is inhomogeneous as such the resistivity varies as the electrode spacing is varied or the whole array is

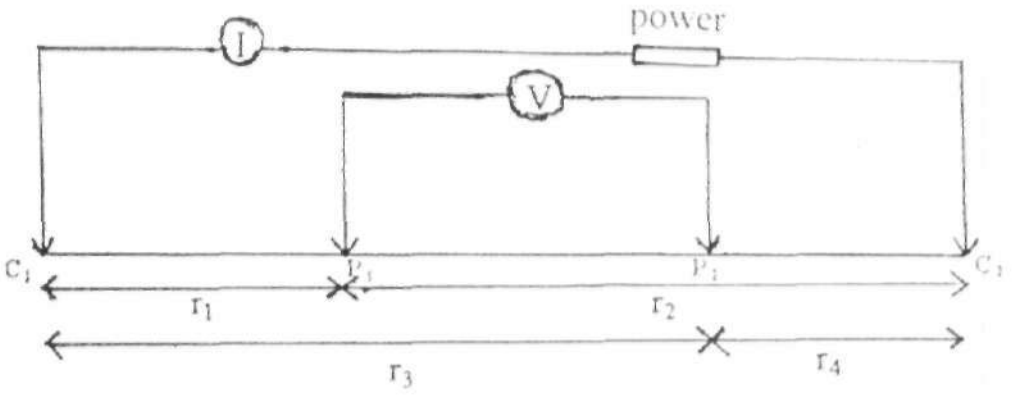


Fig.3.4 General electrode configuration

moved about. This measured resistivity is called the apparent resistivity (ρ_a), which is diagnostic of the real resistivity of the subsurface in the vicinity of the electrode array. The apparent resistivity depends on the geometry and resistivity of the elements constituting the given geologic medium. In any electrode layout, the potential and current electrodes can be interchanged and by the principle of reciprocity, the apparent resistivity should be the same in either case (Telford, et al., 1976).

3.4 ELECTRODE CONFIGURATIONS

There are several types of electrode layout available for use in resistivity survey. In practice the arrangement is always collinear due to the fact that it makes the interpretation of results easier and field procedure less complicated. The Schlumberger and Wenner arrays are most commonly used for exploration surveys. Figure 3.4. illustrates the general electrode configuration while figure 3.5 illustrates the two electrode configurations in common use.

KASUM (GRADUATE LIBRARY

3.4.1. **The Schumberger Configuration.**

This measures the potential gradient at the midpoint of the current electrode spread (i.e. at centre O Fig. 3.5(a)). The current electrodes are always far away from the potential electrodes. From Fig.34 and 3.5a,

$r_1 = (L - x) - l$, $r_2 = (L + x) + l$, $r_3 = (L - x) + l$, and $r_4 = (L + x) - l$,

If P_1P_2 ($= 2l$) << C1C2 (2L). (by a factor of ten or more),

then the apparent resistivity ρ_a, is given by

$$\rho_a = \frac{2\pi\Delta U}{I}\left[\frac{1}{\left(\frac{1}{(L-x)-l} - \frac{1}{(L+x)+l}\right) - \left(\frac{1}{(L-x)+l} - \frac{1}{(L+x)-l}\right)}\right] \quad \ldots(15)$$

For a symmetrical spread, and at the centre (Fig. 3.5(b)) of the system, where x = o it becomes

$$\frac{2\pi\Delta U}{I}\left[\frac{1}{\frac{1}{L-l} - \frac{1}{L+l} - \frac{1}{L+l} + \frac{1}{L-l}}\right]$$

$$\rho_a = \frac{2\pi\Delta U}{I}\left(\frac{1}{\frac{4l}{L^2 - l^2}}\right) = \frac{2\pi\Delta U}{I}\left(\frac{L^2 - l^2}{4l}\right) = \frac{\pi\Delta U}{2l}\left|L^2 - l^2\right|$$

$$\rho_a = \frac{\pi\Delta U}{I}\left(\frac{L^2}{2l} - \frac{l}{2}\right) \quad \ldots(16)$$

and since $L >> l$ we get

$$\rho_a = \frac{\pi L^2}{2l}\left(\frac{\Delta U}{I}\right) \quad \ldots(17)$$

3.4.2 **Wenner Spread**

The electrodes are collinear and uniformly spaced. It measures the potential difference between the potential electrodes (Fig. 3.5c).

The apparent resistivity is given by

$$\rho_a = \frac{2\pi\Delta U}{I}\frac{1}{\left(\frac{1}{r_1}-\frac{1}{r_2}\right)-\left(\frac{1}{r_3}-\frac{1}{r_4}\right)} \qquad \ldots(18)$$

$$= \frac{2\pi\Delta U}{I}\frac{1}{\left(\frac{1}{a}-\frac{1}{2a}\right)-\left(\frac{1}{2a}-\frac{1}{a}\right)} = \frac{2\pi\Delta U}{I}\frac{1}{\left(\frac{1}{a}-\frac{1}{2a}+\frac{1}{2a}-\frac{1}{a}\right)}$$

$$\Rightarrow \rho_a = \frac{2\pi a\Delta U}{I}, \text{ or } \rho_a = \frac{K\Delta U}{I} \qquad \ldots(19)$$

where K = geometrical factor (i.e. K = 2πa).

3.5 **RESISTIVITY SOUNDING**

Resistivity surveys are commonly applied in the vertical electrical sounding (VES) mode for obtaining information or estimating thicknesses and true resistivities in a vertical succession of sub-horizontally layered sequence. In crude terms, the intermediate layer of lower resistivity in the typical sounding curve represents the target zone, lying between a more resistive overburden and the bedrock. The mid point of the electrode configuration is referred to as the sounding point. The centre is kept fixed while the spread is increased

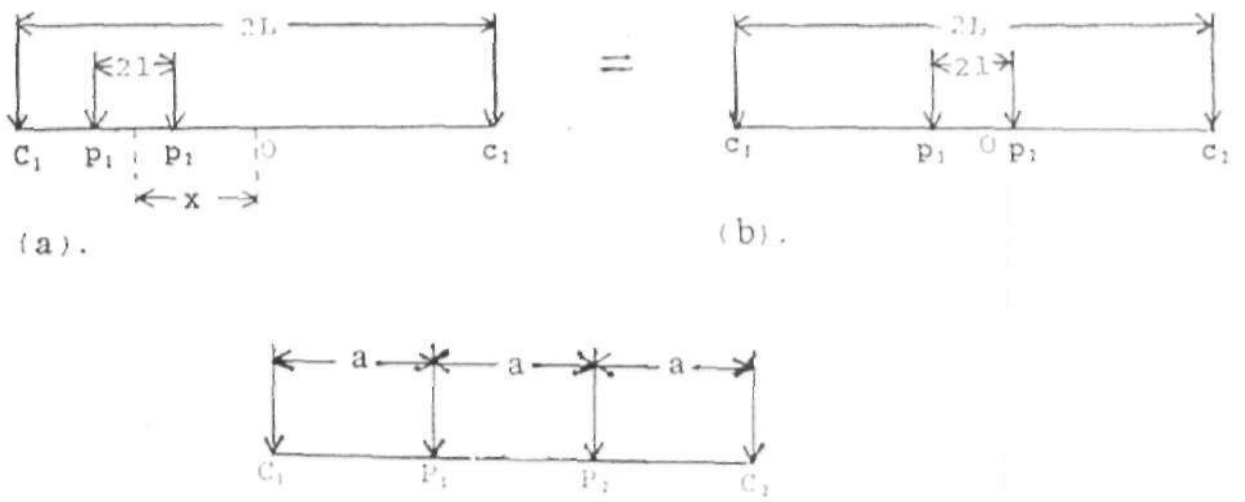


Fig. 3.5 Schlumberger and Wenner arrays

Fig. 3.5 a. Schlumberger spread (electrode spread for the potential gradient at midpoint of current electrodes).

Fig. 3.5b. Schlumberger spread (for a symmetrical spread, and at the centre of the system).

Fig. 3.5c. Wenner spread

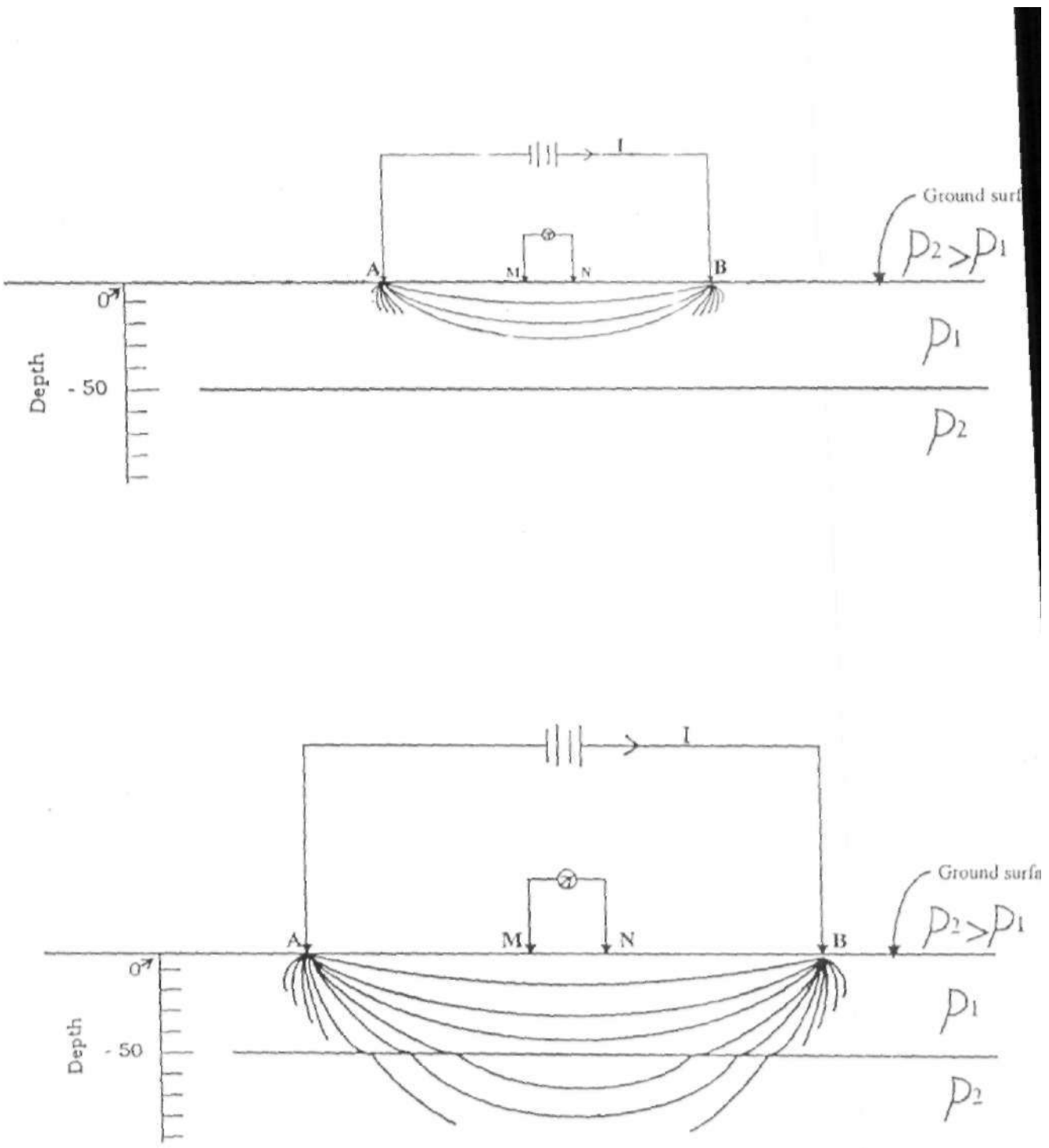


Fig. 3.6 Increase in electrode spread increases depth of current penetration

gradually (i.e. having a fixed centre with an expanding spread). In this way deeper beds of contrasting resistivities become more pronounced and the presence of horizontally or gentle dipping beds of different resistivities can be easily detected (Fig. 3.6 shows how increase in electrode spread increases the depth of current penetration). Both the Wenner and Schlumberger arrays can be employed for this purpose with the Schlumberger method having a greater advantage because only two electrodes are moved at a time. Also the effect of shallow resistivity variation is constant with the fixed potential electrodes. A field curve is plotted using the apparent resistivity values at each sounding point. The curve is digitised and a calculated curve is plotted using the digitised values. The layering models are then obtained using modern software (Zohdy, 1989).

3.6 HORIZONTAL PROFILING

The resistivity profiling technique is used in cases of steeply dipping contacts or for the studying of lateral changes in the resistivity of a particular horizon. In lateral profiling or mapping, the electrode spacing is kept constant while the array as a whole is moved along predetermined profiles or traverse lines. The method is well suited for mineral prospecting especially for the detection

of; (i) Vertical contacts like faults, fractures which can act as secondary aquifers, dykes, shear zones and steeply dipping veins.

(ii) Three dimensional bodies such as massive sulphides of anomalous conductivity. It is usually important to carry out vertical electrical soundings prior to any resistivity profiling even if the interest is only on lateral variation in the subsurface. However, it is important to mention that this technique was not used for this work owing to the high capability of the interpretational technique used in this work which is capable of providing information in the lateral horizon.

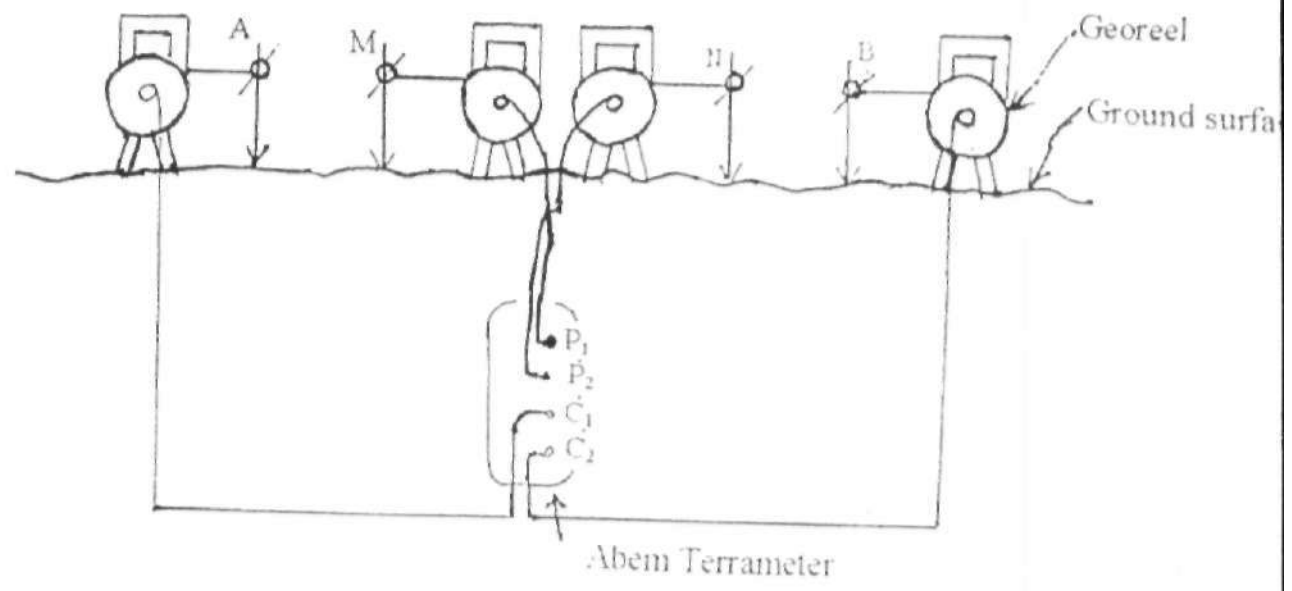
3.7 INSTRUMENTATION

The basic equipment required for resistivity measurement are as follows:

(i) A power source: This may be from an ordinary d.c. battery or low frequency alternating (a.c.) current preferably less than 60Hz.

(ii) Voltmeter and milliammeter for measuring voltage or potential and current respectively. The ABEM Terrameter, model SAS 300, was used for the survey. This instrument measures the ratio of the potential to the current. Fig. 3.7 shows the field resistivity equipment set up.

(iii) Electrodes (preferably non polarizing electrodes e.g. steel or copper).



A and B = current electrodes.

M and N = Potential electrodes.

C_1 and C_2= connections to A and B current electrodes respectively

P_1 and P_2 = connections to M and N potential electrodes respectively.

Fig. 3.7. Field resistivity equipment set up.

(iv) Cables and reels.

3.7.1 ABEM TERRAMETER SAS SYSTEM

GENERAL

The ABEM TERRAMETER SAS SYSTEM is a family of instruments for the measuring of resistivity, self potential and temperature. The TERRAMETER SAS SYSTEM consist of a basic unit called the TERRAMETER SAS 300 which is a transmitter/receiver system in one single box which can be used alone or as a master or supplement as desired with the following:

(i) TERRAMETER SAS 2000 which is a booster transmitter for the extension of the voltage and current ranges of the SAS 300. It can also be used as a separate transmitter.

(ii) TERRAMETER SAS LOG 200 which is a well logging unit for, resistivity, self potential, and temperature. It needs the master unit for operation.

SAS stands for Signal Averaging System. It is a method whereby consecutive readings are automatically being taken and the results averaged

SHIM IBR

continuously. The running average which is continuously updated is presented automatically on the visual display. This continues until the operator is satisfied with the stability of the result. SAS are more reliable than those obtained using single shot systems. Also SAS results are easier to check than results obtained using signal staking (enhancement). The SAS 2000 Booster (optional) can be used to supplement the SAS 300 in situations where the voltage and/or current must be increased. The booster is normally slaved to SAS 300, but it can also be operated separately in special application such as charge potential studies and dipole - dipole surveys. The SAS log 200 (also optional) provides an efficient, and simple way of expanding surveys into wells and drill holes. This consists of a 200m cable with logging probe, electrodes, temperature transducer and resistivity cell, all mounted on a backpacking frame.

3.7.2 DIGITAL TERRAMETER SAS 300

The terrameter SAS 300 can operate in two modes namely: resistivity surveying mode and voltage measuring mode.

. The terrameter SAS 300 contains three main units, all housed in single casing. Well defined and regulated currents are sent out by the electrically

isolated transmitter. The receiver discriminates noise and measures voltages correlated with transmitted signal current (resistivity surveying mode) and also measures uncorrelated DC potentials with the same discrimination and noise rejection (voltage measuring mode). The micro-processor monitors and controls operations and calculates results. With the SAS 300, geophysical survey measurements of natural or induced signals at low levels are possible with excellent penetration and low power consumption. Moreover, it can be used in a wide variety of applications where effective signal/noise discrimination is needed. It can be used to determine the ground resistance of grounding arrangement at power plants and along power lines and (in a pinch) it can even be used as an ohmmeter. In industrial applications, temperature, strain, pressure etc. can be measured using standard transducers in high-noise environments.

3.7.3 TRANSMITTER DESIGNED FOR DEEP PENETRATION

The transmitter current is commutated in a time pattern suitable for resistivity surveying. The transmitted signal (plus SP and ground noise) is measured by the receiver at discrete time intervals when the eddy currents, the IP and the cable transients have decayed to low levels. Standard factory current output

programming (in combination with the receiving principle) provides skin impedance effects equivalent to approximately 0.4Hz for 3.6 seconds of current flow. Other scales of equivalent to 0.2 and 0.1Hz can be selected. These alternatives should be used only under extreme depth and resistivity conditions since corresponding time cycles (7.2 and 14.4 seconds of current flow) increase power consumption. For normal use, the standard factory programming is equivalent to DC surveying. Current leakage and creep can substantially reduce the attainable accuracy and sensitivity and thus the depth penetration.

3.7.4 MICROPROCESSOR MONITORS AND CONTROLS MEASUREMENTS

The microprocessor controls and monitors all measurements to ensure optimal accuracy and sensitivity and make certain that the instrument is used correctly. When the MEASURE button is pressed, the microprocessors runs a thorough check on the circuits, switch positions, checks the battery condition and the usability of the selected parameters. The complete check-up procedure lasts only for one second and, if necessary, warnings and information comprising beeper signals and simple error codes tell the

KASHIM IBRAHIM LIBRARY

operator to change parameters or to check circuits. When satisfied, the microprocessor automatically starts the measurement cycle, and after all readings have been taken it puts the instrument into the standby mode with the final result displayed.

3.8 **DATA COLLECTION**

A reconnaissance survey was undertaken to acquaint one with the survey area so as to plan for the main survey. The entire survey was carried out by a six - man crew, comprising the author, four locally hired workmen and a driver. The equipment for the survey was donated by the International Program in the Physical Sciences Uppsala University Sweden. The geoelectric survey comprised of forty six schlumberger electrical soundings whose center points are located in Fig. 1.2. Six of the soundings consist of three mutually oriented soundings (radial soundings) at sixty degrees (60°) and represent a common point of investigation. The current electrode separation used for this work AB/2 ranges from a minimum of 1 m to a maximum of 150 m. This electrode spread was chosen due to the fact that the survey area is within the basement complex of Nigeria and is expected to be shallow in depth.

The range of the potential electrodes MN/2 was 0.5 m to 10 m. Forty of the vertical electrical soundings were located on a regular grid (each grid being 400 m x 300 m) while the six radial sounding positions were chosen at different locations considering the nature of the topography. Data coverage was confined to the developed areas of the institution and nearby environs which are likely to have the priority of future development. This is done so that borehole sites can be located appropriately in the developed areas or as close as possible to them so as to reduce the cost that may be incurred in laying or conveying water pipes. The entire fieldwork lasted 17 days from April 28 to May 15, 1998. The survey was carried out before the rainy season became severe.

3.9 FIELD PROBLEMS ENCOUNTERED

Problems encountered include the intrusion by farmers inquiring about the purpose of the investigation. Grazing cattle also posed yet another problem in the form of delays as the cattle often dislodged pegs and pulled the cables. At some locations of the survey area water had to be added to the ground to ensure good contact between the electrodes and the ground which had been hardened due to its dryness. This measure prevents erratic readings from the Terrameter.

KASHIM IBRAHIM LIBRARY

CHAPTER FOUR

INTERPRETATION

4.1 INTRODUCTION

The interpretation of resistivity data means;

(i) Studying the given resistivity curve in a view to having a picture of the subsurface causes (Qualitative interpretation).

(ii) Delineating the effect of the individual features on the basis of available eophysical and geological data (i.e. smoothing to remove noise).

(iii) Estimating the likely parameters of the body of interest from the corresponding true or apparent resistivity curve (quantitative interpretation). These may include depths to the various horizons, their thicknesses and true resistivities.

The traditional method for the interpretation of sounding curves employs the use of auxiliary point techniques (Zohdy, 1989) and curve matching procedures using albums of theoretical curves (Orellana and Mooney, 1966; Rijkwaterstaat, 1969). These methods are time consuming. In our modern world of industrial and computer technological advancement, there is the need to revert to higher resolution techniques of interpretation capable of providing more detailed information about the subsurface lithological

composition. Several methods for computerized interpretation of vertical electrical sounding (VES) curves were developed in the 1970s. These methods can be classified into two groups. The first group relies on the transformation of a VES curve into its corresponding resistivity transform curve (or Kernel function) using forward filters such as those developed by Ghosh (1971), Koefoed (1969), and Strakhov and Karelina (1969). The resistivity transform curve is interpreted using methods based on Pekeris (1940) and Koefoed's (1979) formula.

The second group of interpretation is the inversion method. The first inversion method was developed by Parasnis (1979) and later programmed by ABEM (a Swedish corporation) using the filter suggested earlier by Gosh 1971.

The inversion method relies on inverting the sounding curve itself without first transforming it to its resistivity transform curve (Anderson, 1979; Kunetz and Rocroi, 1970; Zohdy, 1975).

For field sounding curves, the present method provides the geophysicist with a theoretical curve that fits the observed curve as closely as possible and produces a corresponding well-behaved layering model (with no extremely thin layers or unusually low resistivities). To achieve this, the number of

layers is equal to the number of digitized points, and the layer boundaries are spaced uniformly on a logarithmic depth scale Zohdy. (1989).

The advantage of the Zohdy method over other interpretational methods is:

(i) It is less time consuming and processing cost are low in relation to other methods.

(ii) Since no initial guess of the number of subsurface layers is required. it is well suited when a survey is being made in areas where absolutely no geological information is available.

(iii) The resulting n-layers model from the interpretation is more advantageous than to layering models obtained by the use of other methods in that, it provides more detailed information about the subsurface variations within any suggested geoelectric layer. In most hydrogeological applications at least some rudimental information is available. This may only consist of a rough idea of the layering sequence; overlying sediments, aquifer and basement. Or, in areas where wells or boreholes have been drilled, very detailed information may exist regarding the number of distinct lithological units and their thicknesses. In these situations it is usually desirable to obtain an interpretation which has the same number of layers as there are distinct lithological units. The geophysicist may accept, simplify, complicate or

IBRAHIM LIBRARY

modify the resulting solution to satisfy known geologic information using other equivalent layering models (Zohdy, 1974).

4.2 OUTLINE OF THE ZOHDY METHOD

The study of the Schlumberger and Wenner theoretical sounding curves for horizontally stratified, laterally homogeneous, and isotropic media shows that regardless of the number of layers or resistivity distribution with depth, the following properties are observed:

(1) Computed apparent resistivities are always positive.

(2) The form of a sounding curve follows the form of the true resistivity-depth curve. As the true resistivities increase (or decrease) with depth, the apparent resistivity increase (or decrease) with greater electrode spacing. This is particularly evident for layers whose thickness increases logarithmically with depth.

(3) The maximum change in apparent resistivity always occurs at an electrode separation which is greater than the depth at which the corresponding change in true resistivity occurs. That is, a sounding curve is "out of phase" with the resistivity depth curve and is always shifted to the right of the resistivity depth curve.

(4) The amplitude of a sounding curve is always less than or equal to the amplitude of the true resistivity-depth curve. The apparent resistivity asymptotically approaches the true resistivity at electrode spacing that are very small with respect to the thickness of the first layer or very large with respect to the depth of an infinitely thick last layer.

(5) In a multilayer model, if the true resistivity of a thick layer is changed, the apparent resistivity along a corresponding segment of the sounding curve also changes accordingly. Furthermore, the maximum changes in the apparent resistivity are approximately equal to the net change in true resistivity.

Properties (1) and (2) led early interpreters to assume that electrode spacing is equal to probing depths and that apparent resistivity are nearly equal to true resistivities. In view of properties (3), (4), and (5), however, it is evident that: (i) the electrode spacing do not adequately approximate the depths to the various layers. Therefore, the assumed depths must be shifted to the left in order to bring the assumed layering more or less in phase with the resistivity depth curve. (ii) The apparent resistivity do not adequately approximate the true resistivities.

(iii) Property (5) can be used to make the required resistivity adjustments.

The essence of the new iterative process is to determine the appropriate amount to horizontally shift the depths and vertically adjust the resistivities without a prior knowledge of the true resistivity depth distribution.

4.3 INITIAL DATA PREPARATION

A field Schlumberger sounding curve is different from a theoretical curve in the sense that it is composed of several overlapping segments. The segmented Schlumberger field curve is processed and reduced to a continuous curve prior to its interpretation in terms of a horizontally stratified model (Deppermann, 1954; Koefoed, 1979; Kunetz; 1966; Mundry, 1980; Zohdy et al., 1973).

4.3.1 ITERATIVE PROCEDURE

The iterative procedure relies on the following initial assumptions:

(i) The number of layers in the model equals the number of digitized points on the observed curve. This assumption remains unchanged throughout the iterative process.

(ii) The depths of the model layers are equal to the digitized electrode spacing which are equally spaced on a logarithmic depth scale.

(iii) The true resistivities of the model equal the apparent resistivities.

4.3.1a. Depth Determination

In practice, the true resistivity depth curve is unknown. Therefore, in order to determine the amount of shift to the left to bring assumed and unknown layering to the nearest "in phase" condition, the following iterative processes have to be done.

(a) Assume that the digitized electrode spacings are equal to the depths and that the apparent resistivities are equal to the true resistivities at those depths.

(b) Compute a theoretical sounding curve for this multilayer model by convolution.

(c) Compute the root-mean-square (rms) percent from the equation

$$rms\% = \sqrt{\frac{\sum_{j=1}^{N} \left(\frac{\rho_{oj} - \rho_{cj}}{\rho_{oj}} \right)^2}{N}} \times 100,$$

Where

ρ_{oj} = jth "observed" apparent resistivity,

ρ_{cj} = jth calculated apparent resistivity, and

N = number of digitized apparent resistivity points (with j = 1 to N).

IBRAHIM IBRAHIM LIBRARY

d. Multiply all the depths by 0.9 to decrease all the layer depths by 10 percent (small arbitrary amount).

e. Repeat steps (b) and (c) and compute a new rms percent.

f. Compare the new rms percent with the previous one (which it will be for the first few iterations), then the newly computed shallower depths are now more in phase and are closer in position with respect to the true, but unknown, depths than the previously assumed depths.

g. Repeat steps (d), (b), (c), and (f) until the rms percent is minimum. A minimum is detected when the rms percent increases as the depths are shifted too far to the left (i.e. made too shallow). In order to speed up the iterative process, the initial depths may be started at a value that is already smaller than the electrode spacings. For example, multiply all the electrode spacings by 0.8 and then successively reduce the depths by 10 percent until a minimum rms percent is found.

4.3.1b Resistivity Determination

After calculating a theoretical curve using shifted depth and apparent resistivities, the amplitudes of those resistivities must be adjusted to obtain a better fit between observed and calculated sounding curves. The iterative process is as follows.

a. At each digitized electrode spacing on the observed and calculated curves, if the computed apparent resistivity, at the jth spacing, is less (or greater) than the corresponding observed apparent resistivity, the corresponding true resistivity of the jth layer should be increased (or decreased) so that the calculated apparent resistivity will rise (or fall) and approach the observed resistivity. The amplitude of a layer resistivity is iteratively adjusted as:

$$\rho_{i+1}(j) = \rho_i(j) \times \rho_o(j) / \rho_{ci}(j),$$

Where

i = number of iteration,

j = jth layer and jth spacing,

$\rho_i(j)$ = jth layer resistivity at the ith iteration,

$\rho_{ci}(j)$ = calculated apparent resistivity at the jth

Spacing for the ith iteration, and

$\rho_o(j)$ = observed apparent resistivity at the jth spacing.

The ratio of observed to calculated apparent resistivity is multiplied by the corresponding layer resistivity to adjust it to a higher or lower value.

b. A new sounding curve is calculated using the adjusted layer resistivities.

c. A new rms percent is computed and compared with the previously obtained rms percent.

d. Steps (a), (b), and (c) are repeated until a match is found to the observed curve or until another condition is met to terminate the iterative process.

The iterative process is terminated when one of the following conditions is met: a prescribed minimum rms percent (less than 2 percent for field data) is obtained; a slowness in further improvement in fit is detected (less than 5 percent reduction in successive rms percent); a maximum number (30) of iterations is reached; or the rms percent increases instead of decreasing. The average number of iterations is about 10.

4.4 Ambiguity In The Relation Between The Resistivity Curve and The Subsurface Layer Distribution

Strongly differing layer resistivity distributions in the subsurface may yield apparent resistivity curves that are not strictly equal, but differ so slightly that they cannot be separately distinguished as different formations with the accuracy of the resistivity measurements/instrument. This ambiguity lies entirely in the relation between the resistivity transform and the parameters of the subsurface layer distribution.

These ambiguities are generally reffered to as "equivalence" and or "suppression". The term "equivalence" is used either in cases were ρ_t-1 >

KING FAHD UNIVERSITY OF PETROLEUM & MINERALS LIBRARY

ρ_i+1 (i.e. the so called "bowl-type" resistivity sequences), or where ρ_i -1 < ρ_i > ρ_i +1' (i.e. "bell-type" resistivity sequences). In the bowl-type case two resistivity stratifications can be equivalent, i.e., distinguishable on the apparent resistivity curves, if they have the same value for the quotient t_i/ρ_i. For bell-type cases this situation arises for two resistivity stratifications which have the same value for the product $t_i \times \rho_i$ The term "suppression" is used either where ρ_i -1 < ρ_i < ρ_i +1' (i.e., "ascending-type" resistivity sequences) or where ρ_i -1 > ρ_i > ρ_i +1' (i.e., "descending-type" resistivity sequences). In both the ascending and descending types the effect of the phenomena is such that it may be impossible to detect the existence of the intermediate layer at all from the apparent resistivity curve.

These limitations were resolved by sounding at some borehole locations where the resistivities and thicknesses obtained were verified with the corresponding stratification in the borehole lithology log within the area of survey.

4.5 OPTIONS AND CHARACTERISTICS

Different options and characteristics can be used to generate equivalent models and to impose constraint so that the eventual model chosen actually represents the resistivity and layering sequence for each of the resistivity/formation identification. In this work a shift factor of 0.3 was used for the sounding curves to bring the observed and unknown layering to the the nearest in phase condition. Some of the options that can be applied are discussed below.

1) Fixed shift factor: Each sounding has its unique depth shift factor that yields a minimum root-mean-square percent. The value of this shift factor depends on (a) the curve type; i.e., H($\rho_1>\rho_2<\rho_3$), K($\rho_1<\rho_2>\rho_3$, ρ_4), A($\rho_1<\rho_2<\rho_3$), KH($\rho_1<\rho_2>\rho_3$, ρ_4), etc (Zohdy, et al., 1974); (b) The completeness of the left and right branches of the field curve; and (c) the amount of noise present. It was found, however, that because of equivalence, determining the optimum shift factor is not critical for the final fitting of the curve. Thus; a fixed shift factor can be selected within the range between 0.3 and 0.6 (approximately) as suggested by Zohdy (1989).The fixed shift factor selected for this work was as mentioned earlier 0.3 for all schlumberger curves, and the observed curve always match when the resistivity amplitude adjustment was applied.

The use of a fixed shift eliminates a few iterations that would have been necessary to find optimum shift factor for each curve type. However, the number of iteration saved in using a fixed shift factor results in a larger number of amplitudes adjustment iterations. Furthermore, if the selected fixed shift factor is too small (layering is shifted too far to the left), overshoots and undershoot develop at shallow depths, and the depth to the last layer is defined by an abrupt change in resistivity. Conversely, if the selected fixed shift factor is too large (layering is shifted too far to the right) then over shoots and undershoot develop at large depths, and the depth to the shallow layers are defined by abrupt changes in resistivity.

2) Layer compression: layer compression becomes necessary where severe K-type curves ($\rho_1 << \rho_2 >> \rho_3$) are encountered, like in permafrost areas (Cagniard, 1959); Kalenov, 1958) or over dry lava flows covered by a thin layer of layer compression soil (Zohdy, and Stanley, 1973).This constrain was not applied because the curves do not exibit conditions necessary for its application. A severe K-type curve is a curve that rises steeply at an angle of nearly forty-five degrees(45°) continues to rise for nearly two logarithmic cycles, forms a somewhat sharp maximum, and then falls to low resistivity values (Zohdy, 1989). Interpreting observed curves of the severe K-type results in rms percent values in the range of 5 to 10 percent in which case the curves cannot be fitted within 2 percent, probably because of the distribution of layer depths obtained from digitized electrode spacing, extends over a much larger depth profile than does the true (or any equivalent) layer-depth profile. Hence the layer depths are compressed so that the resisitivity adjustment procedure may succeed to yield a good fit.

Layer compression is achieved by increasing the number of layers per decade. i.e. greater than six. The total number of layers is still the same as the number of digitized points and the thicknesses of all layers beneath the first layer still increase at a uniform logarithmic rate, but now the depth interval is less than the electrode spacing interval from which it was originally derived.

3) Layer Expansion: This is a direct converse of layer compression; it results from decreasing the value of the number of layers per decade.

4) Fixed Last Layer Resisitivity: The resisitvity of the last layer may be fixed for all sounding curves within the same geologically identified formation that show a rising right branch and interpreted in terms of a constant resisitivity value for geoelectric basement and hence geoelectric cross-section are produced with a common basement resistivity; the last layer's resisitvity does not change during the iterative process. The last layer factor was not fixed.

5) Interpretation of Incomplete curves: Most field sounding curves are incomplete, i.e. a sounding curve in which the left and (or) right asymptotes to the resistivity of the first and (or) last layer, respectively, are not measured. A field sounding curve whose last right branch rises at an angle of 45° for at least three or four points (sampled at the rate of six points per decade) is considered to have a complete right-hand branch (Zohdy, 1989). Provided the curve is not distorted, the resistivity value of the first point will fit because the depth to the bottom of the first layer is always less than the first electrode spacing, and similarly for the last layer. Incomplete sounding curves were not encountered in any of the curves used in this work.

4.6 INTERPRETATION OF AZIMUTHAL (RADIAL) SOUNDING

A medium is said to be isotropic if its electrical properties are independent of direction (i.e. no matter the direction in which the axes are taken, the resistivity will be the same). In such a medium, the pattern of anisotropy is a sphere. If the electrical properties of the medium have reference to certain directions fixed relative to the medium, the medium is said to be anisotropic. In such a case the transverse resistivity of the medium would be different from the longitudinal resistivity. The pattern of resistivity anisotropy for such a medium is an ellipse in which the major axes equal to the numerical value of the transverse resistivity while the minor axes equals numerically to the horizontal resistivity. For a rock having three orthogonal fracture systems, and in which the current flow is perpendicular to the fracture system, the pattern in such a case would neither be spherical nor elliptical (Keller and Frischknecht, 1970). Azimuthally resistivity has been used to determine fracture geometry in crystalline rocks and glacial till by lane et al. (1995), Carlson et al. (1996a and b), Hansen and Lane(1996), Chapman and Lane (1996). Lane et al. (1996), Busby (2000). The radial soundings were used to locate positions were fractures are present in the survey area.

KASHIM IBRAHIM LIBRARY

CHAPTER FIVE

RESULTS

5.1 ANALYSIS OF RESULTS

The analysis of the data was performed using suitable modern software called Zohdy program. A special basic program (Zohdy, 1989) was used to obtain the equivalent n-layers model from the apparent resistivity curve of each sounding. One of the advantages of the n-layers model over other layering models is that it can provide additional information about the subsurface variations within any suggested geoelectric layer.

Fig. 5.1 and Fig. 5.2 show the apparent resistivity curve obtained from the field data and the corresponding interpreted (n-layers) model obtained by the use of the software respectively. The Field curves were obtained by the plots from the field data while multilayer sounding curves were obtained from the processed and digitized field curves. The multilayers were shifted to the left to make the layers be in the nearest in phase condition with the true unknown resistivity depth curve by using a shift factor of 0.3.

A quantitative interpretation or analysis of all the vertical electrical sounding curves indicates that most of them range from three to four layer cases of the h type or a combination of both h and k types. All the curves are

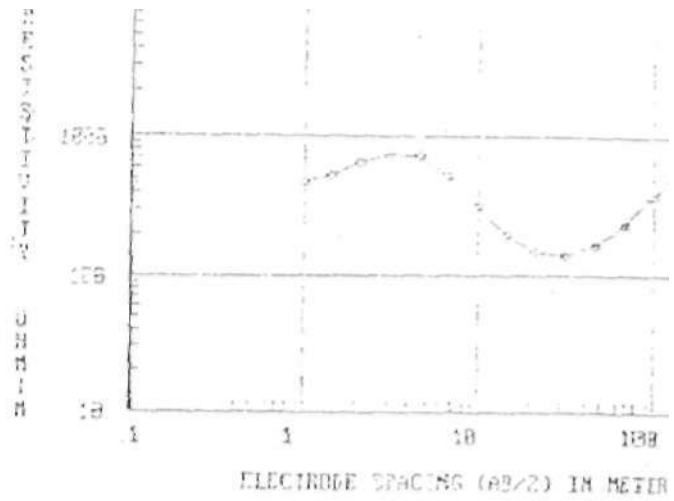
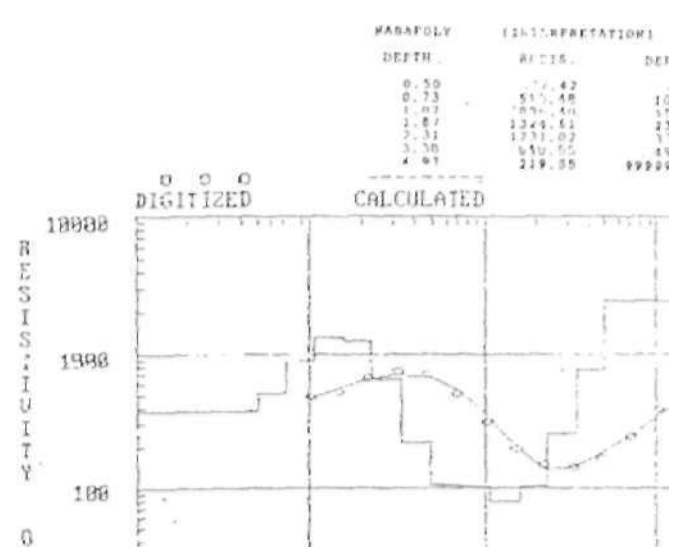


Fig.5.1 Apparent resistivity field curve



characterized by a final segment of positive gradient which, in most cases, approximates 45 degrees. This indicates a semi-infinite basal unit of relatively high resistivity which is considered to correspond to the Nigerian basement.

5.2 **Iso-resistivity contour maps**

The iso-resistivity contour maps represent the horizontal sheing of the survey area at different depths in the subsurface. The resistivity ranges selected were based on previous geophysical works carried by individuals at different locations within the basement complex of Nigeria and the survey area. The range of resistivity values used for this work is shown in Table 5.1.

The Figures 5.3 – 5.15 are the iso-resistivity contour maps for subsurface depths depths corresponding to the surface, 5 m, 10 m, 15 m, 20 m, 25 m, 30 m, 35m, 40 m, 45 m, 50 m, 55 m, and 60 meters respectively. (Figures 5.8 – 5.15 are shown in the appendix). They also suggest changes in conductivity since conductivity is the reciprocal of resistivity. It should be borne in mind that the surface is taken at a depth of 0.4 m in the subsurface to assume a level surface.

KASHIM IBRAHIM LIBRARY

5.2.1. **Resistivity map of the surface layer**

The map Figure 5.3 was obtained by contouring the resistivity values for all the sounding points measured at the surface. The map shows the resistivity for the topmost layer and reveals that the surface is covered mostly by lateritic soil. One major anomaly is prominent at around sounding point 32 on the map by the clustering of the contour lines. This anomaly may be due to the presence of fresh laterite which may be highly consolidated due to its high resistivity (greater than 500 ohm-m). An advantage of such an area is that it could serve as a good location for the erection of buildings due to the high consolidation of the rocks in the area.

5.2.2. **Iso-resistivity Map at 5 m depth.**

Figure 5.4 shows that the area is generally characterized by relatively low resistivity values. An explanation for this low value of resistivities could be due to the fact that the area is saturated with water. This is an indication that such a depth is in the aquiferous zone of the survey area. There is a shift of the anomaly at VES 32 for the surface plot to VES 33 at the depth of 5m. This may be moderately weathered at resistivity ranges from 200 to 500 ohm-m and finely weathered at resistivities greater than 500 ohm-m (Fig. 5.4).

Table 5.1 Resistivity ranges used for this survey work

ROCK TYPES	RESISTIVITY (OHM-M)
Lateritic Soil	201-500
Fresh laterite	Greater than 500
Strongly or deeply weathered basement	30-200
Moderately weathered basement	201-500
Finely weathered basement	501-1000
Fresh basement	Greater than 1000

KASHIM IBRAHIM

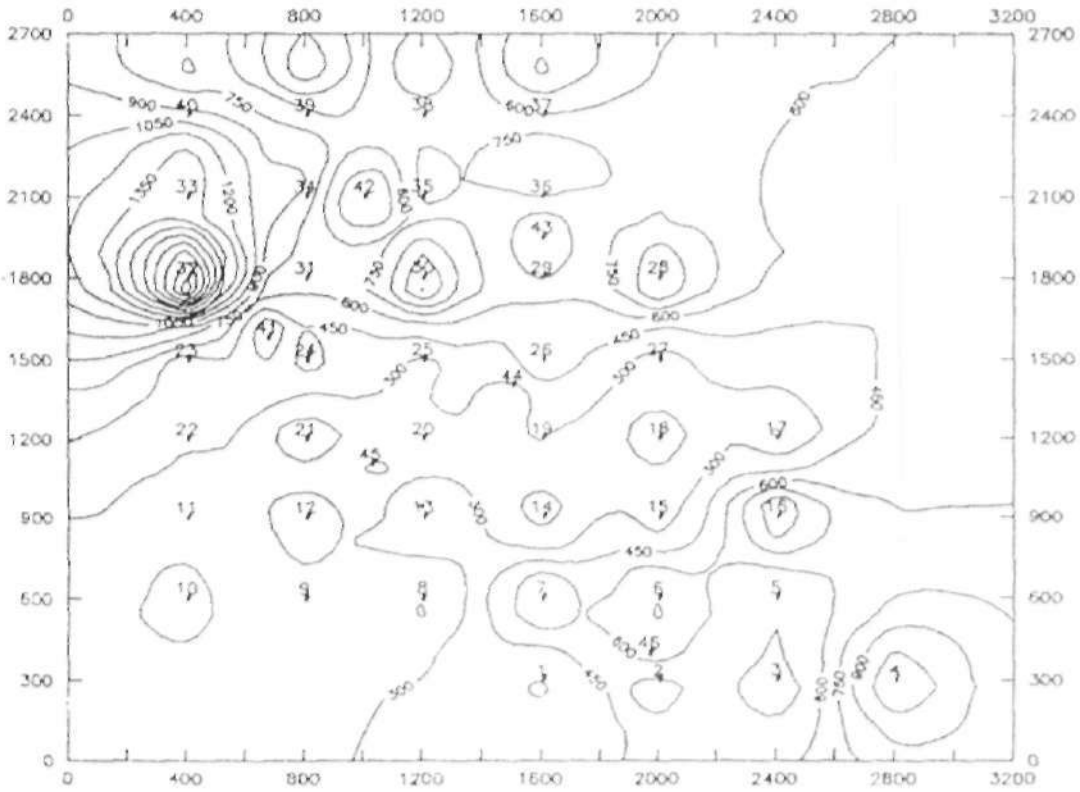


Fig. 5.3. Iso - esistivity contour map at the surface.

Contours at 150m interval

5.2.3. Iso-resistivity contour Map at 10m, 15m, etc.

At a depth of 10 m (Figure 5.5) it is seen that the saturated zones are more prominent at areas bordering the upper part of the contour line of 200 ohm-m which passes between VES (27 and 28), VES (26 and 27), VES (20 and 25), VES (21 and 45), VES (12 and 13), and finally between VES (8 and 9). The lower part of the contour line may comprise moderately weathered gneisses of the basement. As the subsurface is progressively unraveled by the iso-plots, the basement is struck at a depth of 20 m at around VES 14, 15 and 16 Fig. 5.7). This is evident by the presence of concentric circles or closures and a high resistivity value of above 1000 ohm-m. The process of gradual decrease in weathering is evident at greater depth in the subsurface (i.e. at 25m, 30m, 35m, 40m, 45m, 50m, 55m, and 60m) until the fresh basement is struck at all the VES points (Figures 5.8 to 5.15) as shown in the appendix.

5.3. GEOLOGIC SECTIONS

5.3.1 GENERAL INTRODUCTION

The geologic sections equivalent to geoelectric sections were obtained by taking profiles along different directions on the survey area. The resistivity

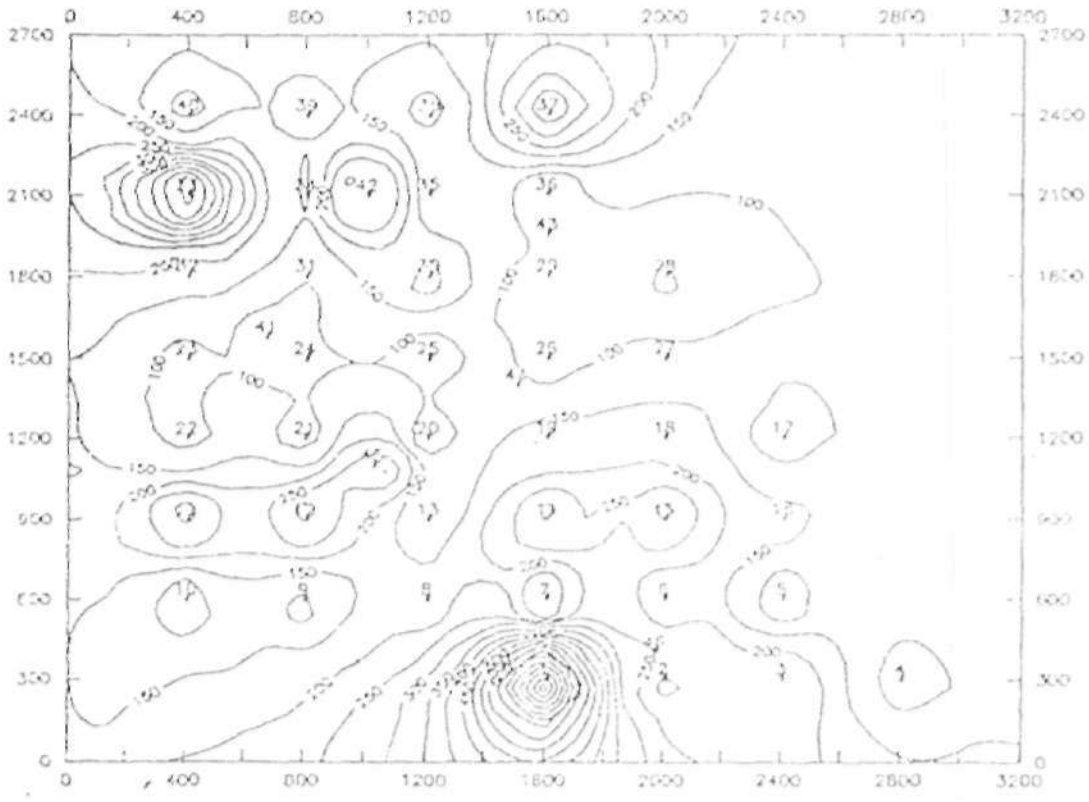


Fig. 5.4. Iso - resistivity contour map at 5m depth.

Contours at 50m interval

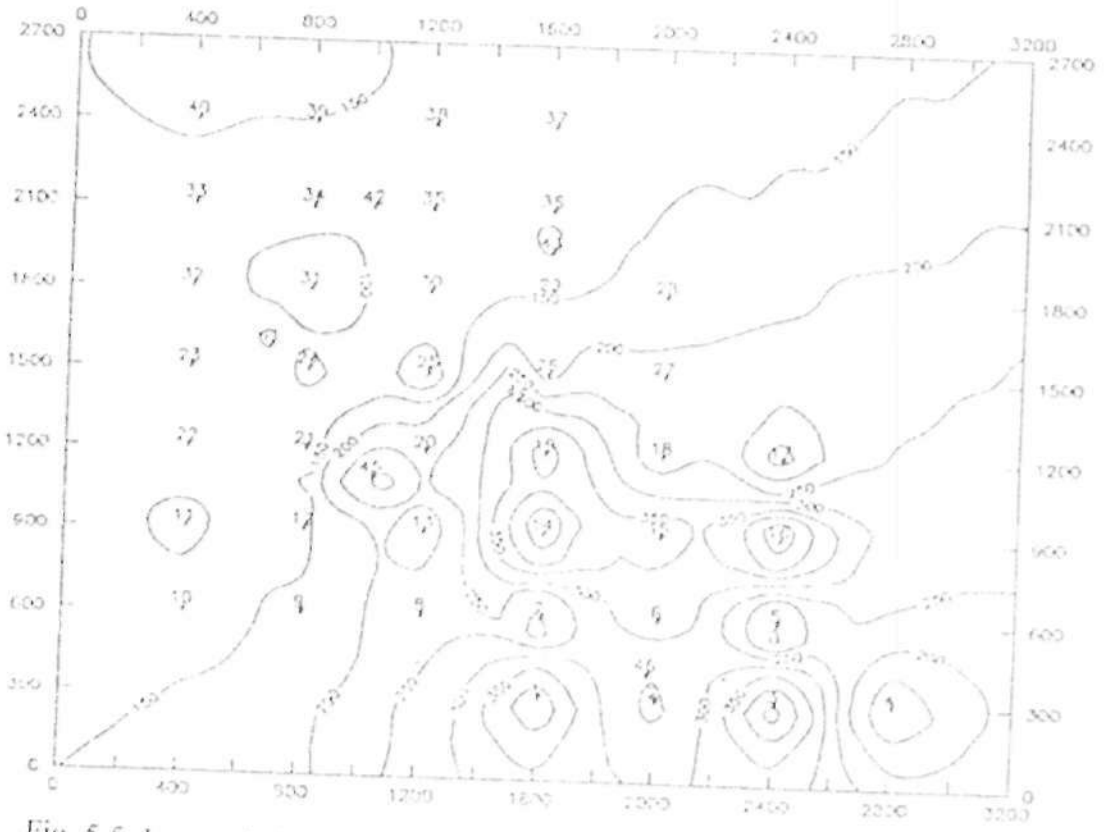


Fig. 5.5. Iso - resistivity contour map at 10m depth

Contours at 50m interval

KASHIM IBRAHIM LIBRARY

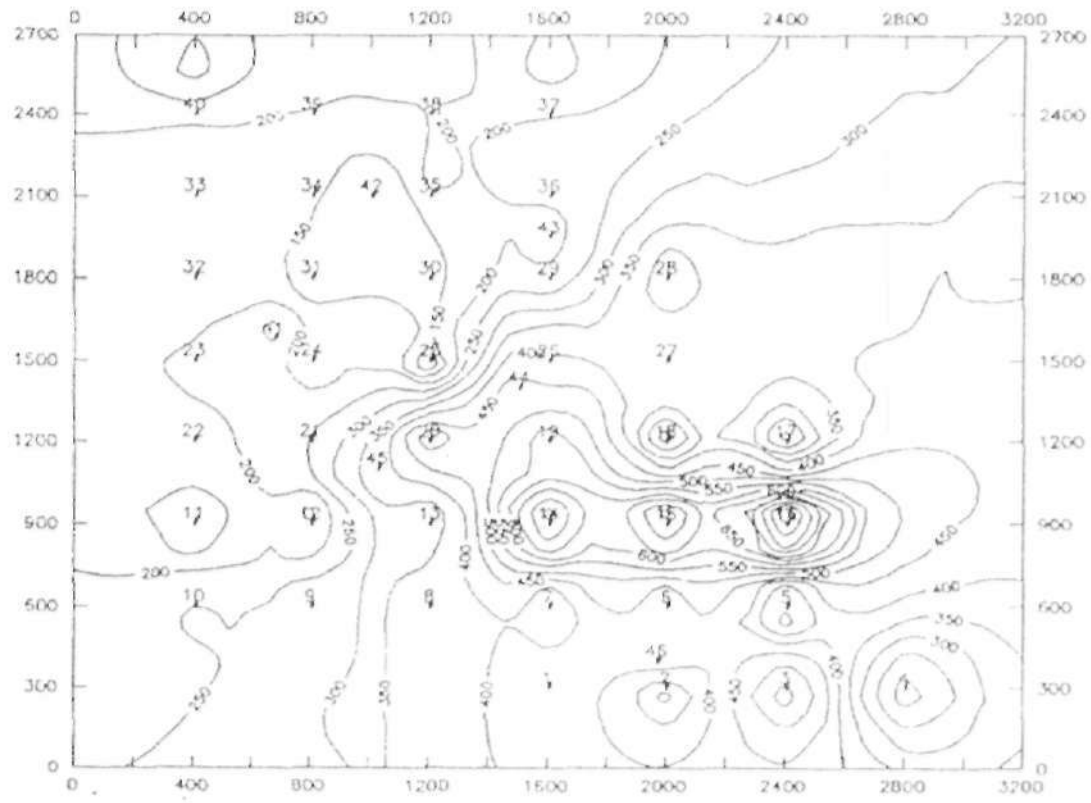


Fig. 5.6 Iso - esistivity contour map at 15m depth

Contours at 50m interval

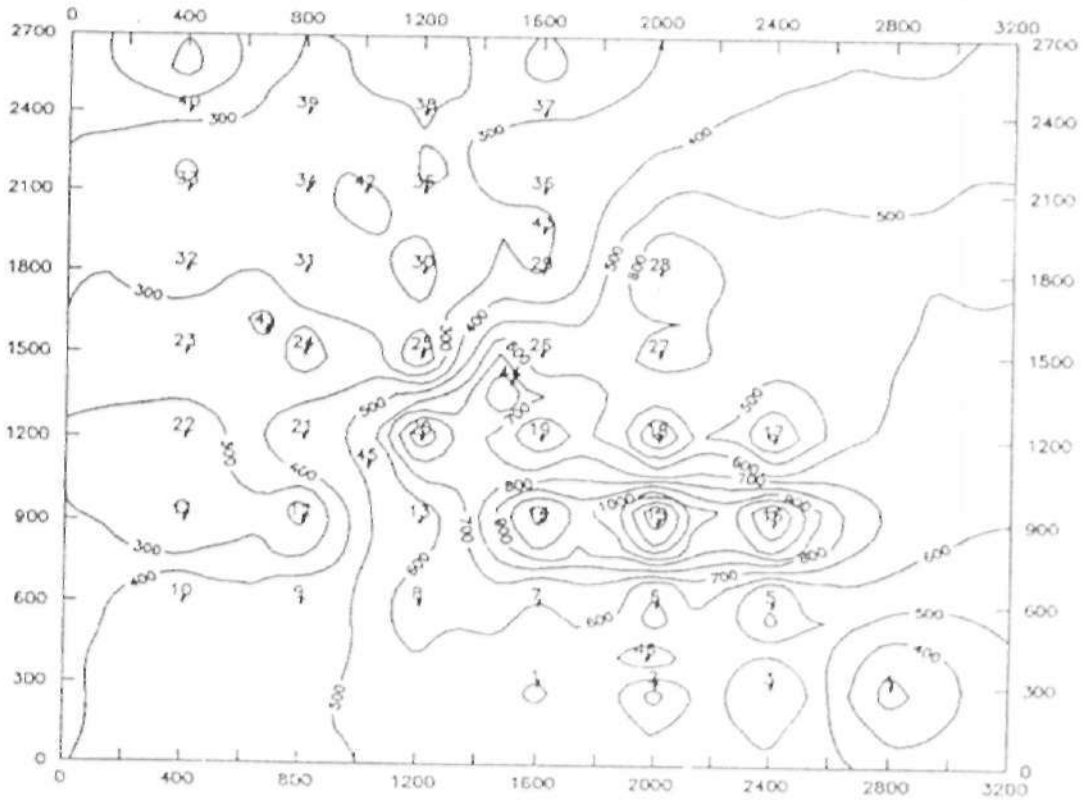


Fig 5.7 Iso - esistivity contour map at 20m depth

Contours at 1 0m interval

KASHIM IBRAHIM LIBRARY

models obtained from the n-layers analysis were used to produce subsurface resistivity contour sections along sounding profiles and subsequently used to obtain the equivalent geologic sections Fig. 5.16 shows the profiles chosen. The resistivity contour sections were obtained by plotting the resistivity values of each of the n-layers of each sounding at different points on the layers below the sounding location, and the resistivity values were thus contoured in the vertical plane of this section. The geologic sections were obtained by interpreting the subsurface resistivity contour sections. This was done by careful examination of the contour behavior at the different depth and taking into consideration the range of resistivity values suitable for the Nigerian basement complex and previous geophysical work around the survey area.

5.3.2 Subsurface Geologic Section Along Profile AB

It should be recalled that since water can reside in the weathered mantle of the crystalline basement, it follows that a geophysical target in ground water search is an area of high degree weathering.

The geologic section along this profile Fig. 5.17 shows that the areas of deep or strong weathering are thickest beneath VES (33 and 11) with VES 33 being 14.9 m thick, while VES 11 is 14.5 m thick. In the moderately

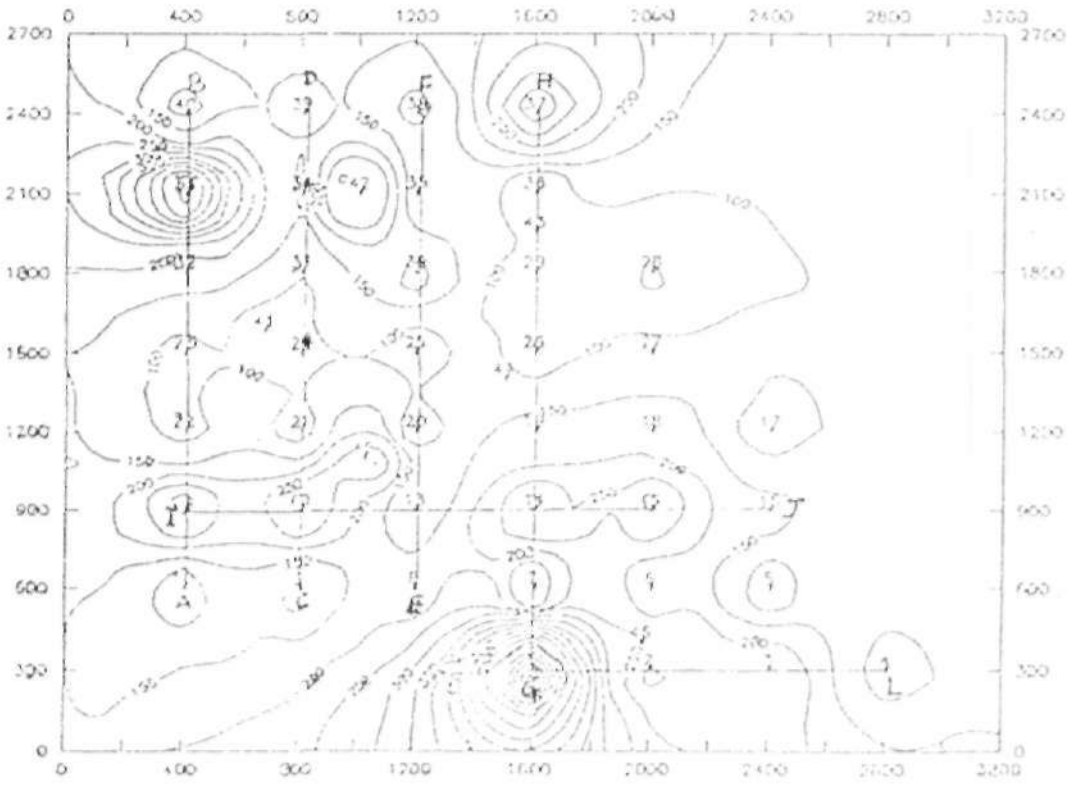


Fig. 5.16 Iso - resistivity contour map at 5m depth
(Showing the profiles chosen)

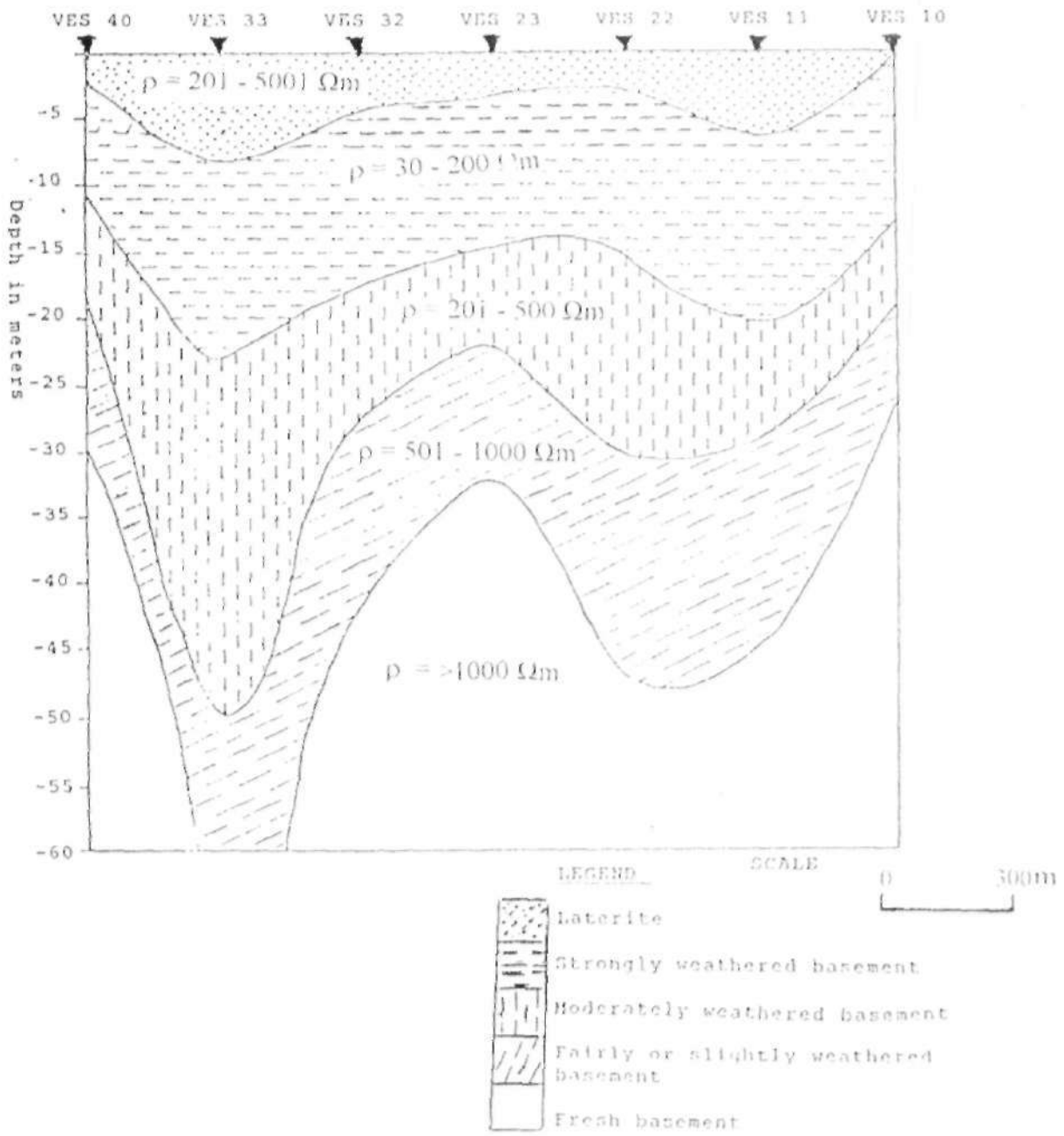


Fig. 5.17 Geologic section equivalent to geoelectric contour section along profile AB.

KASHIM IBRAHIM LIBRARY

weathered zone, VES 33 is thicker than at VES 11. The flow of ground water occurs more towards VES 33 than to VES 11, since the gravity beneath the weathered profile at VES 33 is greater than that beneath VES 11. This follows from the fact that ground water flows from areas of low gravity to high gravity.

In the light of the above discussion ground water potential is most evident at VES (33 and 11), with VES 33 being more promising. Boreholes should be drilled to the slightly weathered basement. This is to say at least for VES 33 it should be dugged to a depth of 50m and for VES 11 to a depth of 29m.

5.3.3 **Subsurface Geologic Section along Profiles CD, EF, GH, IJ, and GL.**

The subsurface geologic sections obtained along these profiles in Figures 5.18 to 5.22 are similar to that obtained in Fig.5.17. From these profiles it would be easy to detect the thicknesses of the various horizons as areas of thick weathering suggest areas of high groundwater potential.

5.4 **Map of Aquifer layer**

5.4.1 **Depth to Aquifer**

This contour map was obtained using the depth to the top of the strongly weathered basement at all the sounding points. The depth to aquifer varies from 1m to 10m. It should be noted that shallower depth to aquifer does not necessarily denote the best locations for sitting of boreholes since the

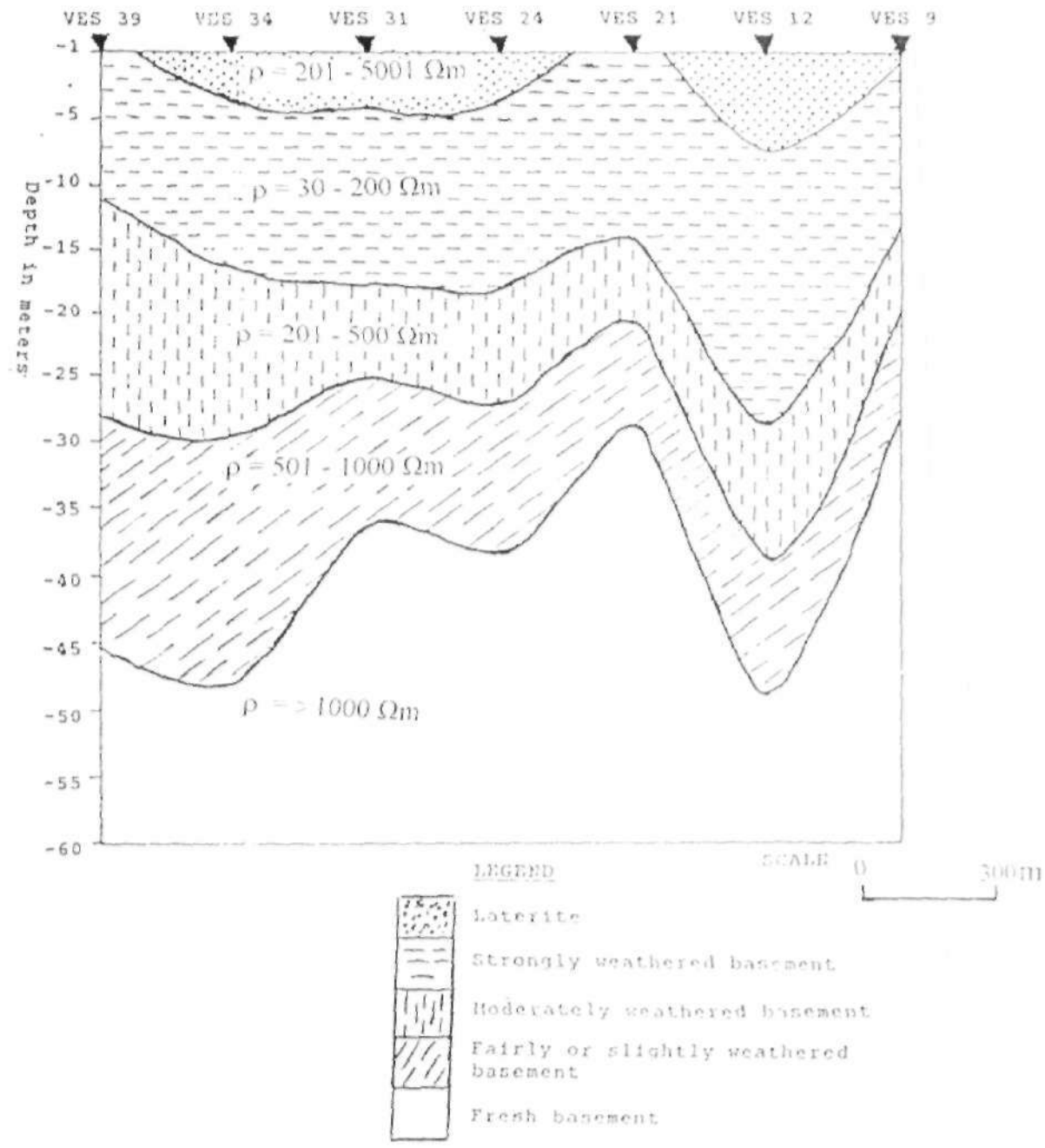


Fig. 5.18 Geologic section equivalent to geoelectric contour section along profile CD

KASHIM IBRAHIM LIBRARY

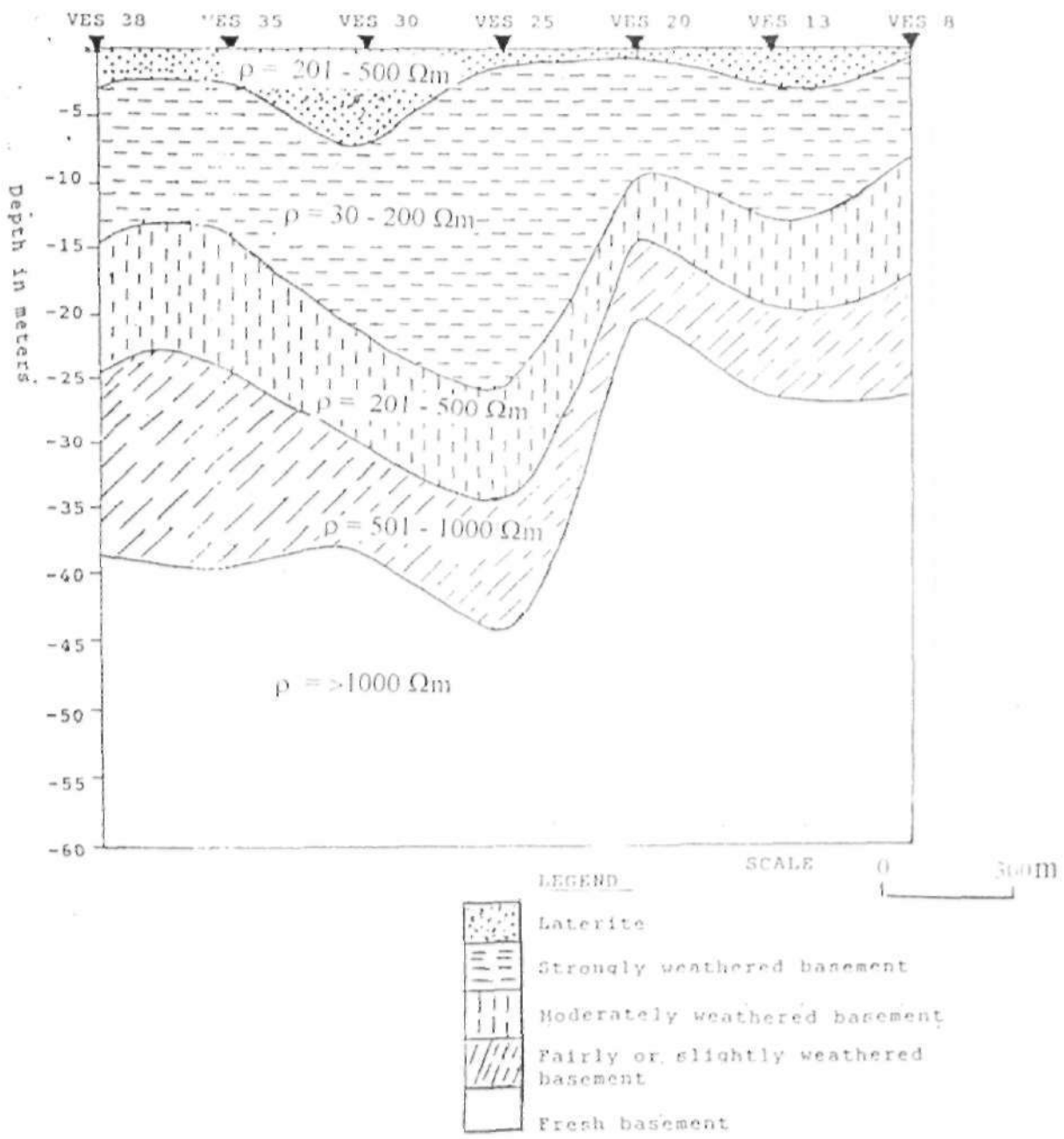


Fig. 5.19 Geologic section equivalent to geoelectric contour section along profile EF

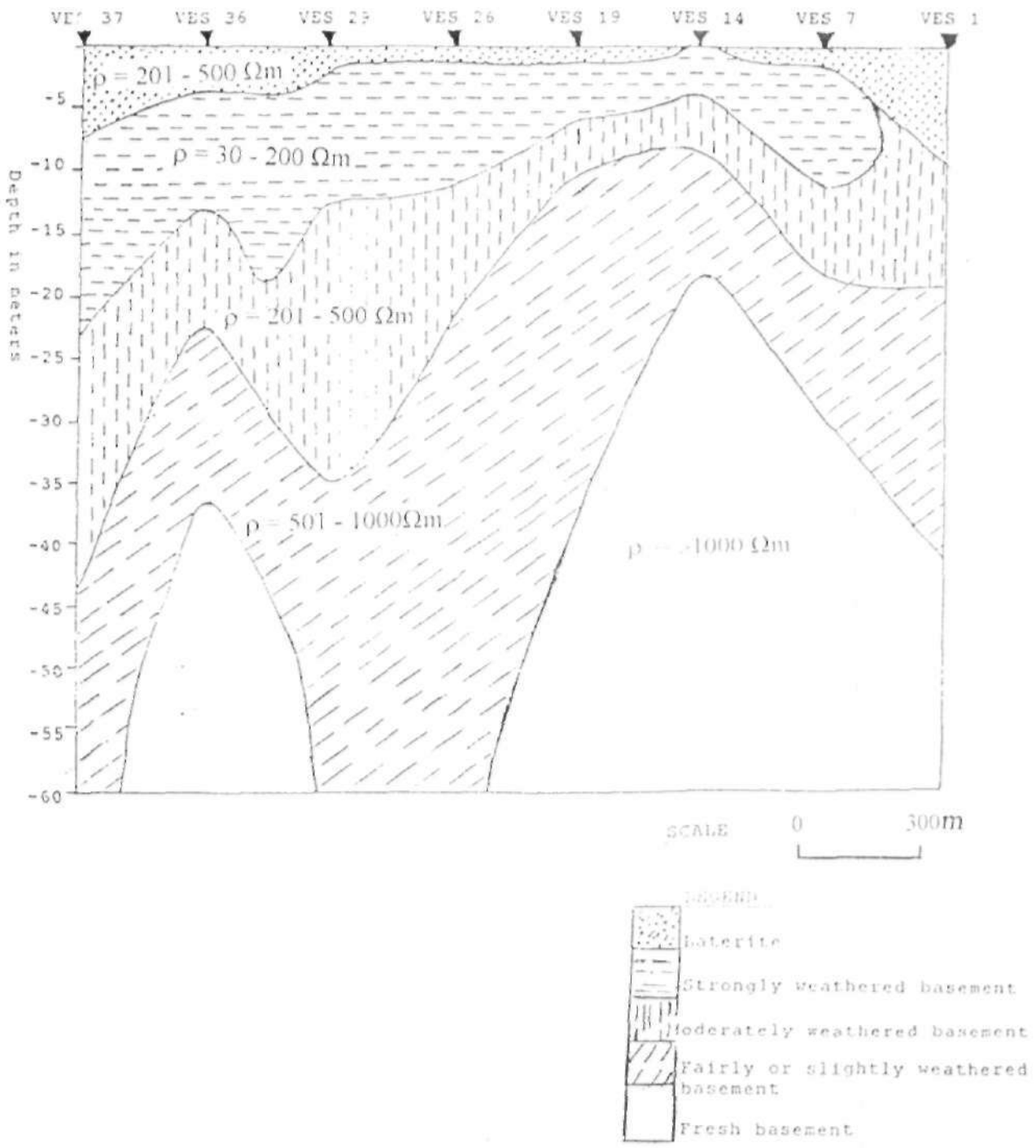


Fig. 5.20 Geologic section equivalent to geoelectric contour section along profile GH.

UNIVERSITY OF NAIROBI LIBRARY

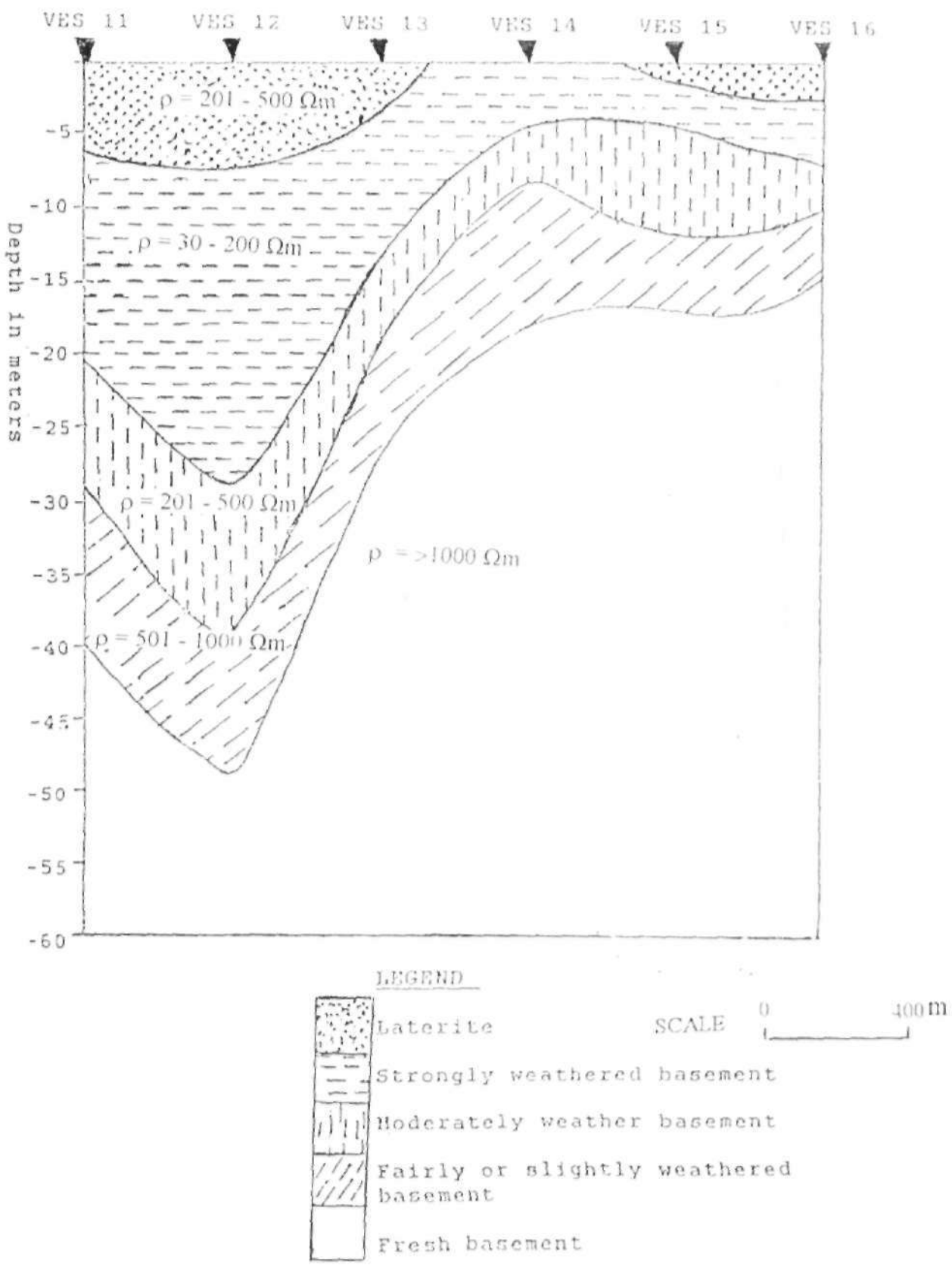


Fig. 5.21 Geologic section equivalent to geoelectric contour section along profile IJ.

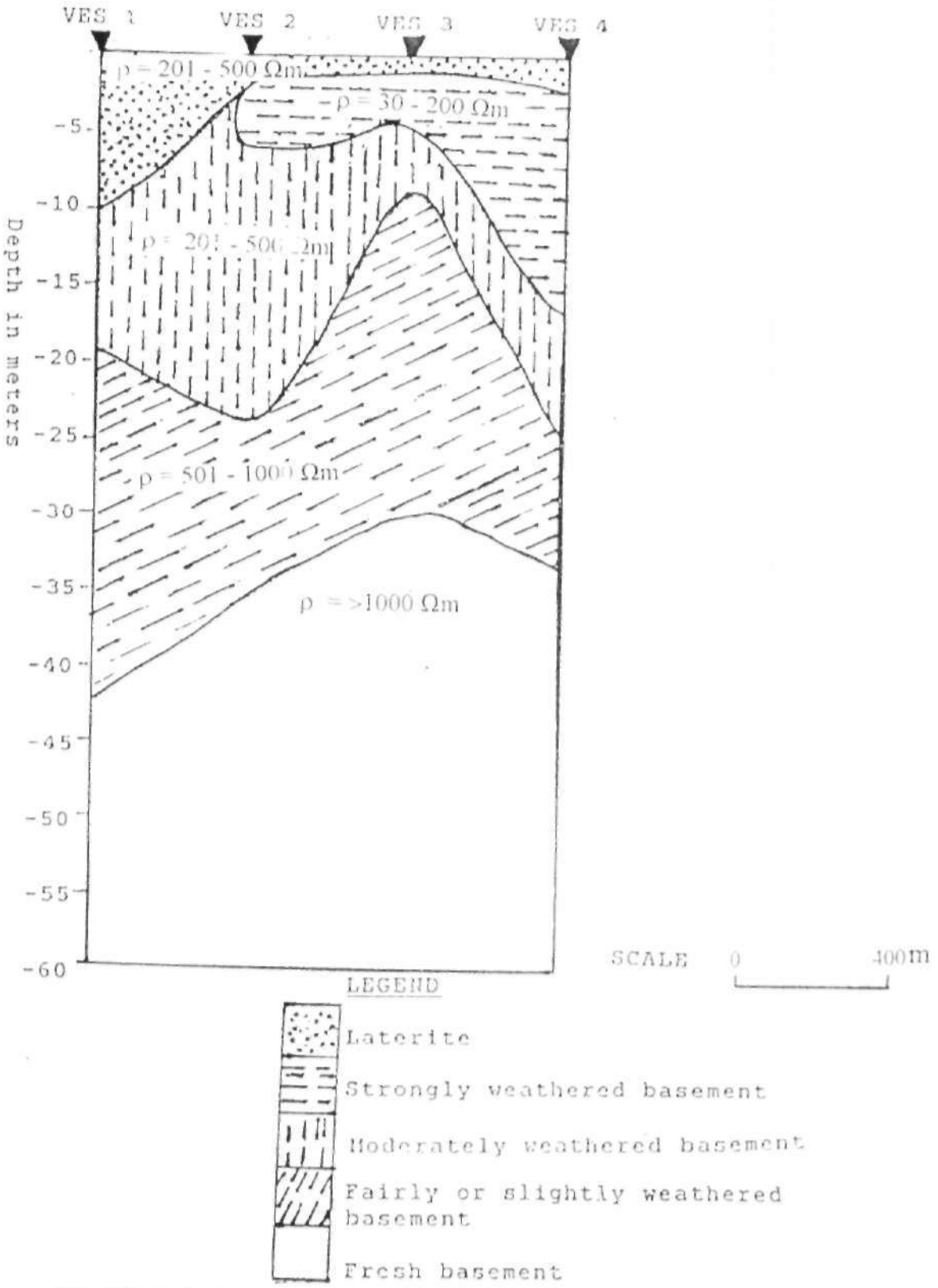


Fig. 5.22 Geologic section equivalent to geoelectric contour section along profile GL.

LIBRARY

thicknesses of the weathered profile needs to be taken into consideration. The depth to aquifer tends to trend westwards (Fig. 5.23).

5.4.2 **Aquifer Layer Thickness Map**

The map (Fig. 5.24) was produced from the thickness of the strongly weathered (low resistivity) layer which was obtained during the interpretation. The contour interval used for the weathered layer thickness in all the VES points is 2 m. The purpose of producing this map is to see how the aquifer layer varies in thickness within the subsurface of the survey area. The map shows that the thickness varies in thickness from 3 m to 23 m.

A general observation of the map reveals that areas of shallow basement correlate with areas of shallow thickness while areas with large aquifer thickness are seen generally to correlate with areas of basement depressions.

5.5 **Depth to Basement Map**

The depth to basement map Fig. 5.25 was obtained by contouring the depths to basement at all the sounding locations in the survey area. It shows the depth to basement at various points within the survey area. The basement represents regions of infinite resistivity (greater than 1000 ohm-m) as typical with the basement terrain of Africa and in particular Nigeria where it

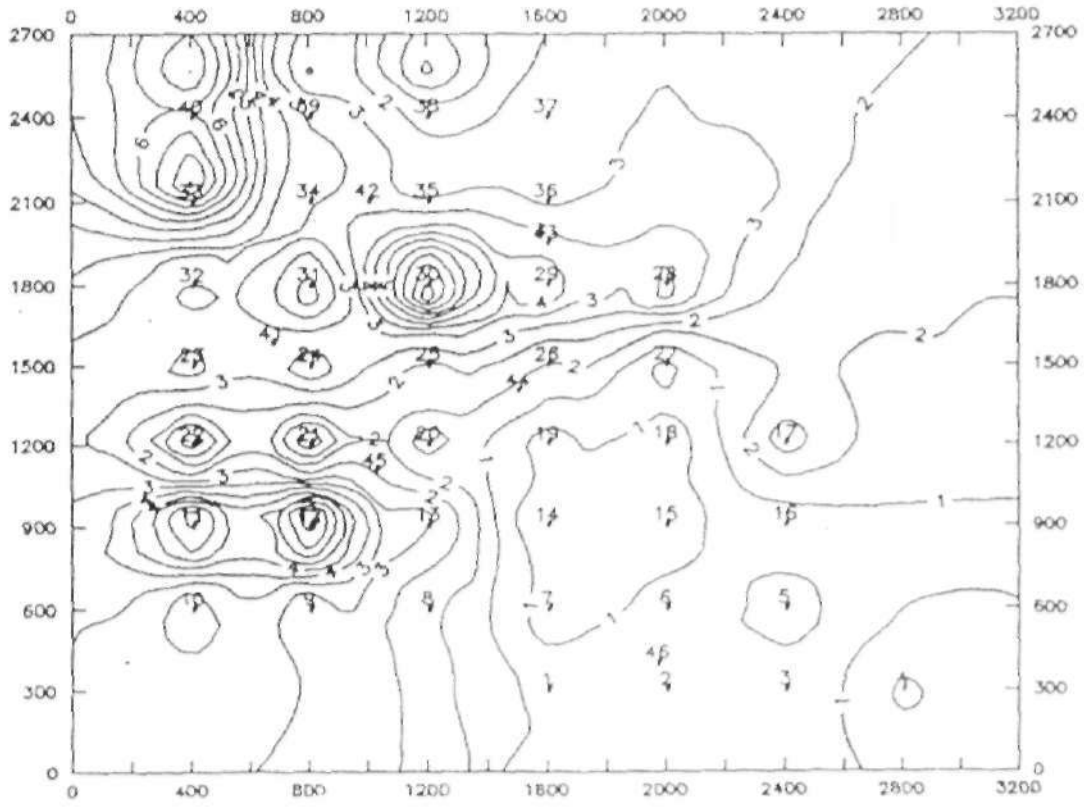


Fig. 5.23 Depth to aquifer contour map Contours at 1m interval

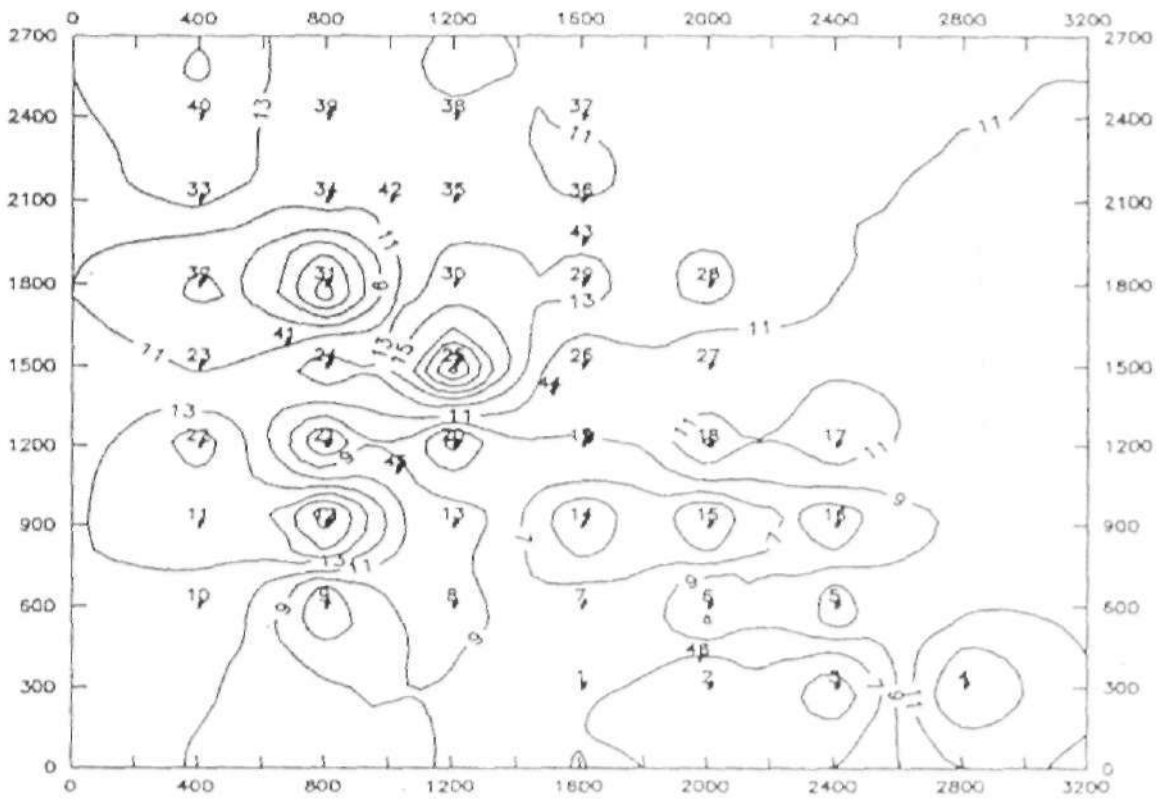


Fig 5.24 Aquifer thickness contour map

Contours at 2m interval

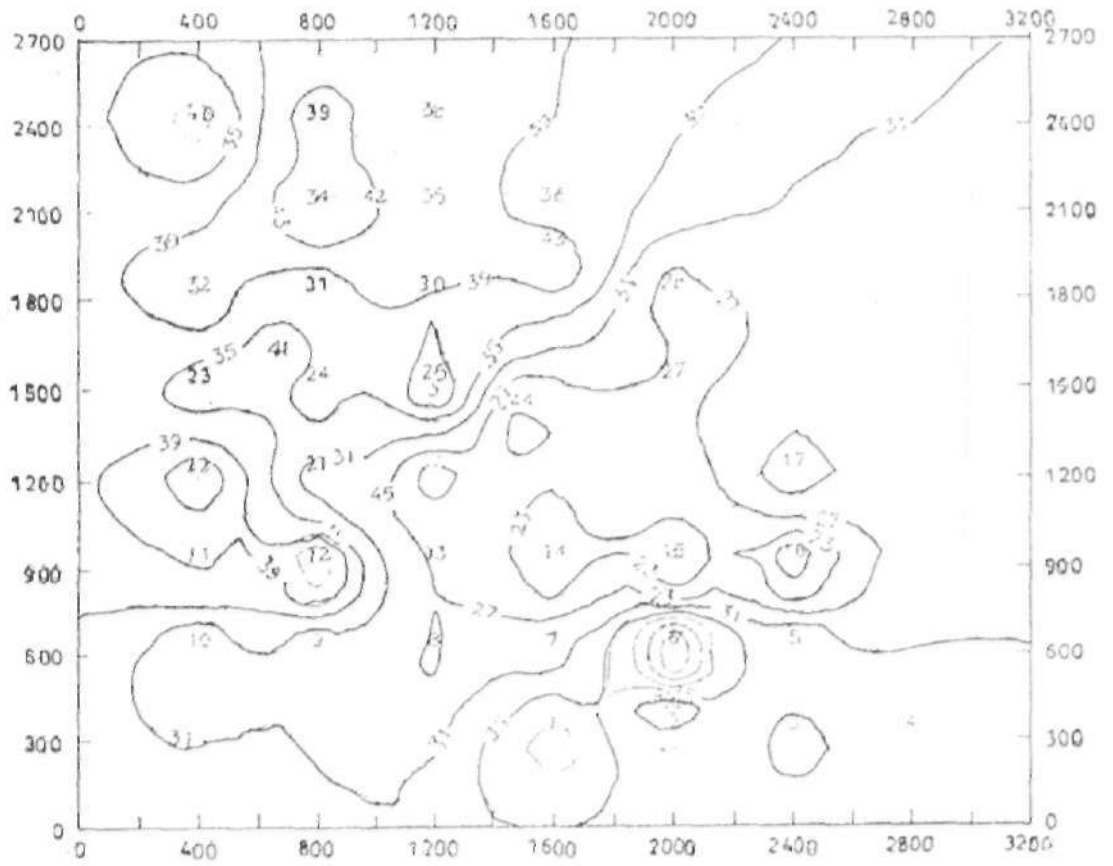


Fig. 5.25 Map of depth to fresh basement.

Contours at 4m interval

KACHERI IBRAHIM LIBRARY

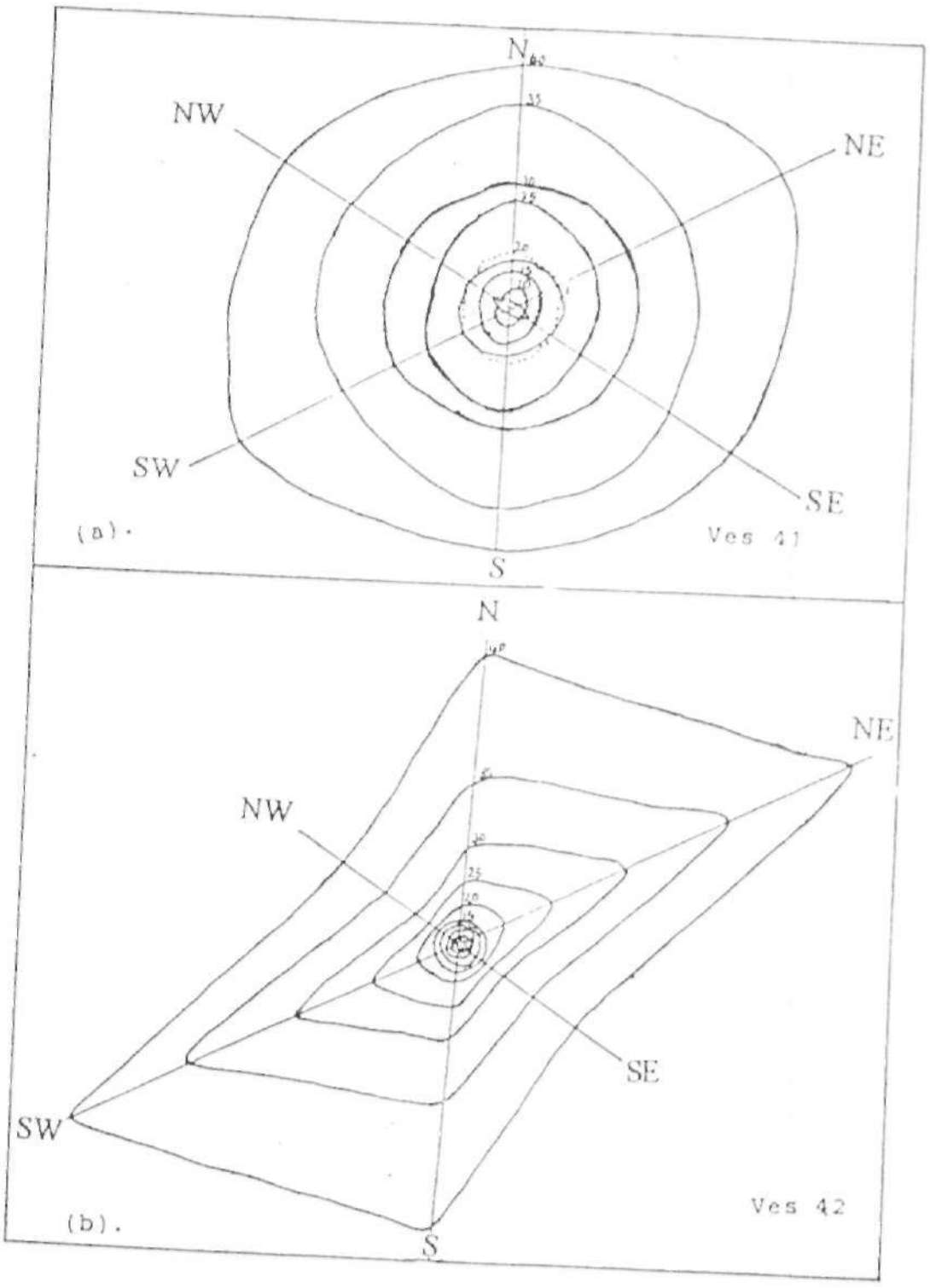
is shallow. The depth to fresh basement varies at different points within the survey area. Its minimum value is about 2 m and occurs at around VES 15. The average depth to basement is 33m, which falls within the range of the depths to basement with those that have carried out similar works within the basement complex of Nigeria.

The surface plot was made in order to have a visual understanding of the surface behavior or configuration of the basement. The plot Fig. 5.25 shows that the basement is an undulating surface.

5.6 AZIMUTHAL (RADIAL) SOUNDING

The patterns of resistivity anisotropy were obtained from the true resistivity values obtained from the interpreted depths and corresponding resistivities as a function of direction at each of the six radial sounding points (Fig. 5.26 and 5.27).

Fig. 5.26 (a). The patterns of resistivity anisotropy generally describes a sphere and this suggests that the medium at such depths is isotropic (the resistivities are not functions of direction). The minor variations from sphericity could be interpreted as being attributed to noise at these depths. In



Scale: 1:50 OHM-M

Fig. 5.26 Patterns of resistivity anisotropy map

(Radial soundings).

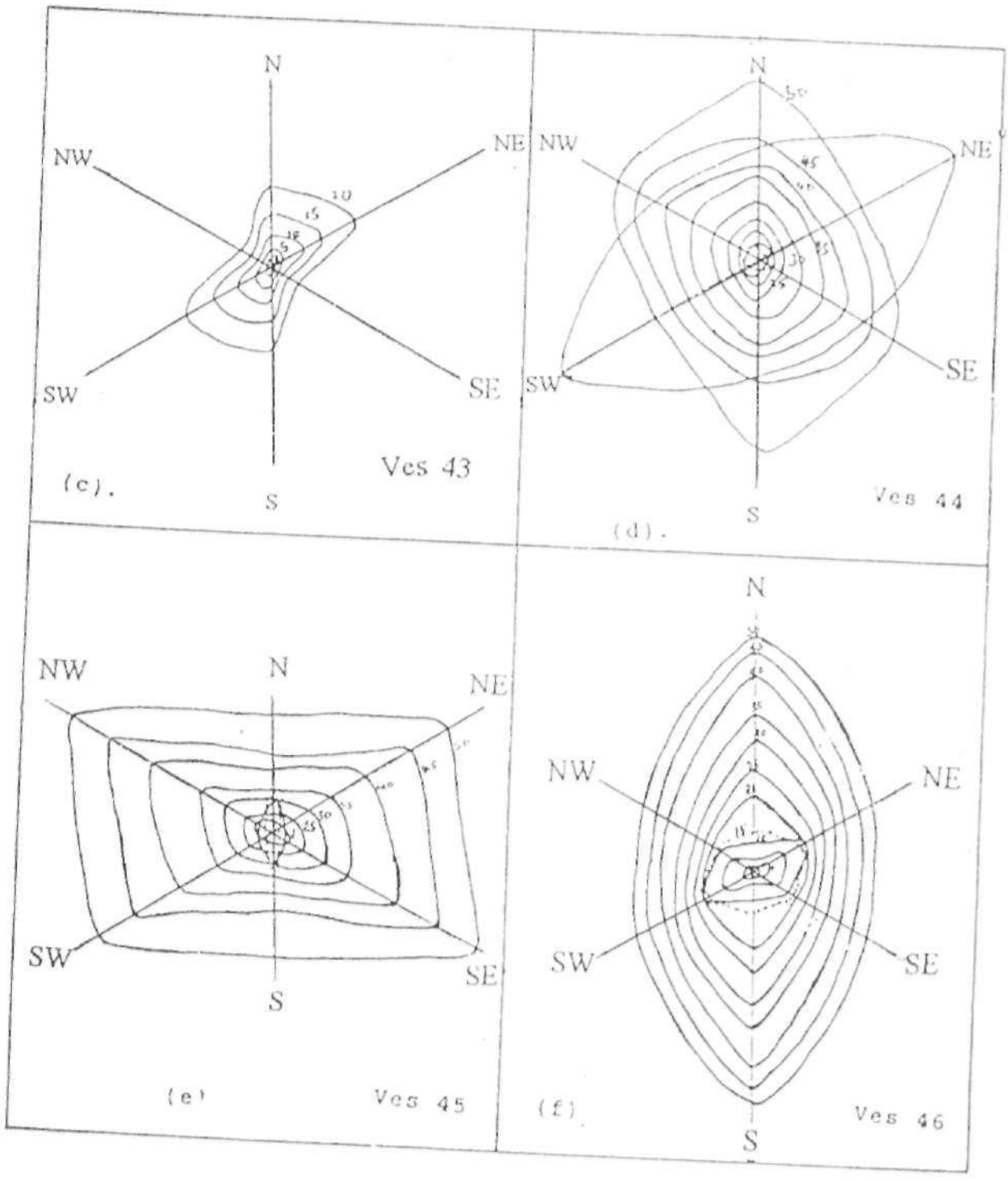


Fig. 5.27 Patterns of resistivity anisotropy map

(Radial sounding s.).

a wholly isotropic medium, as earlier mentioned, the pattern would be a sphere.

Fig. 5.26 (b). At depths of 15 m the subsurface is isotropic. It is anisotropic at depths of 20 m and beyond with the form of the patterns deviating more seriously from ellipcity at depths of 25m, 30m etc. These consistent departures could be due to the presence of fractures within the subsurface layers. The direction of the bedding plane is the SE - NW direction.

Fig. 5.27 (c). The subsurface is entirely anisotropic. The bedding plane is in the direction NW - SE. In general, fractures in the survey area occur at different depths and at defferent locations of investigation.

Fig. 5.27 (d). The bedding planes are in the direction NE-SW. The subsurface is entirely anisotropic.

Fig. 5.27 (e). As in d. above, the subsurface layers are entirely anisotropic with directions of bedding planes being N-S.

Fig. 5.27 (f). These patterns clearly show that the subsurface medium at that location is entirely anisotropic, except at a depth of 1m which is isotropic. The major axes of the ellipse represents the numerically the transverse resistivity, while the minor axis represents the longitudinal or horizontal resistivity and indicates the direction of the bedding plane at that depth. At a

depth of 3m, 5m, 10m, and 15m, the direction of the bedding plane is in the direction N-S, while at depths of 20m, 25m, 30m, 35m, 40m, 45m and 50m. it is in the E-W. One important deduction from these is that the bedding planes direction may differ at depths beneath a sounding location. In addition to these the subsurface layers are less resistive along the bedding plane implying that the conductivity is always higher in the bedding plane direction than in the transverse direction.

KASHIM IBRAHIM LIBRARY

CHAPTER SIX

CONCLUSION AND RECOMMENDATIONS

6.1 CONCLUSION

The major rock type in the survey area was found to be gneisses which where weathered to varying degrees. The sequences of weathering or the weathering profile is from top soil or lateritic soil underlain by a thin layer of clay, followed by strongly weathered basement gneisses, moderately weathered basement, slightly or finely weathered basement and finally, the fresh basement. The vertical electrical sounding curves depict the three layer to four layer cases of the h - type or a combination of both h - and k - types. Generally the average depth to basement in the area is 33m and this is shallow as is usual with basement terrains. The use of the n-layer multilayer models enables us to have an in depth investigation and exposure of the subsurface. The use of resistivity ranges and contour behavior make it easier to delineate the layer boundaries. The layers distinguished are as follows.

(1) Lateritic layer. This layer is considered to be composed mainly of laterite and underlain by a thin layer of clay. The layer varies in thickness within the survey area. At certain locations fresh laterites may be encountered due to their high consolidation.

(2) Strongly weathered layer: This highly weathered layer serves as a good reservoir for groundwater. The layer is of variable thickness as can be seen on the geologic sections taken along the profiles (Fig. 5.17 - 5.22) and the Map of aquifer thickness (Fig. 5.24). The locations with very thick aquifers are most suitable for sitting boreholes and this can easily be selected along any of the profiles. The resistivity range for this layer is between 30 ohm-m to 200 ohm-m.

(3) Moderately and slightly or finely weathered layer

These layers add to the groundwater potential as it can hold additional water. The layer also varies in thickness from location to location.

(4) Fresh basement. This is the impervious basal unit of infinite resistivity. The resistivity of this layer is greater than 1000 ohm-m. As earlier mentioned the average depth to this unit is 33m. It is noticeable that areas of shallow weathering thickness correspond to areas of shallow basement and conversely. It thus follows that depressions in the basement are groundwater collecting centers which are priority areas for groundwater development.

The patterns of anisotropy maps reveal that in the survey area the subsurface is generally anisotropic. This implies that the subsurface of the real earth is inhomogeneous. Also it shows that the direction of profiles of the vertical

KASHIM IBRAHIM LIBRARY

electrical soundings is important as the resistivity values beneath a given point may differ with direction. As a result, in any resistivity work (VES), radial soundings should precede the conventional soundings. This is necessary to choose the preferred direction of soundings to be employed and maintained throughout the survey. When this is done the data collected will be more reliable. The direction of profiling adopted for this is the NS.

6.2 RECOMMENDATIONS AND FUTURE WORK

In order to achieve a full exploitation of an area for groundwater potential, other geophysical techniques should be employed in conjunction with the geoelectric method. These methods include seismic refraction method and electromagnetic methods. Also the lateral resistivity variation (profiling) in the in the geoelectric method should be used to detect fracture zones within the area. When these methods are employed, it would be easier to demarcate the different subsurface layers, structures and fracture zones. The following are the recommendations:

(1). Two sites are strongly recommended for groundwater boreholes. These are at VES 12 and VES 25 (Fig. 5.19 and 5.21), with VES 12, having a higher groundwater potential. It should be noted that there are other

recommendable groundwater locations along the geologic sections (Fig. 5.17, and Fig. 5.20) and their choice may depend on the users interest or demand. The boreholes should be drilled to the finely weathered basement. For example, in VES 12 the borehole should be drilled to a depth of 45m (Fig. 5.19, and Fig. 5.21) while for VES 25 a depth of 40m is recommended.

(2). The boreholes should be properly logged both geophysical and geologically. This would make it possible to check and compare with other VES results. Aquifers must be properly screened to achieve maximum yield.

(3). To avoid the contamination of boreholes in the course of exploitation care must be taken as pollutants from the surrounding may be drawn from long distance recharge due to excessive pumping. The boreholes should be grouted (cement seal) to the depth of at least 7.0m to prevent contamination from septic tanks, surface drainage, lateritic covers and other sources of pollution.

(4). The shallow hand dug well around the engineering complex whose water usually turns milky when it is almost dry could be due to the presence of soluble minerals veins that cut across the well. These could be kaoline, carbonate, etc. It is therefore advisable to increase the depth of the well so as to avoid the mineral vein path.

LIBRARY

REFERENCES

Akpoborie, I. A., 1972, Hydrogeological control of the structures along Samaru Creek: B.Sc. thesis Geology department, Ahmadu Bello university, Zaria.

Anderson, W. L., 1979, Programme MARQDCLAG, Marquardt inversion of D.C. Schlumberger Soundings by lagged – Convolution: U.S. Geological Survey open file rep. 79-1432, 58.

Busby, J. P., 2000, The effectiveness of azimuthally apparent- resistivity measurement as a method for determining fracture strike direction: Geophysical prospecting, 48, 677 – 693.

Cagniard, L., 1959, Abaque pour sondages electriques sur glace: Annal. De Geophys., 15,561 – 563.

Carlson, D. A., Talor, R. W. and Cherkauer, D.S., 1996(a), Azimuthal resistivity as a tool for determination of the orientation of preferred hydraulic transmissivity for a dolomite aquifer in south western Wisconsin: SAGEEP 1996 Conference, Environ. Eng. Geophys. Soc. Proceedings, 1085 – 1094.

(b), Use of azimuthally electrical resistivity method used for determining joint orientations in glacial tills around milwaukee, wisconsin: SAGEEP 1996 Conference, Environ. Eng.Geophys. Soc. Proceedings, 51 – 59.

Chapman, M. J. and Lane, J.W., 1996, Use of directional bore hole radar and azimuthally square – array D. C. resistivity methods to characterize a crystalline – bedrock aquifer: SAGEEP 1996 Conference, Environ. Eng.Geophys. Soc. Proceedings, 833 – 842.

Davis, S.N., and Dewiest, R.J.M, 1966, Hydrogeology:, J. Wiley and sons, Inc. New York.

Deppermann, K., 1954, Die Abhangigkeit des Scheinbaren Widerstandes von Sondenabstand bei der Veirpunkt-Method: Geophys. Prosp., 2, 262-273.

Ghosh, D. P., (1971), The application of linear filter theory to the direct interpretation of geoelectrical resistivity sounding measurements: Geophy. prosp. 19, 192 - 217.

Hansen, B. P. Lane, J. W., 1996, Orientation and characteristic of fractures in crystalline bedrock determined by surface and bore hole geophysical surveys, Millville and Uxbridge, Massachusetts: SAGEEP 1996 Conference, Environ. Eng. Geophys. Soc. Proceedings, 927 – 940.

Ibisam, C., 1997, Geophysical report for groundwater at the temporary site of the Federal polytechnic Nasarawa. Ibisam Nigeria Limited, Keffi, Nigeria.

Kalenov, E.N., 1958, Application of electrical prospecting in permafrost conditions (in Russian): Razved. i promyslov Geofiz., 23, 44 – 57.

Keller, G.V. and Frischknecht, F.C., 1970, Electrical methods in geophysical prospecting. Oxford. Pergamon Press.

Kollert, R., 1969, Groundwater exploration by the electrical resistivity method. Memorandum 3/69 Atlas Copco Abem AB, S – 121 20 Bromma 20, Sweden.

Koefoed, O., 1969, An analysis of equivalence in resistivity sounding. Geophys. Pros. Vol.17, No.3 P.327-335

Koefoed, O., 1979, Geosounding principles, 1, restivity sounding measurements, Methods in Geochemistry and Geophysics: Else-vier.

Kunetz, G., 1966. Principles of direct current resistivity prospecting: Berlin, Gebruder Borntrager.

Kunetz, G., and Rocroi, P. J., 1970, Traitment automatique des sondages electrique: Geophys.Prosp., 18, 157-198.

Lane, j. W., Haeni, F. P., and Watson, W. M., 1995, Use of a square – array direct- current resistivity method to detect fractures in crystalline bed rock in New Hamspshere: Ground Water, v. 33, no. 3, p. 476 – 485.

Lane, j. W., Haeni, F. P., Soloyanis, S., Placzek, G., Williams, J.H., Johnson, C.D., Muursink, M. L., Joesten, P. K. and Knutson, K.D., 1996, Geophysical characterization of a fracture – recovery trench: SAGEEP 1996 Conference, Environ. Eng. Geophys. Soc. Proceedings, 427 – 441.

Mundry, E., 1980, The effect of a finite distance between potential electrodes on Schlumberger resistivity measurements – A simple correction graph: Geophysics, 45, 1969 – 1875.

Orellana, E., and Mooney, H. M., 1966. Master tables and curves for vertical electrical sounding over layered structures: Madrid. Intereciencia.

Oyawoye, M. O., (1964).. Geology of the Nigerian basement complex. Journal of Nigerian Mining, Geological and Metallurgical Society, vol. 1, 87 - 102.

Parasnis, D.S, 1979, Mining Geophysics; Amsterdan, Elsevier.

Pekeris, C. L., (1940). Direct method of interpretation in resistivity prospecting: Geophysics 5, 31 - 46.

Preez, D. and Barber, W. 1965, the distribution and chemical quality of ground water in Northern Nigeria. Geological survey of Nigeria. Bulletin, 36,67.

Strakhov, V. N., and Karelina, G. N., 1969 On the intepretation of vertical electrical sounding data with an electronic calculating machine (in Russian): Prikladnaya Geofiz., 56, 118-129

Telford, W.M., Geldart L.P. Sheriff, R.E. , Keys, D.A., 1976. Applied geophysics, Cambridge Univ. Press. . London.

Todd, D. K., 1959. Groudwater hydrology. John wiley. London.

Vingoe, P, 1972, Electrical resistivity Surveying: Geophysics Memorandum 5/72 Atlas copco-Abem AB, 5-121 20 Bromma 20, Sweden.

Wienbenga, W. A., 1955, Geophysical Investigation of water deposits. Western Australia Canberra, Bureau for Mineral Resources. Geol. And geophysics. Bull. No. 30, p. 1 - 48.

Worthinton, P. F., (June, 1977). Geophysical investigation of groundwater resources in the Kalahari Basin.

Worthinton, P. F., 1975. Quantitative investigations of granular aquifers: Geophys. Surv., v 2, p. 313 - 366.

Wright, E. P. and Burgess, W. G. , 1992. Hydrogeology of Crystalline Basement Aquifers in Africa. Geological Society Special Publication No 66.

Zohdy, A. A. R., Anderson, L.A., and Muffler, L.P.J., 1973. Resistivity, self geothermal system: Geophysics, 38, 1130 – 1144.

Zohdy, A. A. R, Eaton, G. P., and Mabey, D. R., (1974). Application of surface geophysics to groundwater investigation: Tech. of water - resources investigations of the U. S. Geol. Surv., Book 2, chap. D1.

Zohdy, A. A. R., and Stanley, W.D., 1973. Preliminary interpretation of electrical sounding curves obtained across the Snake River Plain from Blackfoot to Arco, Idaho: U.S. Geol. Sur. Open file rep. 20.

Zohdy, A. A. R., (1974). Electrical methods. In application of surface geophysics to groundwater investigations technique of the United States Geological survey. Book 2, Chapter D1, pp 47 - 55.

Zohdy, A. A. R., (1975). An automatic intepretation of schlumberger sounding curves using Dar Zarouk functions: U. S. Geol. Surv. Bull. 1313 - E, 39.

Zohdy, A. A. R., (1989). A new method for the automatic intepretation of schlumberger and Wenner sounding curves: Geophysics, vol. 54, No. 2, pp 245 - 253.

Appendix: C

Iso resistivity contour data

	Depth								
VES	Surface	5m	10m	15m	20m	25m	30m	35m	40m
					ρ(Ωm)				
1	305	801	448	450	510	600	1610	1050	917
2	450	224	250	315	400	750	930	450	2000
3	345	241	500	620	690	671	900	810	1100
4	1000	153	120	178	290	361	603	718	1764
5	545	56	100	220	380	600	782	410	840
6	645	184	305	340	345	450	1113	1050	1871
7	540	62	152	345	510	710	2013	1600	2000
8	40	247	200	390	660	1030	1300	1815	2360
9	168	100	148	250	500	650	967	1645	1500
10	120	76	148	295	690	72	1117	1810	2610
11	136	300	100	100	200	251	250	814	975
12	110	31	150	150	150	300	345	600	1000
13	350	104	150	295	600	900	1500	2450	2350
14	110	300	550	770	1200	1750	2250	2850	3800
15	275	300	400	700	1500	2750	3500	5460	8500
16	1030	163	320	705	850	163	1261	750	517
17	149	71	130	236	290	450	500	600	1000
18	350	190	236	260	291	450	2760	450	500
19	300	161	450	130	600	161	561	2032	3150
20	245	67	250	526	1000	1300	1115	1550	2120
21	135	65	110	260	450	750	481	551	890
22	352	76	150	200	170	200	901	1233	1210
23	450	64	100	230	328	300	545	316	1751
24	218	62	80	150	250	450	481	473	953
25	300	72	570	70	100	172	981	945	870
26	560	131	190	310	420	843	220	1540	2100
27	358	50	200	375	640	300	1161	1640	1763
28	1010	57	150	440	700	442	486	1440	1114
29	600	237	165	236	300	313	623	480	1200
30	1200	122	150	150	175	2171	350	813	1200
31	673	183	45	148	290	360	331	913	1780
32	3650	550	100	150	242	541	551	845	100
33	1540	285	150	150	280	450	523	415	871

34	500	143	150	148	265	351	473	465	735
35	600	58	145	250	350	544	561	841	931
36	750	376	110	75	180	260	544	700	967
37	600	67	130	170	185	315	533	781	1335
38	710	241	136	225	326	311	371	700	500
39	601	73	184	290	300	300	861	1213	783
40	900	237	190	328	490	323	541	388	1134
41	286	60	100	250	300	60	342	500	700
42	310	210	120	110	200	1110	250	1320	1205
43	546	60	100	170	285	815	1115	2000	1667
44	300	210	300	450	500	1110	350	1320	1205
45	150	300	300	375	550	815	1115	2000	1667
46	710	250	210	420	500	456	1113	450	2700

Depth

VES	45m	50m	55m	60m
		ρ(Ωm)		
1	1000	1600	4616	4000
2	3911	3500	2500	2915
3	1975	1145	400	5601
4	2415	3871	1731	3000
5	1800	1200	3200	2250
6	1755	2300	2100	3731
7	2500	3000	3335	4415
8	3350	4320	4325	5201
9	3916	4071	5710	6200
10	3710	5200	6305	3416
11	1500	2000	2500	3051
12	1500	2000	2400	7000
13	4000	6680	6730	4451
14	4700	4330	400	8000
15	8000	8000	8000	1633
16	1480	1131	1315	500
17	200	2700	3570	1500
18	500	1000	1000	500
19	500	500	501	500
20	5601	6000	6000	6000
21	3761	7000	3670	4210
22	1300	1630	1500	1500
23	1864	2650	3000	3500
24	1640	2880	3200	3647

25	943	1914	2320	2500
26	1750	1050	1000	1000
27	2500	3100	3500	4001
28	2345	2300	2650	3000
29	963	1050	1320	901
30	1454	2671	4000	4202
31	1750	2350	2210	3200
32	1225	1661	1700	1825
33	893	983	1000	1000
34	1345	1420	2001	2315
35	1100	1570	2000	1861
36	1328	1623	2000	2430
37	1000	1345	1500	1603
38	1320	781	1500	2000
39	681	1700	1761	1600
40	1350	1120	2000	1500
41	1124	8000	8000	2910
42	1200	1700	1900	1932
43	4520	1400	1500	2250
44	1200	2550	2401	1000
45	4520	6000	4600	5000
46	3600	2300	8000	6000

Appendix: D Aquifer depth contour data

VES No.	Depth (m)
1	5.3
2	6.2
3	4.4
4	14.3
5	12.0
6	10.2
7	9.0
8	9.3
9	6.5
10	14.0
11	19.0
12	19.0
13	10.0
14	3.5
15	3.5
16	10.1
17	12.4
18	12.4
19	9.0
20	5.0
21	7.0
22	11.0
23	11.0
24	13.0
25	23.0
26	10.0
27	10.4
28	8.3
29	13.8
30	13.7
31	3.0
32	7.0
33	13.0
34	10.4
35	10.6
36	11.0
37	11.8
38	10.6

39	10.5
40	13.6
41	11.0
42	10.3
43	11.3
44	10.5
45	9.0
46	7.0

Appendix: E Aquifer thickness data

VES No.	Thickness (m)
1	8
2	6
3	4
4	14
5	4
6	6
7	8
8	10
9	6
10	14
11	14
12	19
13	10
14	4
15	4
16	6
17	12
18	12
19	9
20	5
21	6
22	16
23	10
24	13
25	23
26	10
27	10
28	18
29	14
30	14
31	3
32	7
33	14
34	12
35	12
36	10
37	12
38	12
39	12

TD
403
099

RECEIVED
KASHIJI ...

A54

40	14
41	11
42	12
43	12
44	10
45	12
46	12



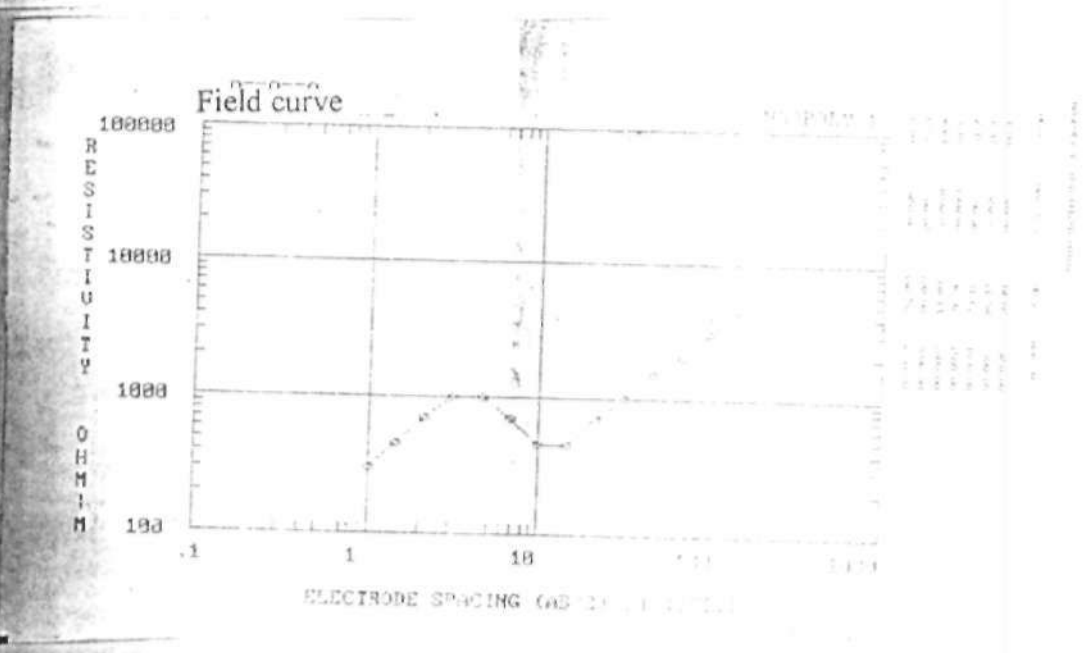
Appendix: F Depth to Basement contour data

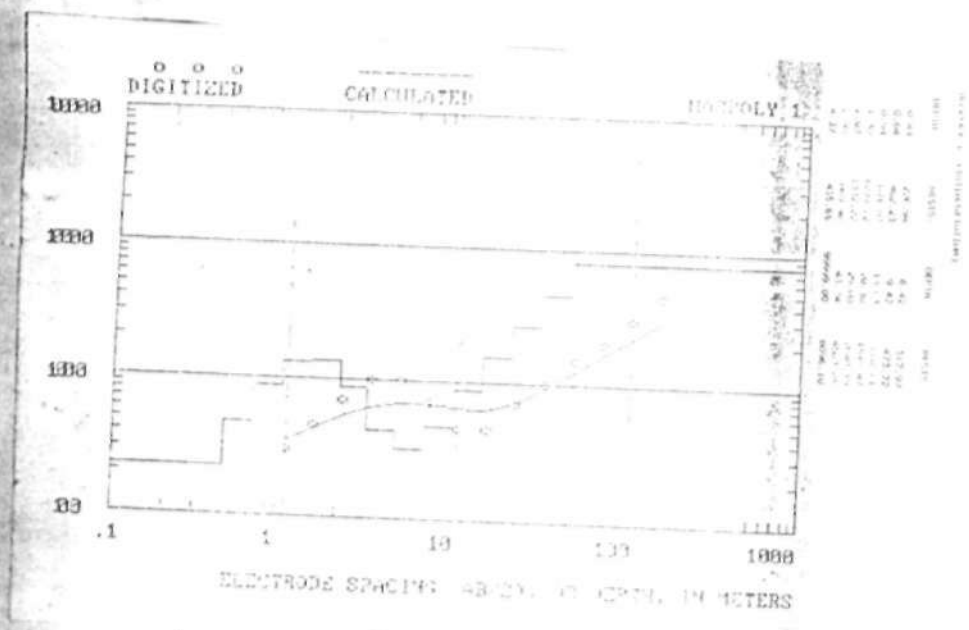
VES No.	DEPTH (meters)
1	35.5
2	29.5
3	33.6
4	35.0
5	57.3
6	30.3
7	26.2
8	27.3
9	26.4
10	39.8
11	48.9
12	26.6
13	18.2
14	17.3
15	26.8
16	34.1
17	50.1
18	30.6
19	20.0
20	28.6
21	47.3
22	32.0
23	38.4
24	44.2
25	50.3
26	26.6
27	24.8
28	53.9
29	38.5
30	36.0
31	42.2
32	50.3
33	48.1
34	39.5
35	40.2
36	41.9
37	38.8
38	45.1
39	29.2

40	31.0
41	36.0
42	43.0
43	39.0
44	25.0
45	27.0
46	49.0

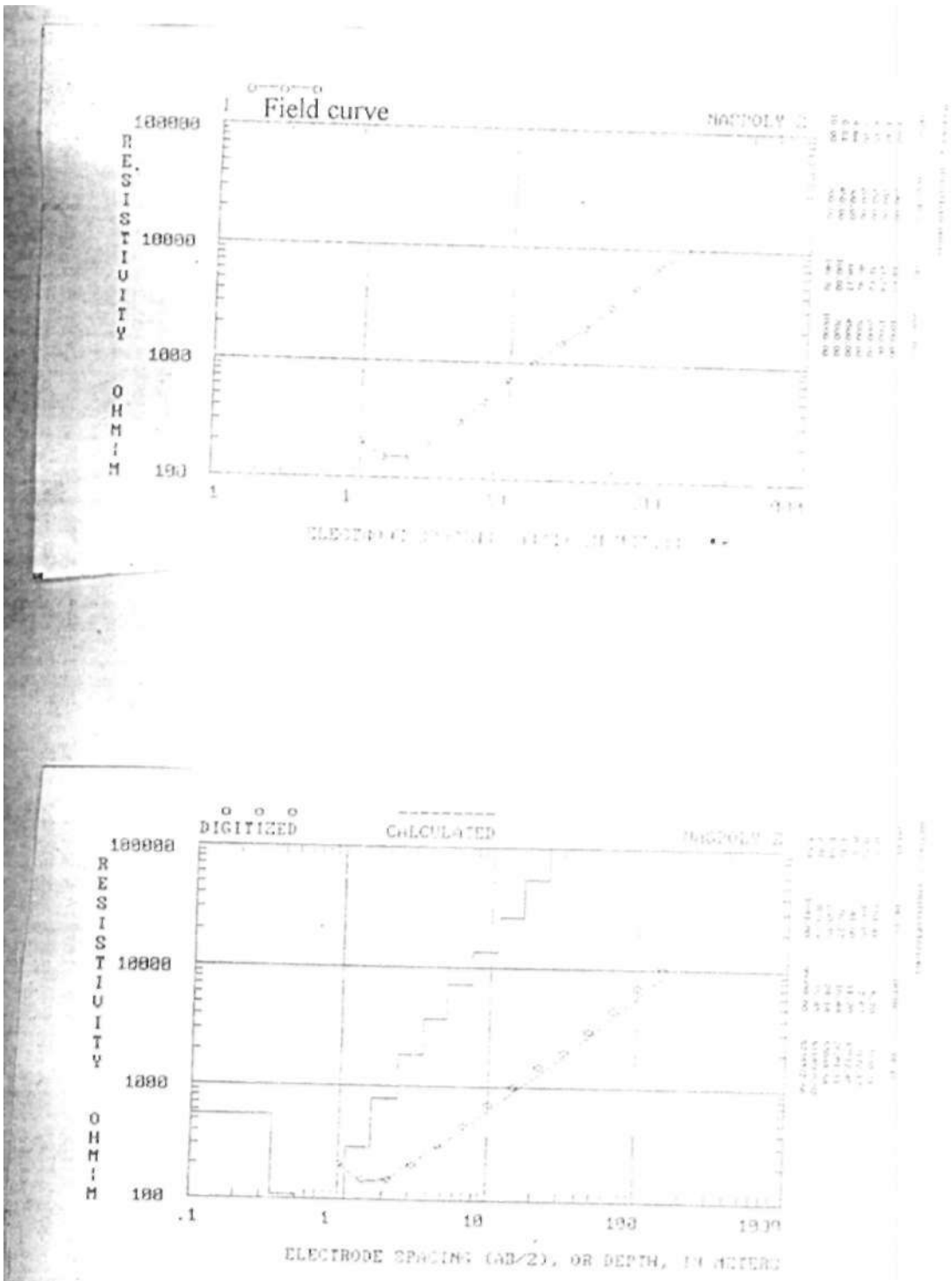
Appendix A:

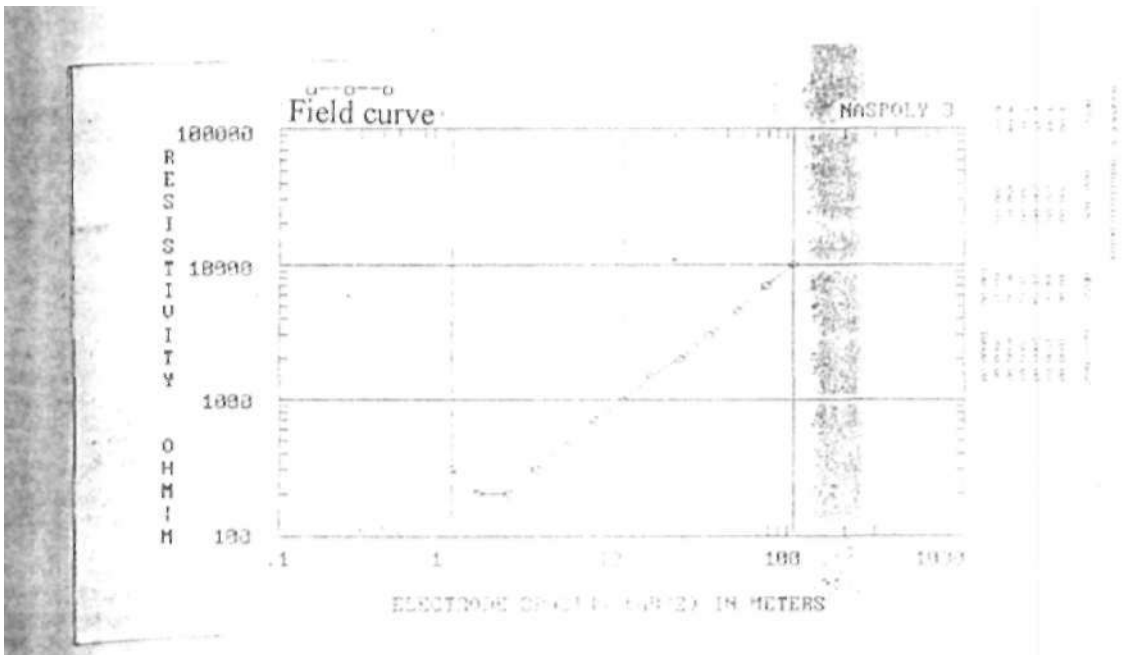
Field curves and Interpreted model layer curves

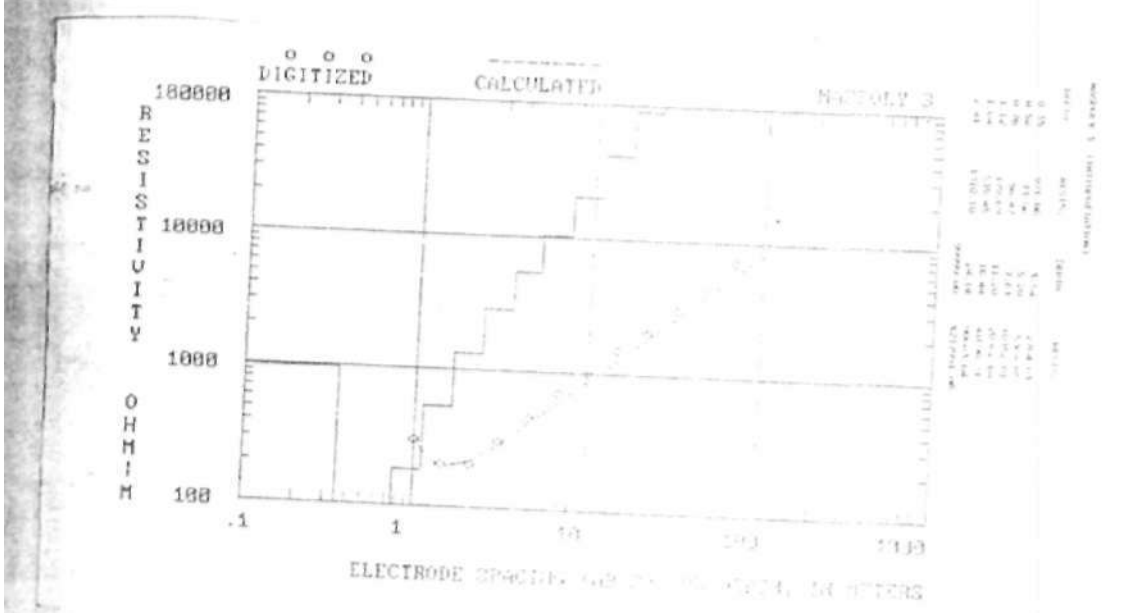


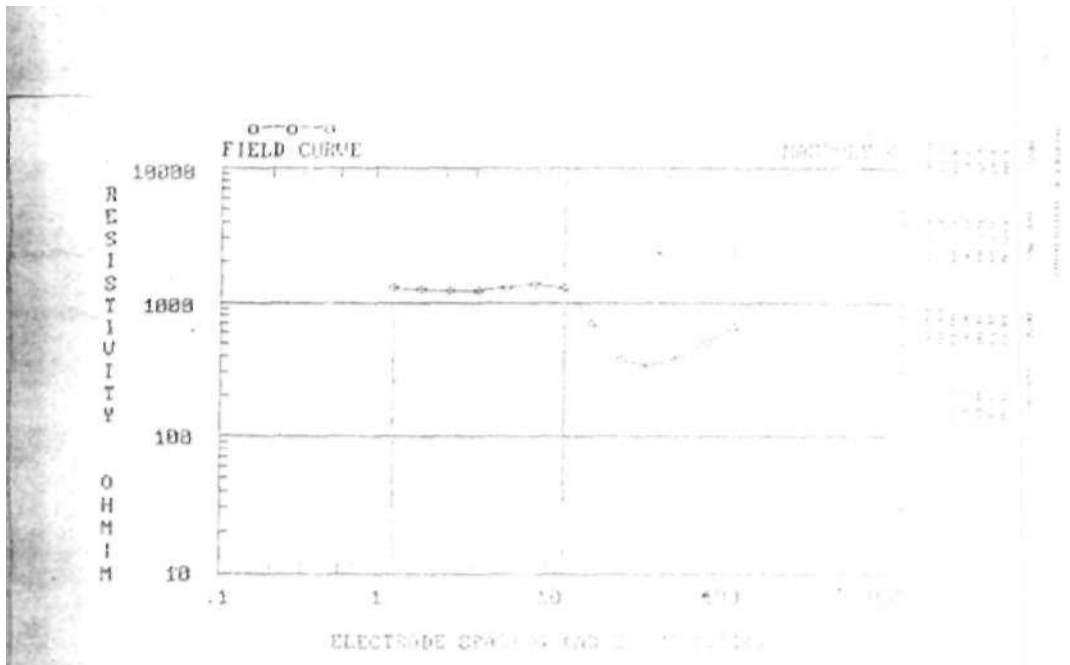


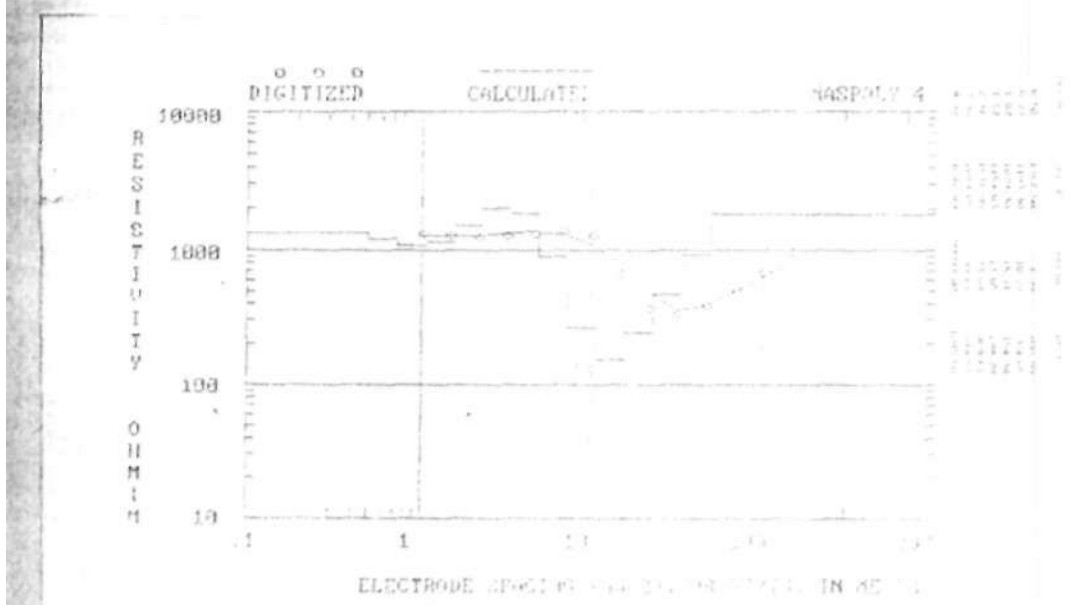
HASHIM IBRAHIM LIBRARY


Field curve
RESISTIVITY OHM-M
100000
10000
1000
100
1
ELECTRODE SPACING (AB/2), OR DEPTH, IN METERS
DIGITIZED
CALCULATED
.1
10
100

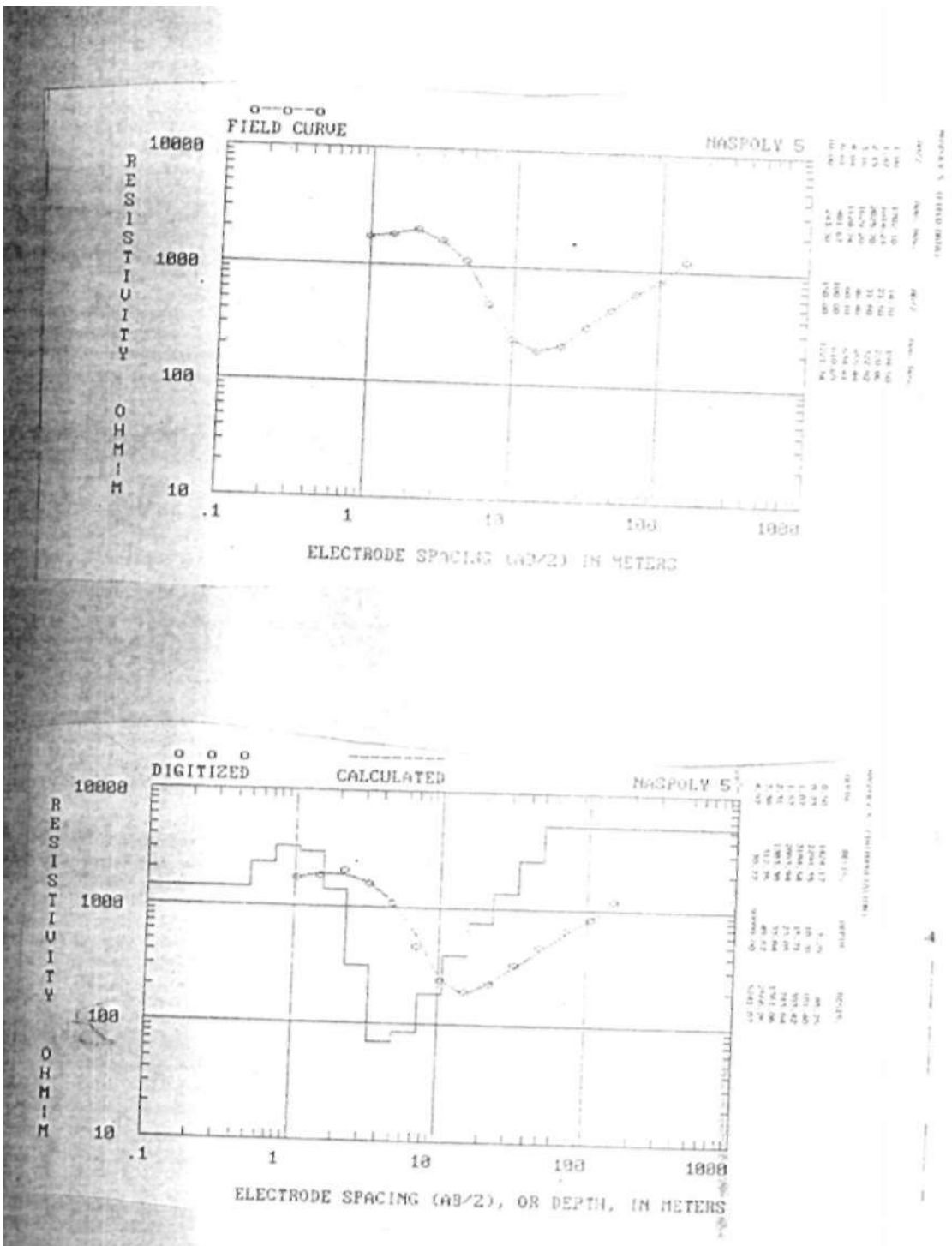

Field curve
NASPOLY 3
RESISTIVITY OHMIM
100000
10000
1000
100
.1
1
100

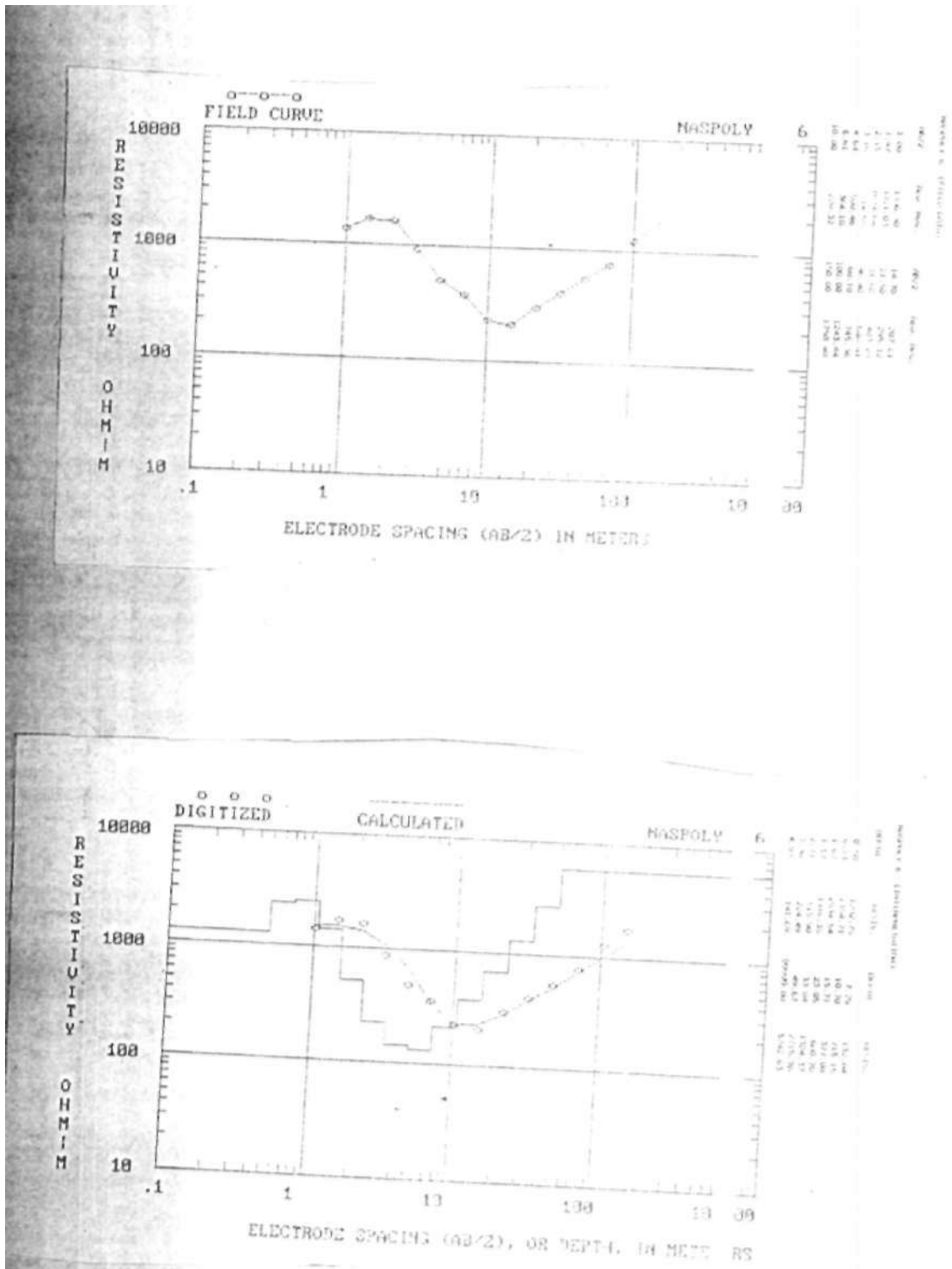

DIGITIZED
CALCULATED
RESISTIVITY OHMIM
100000
10000
1000
100
.1
1



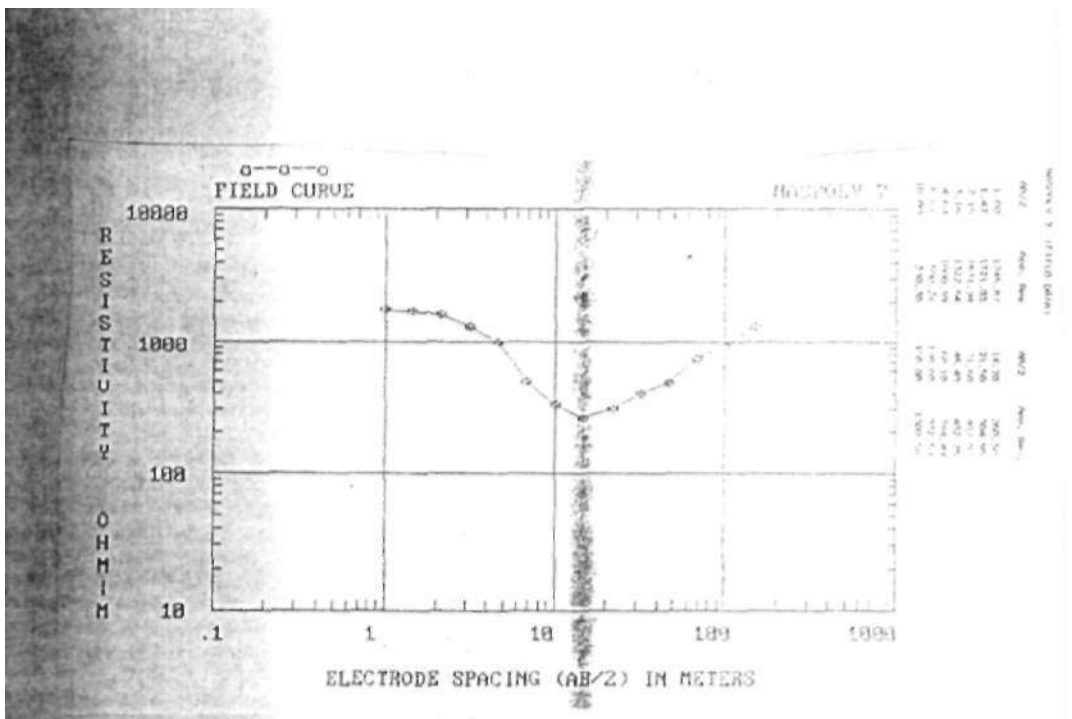


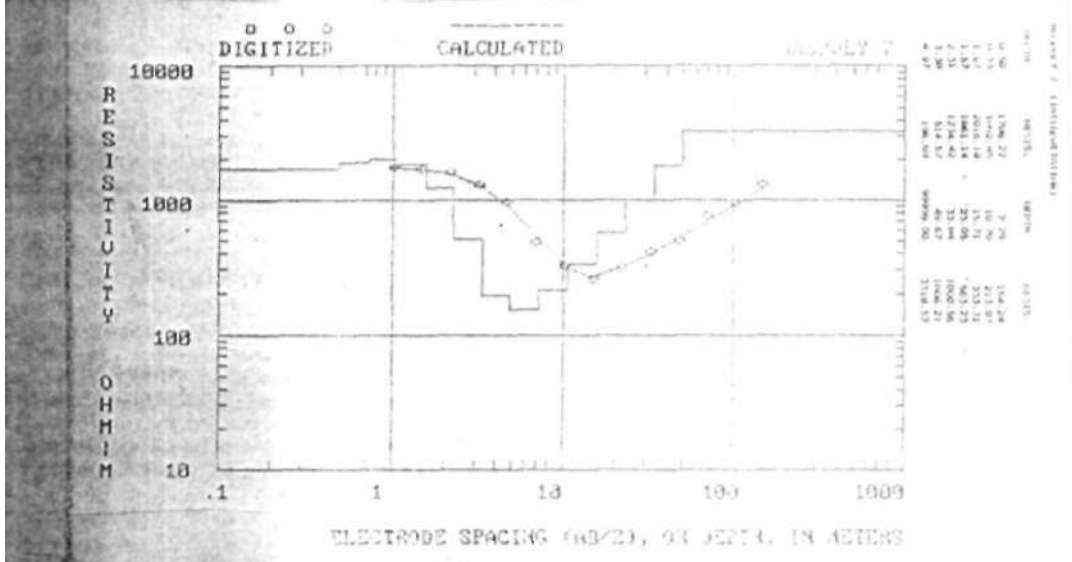
KASHIM IBRAHIM LIBRARY

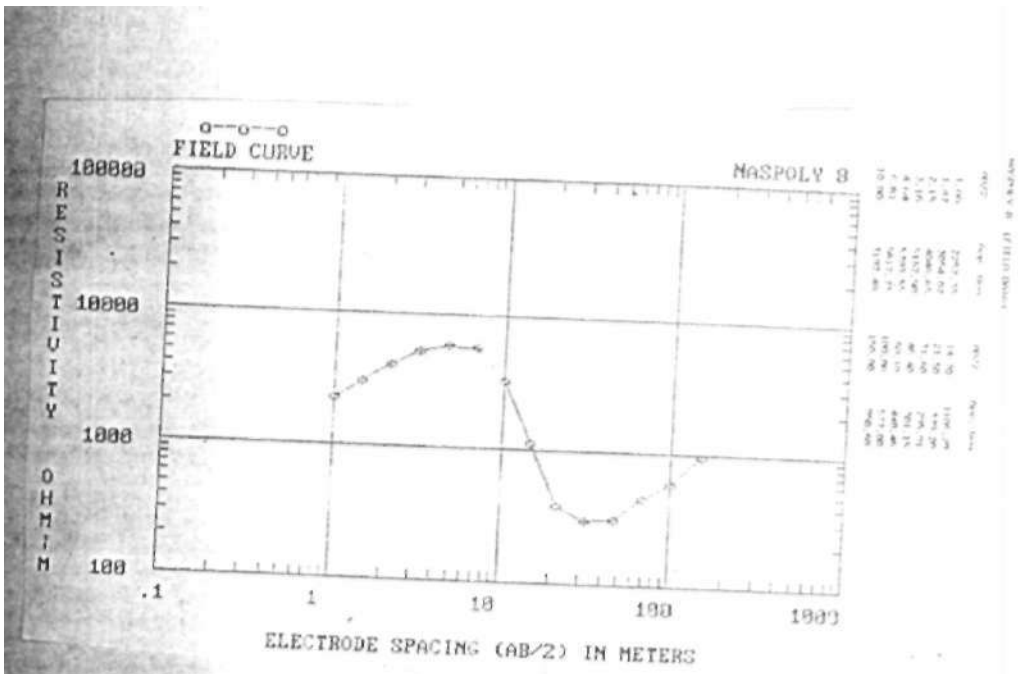

o--o--o
FIELD CURVE
MASPOLY 5
RESISTIVITY OHMIM
10000
1000
100
10
.1
1
10
100
1000
ELECTRODE SPACING (AB/2) IN METERS
o o o
DIGITIZED
CALCULATED
MASPOLY 5
RESISTIVITY OHMIM
10000
1000
100
10
.1
1
10
100
1000
ELECTRODE SPACING (AB/2), OR DEPTH, IN METERS

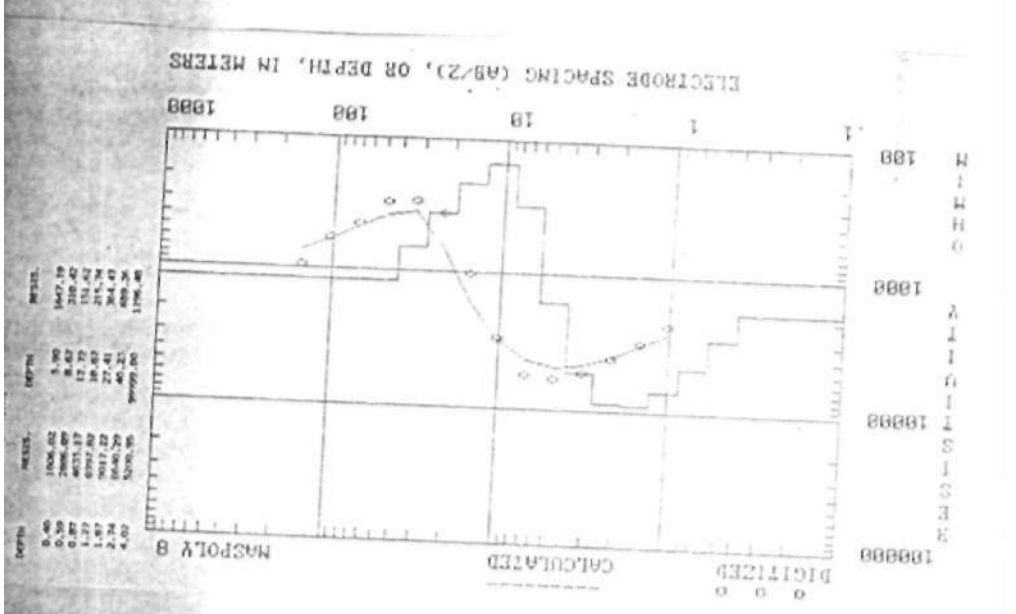


KASHIM IBRAHIM LIBRARY

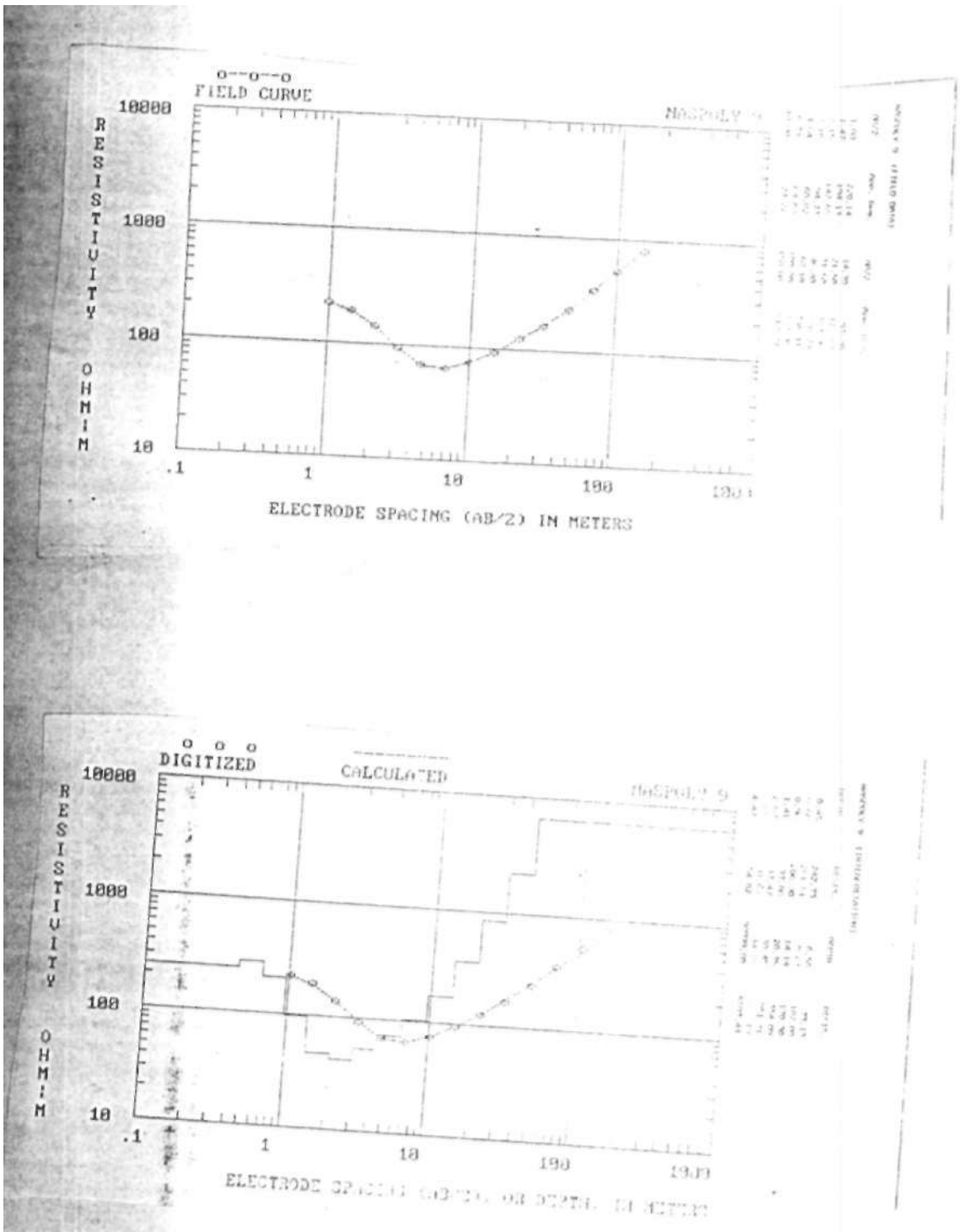

o--o--o
FIELD CURVE
RESISTIVITY OHMIM
10000
1000
100
10
.1
1
10
100
1000
ELECTRODE SPACING (AB/2) IN METERS

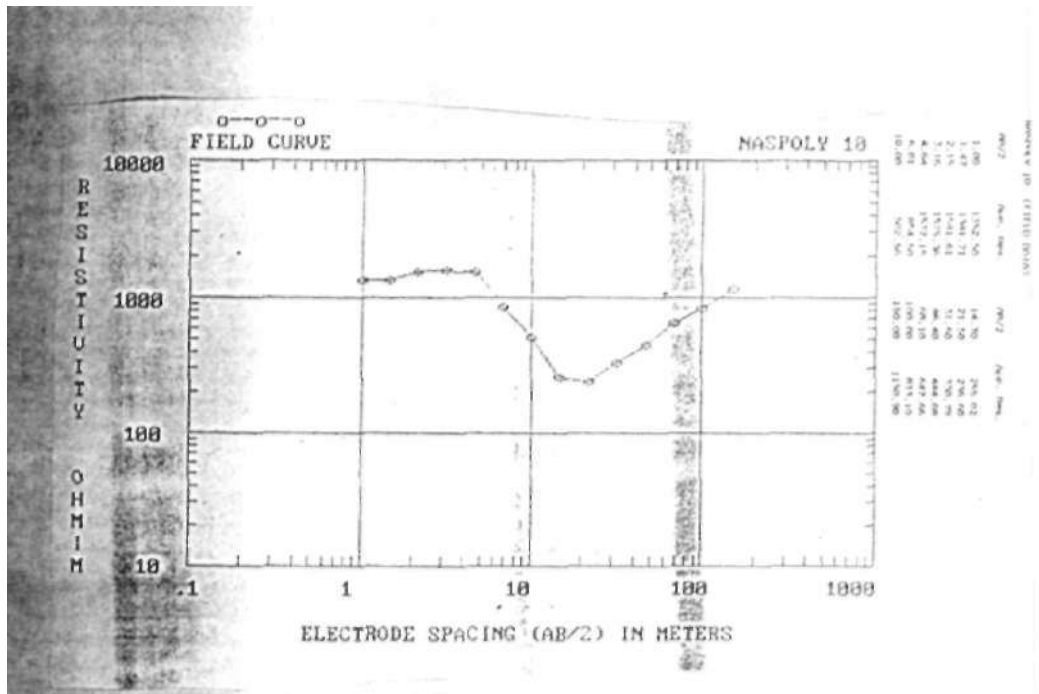

DIGITIZED
CALCULATED
RESISTIVITY OHMIM
10000
1000
100
10
.1
1
10
100
1000

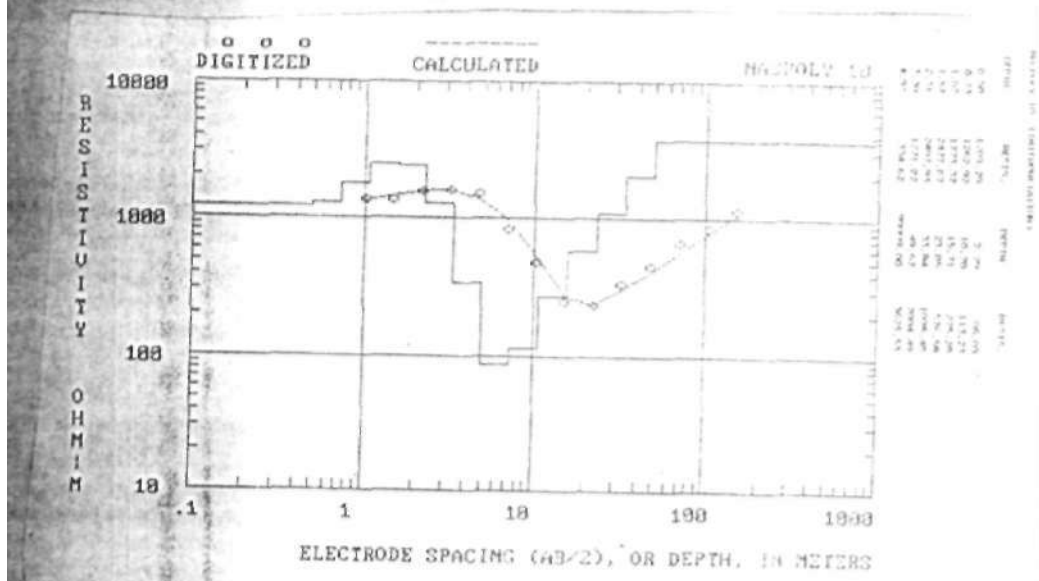




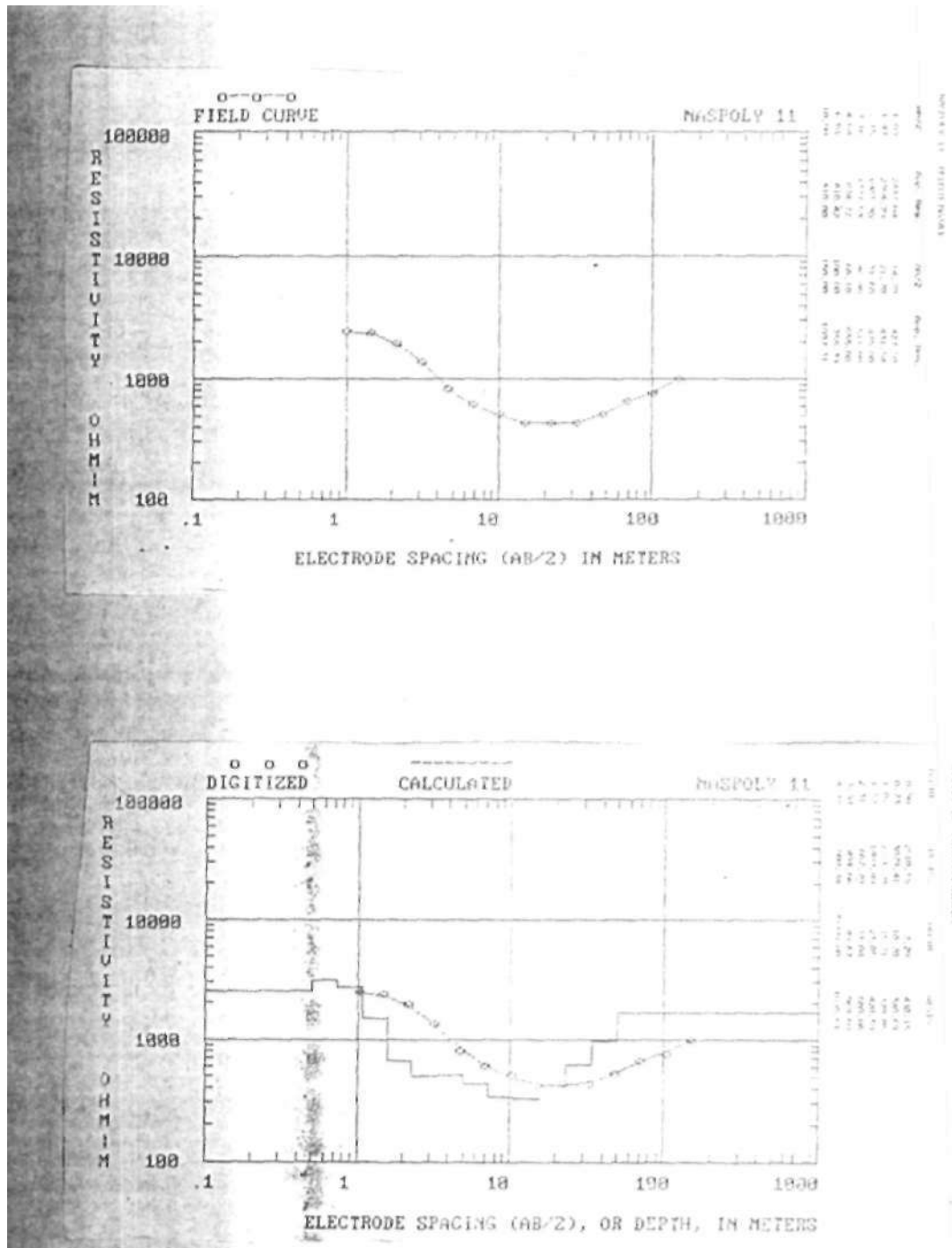
KASHIM IBRAHIM LIBRARY

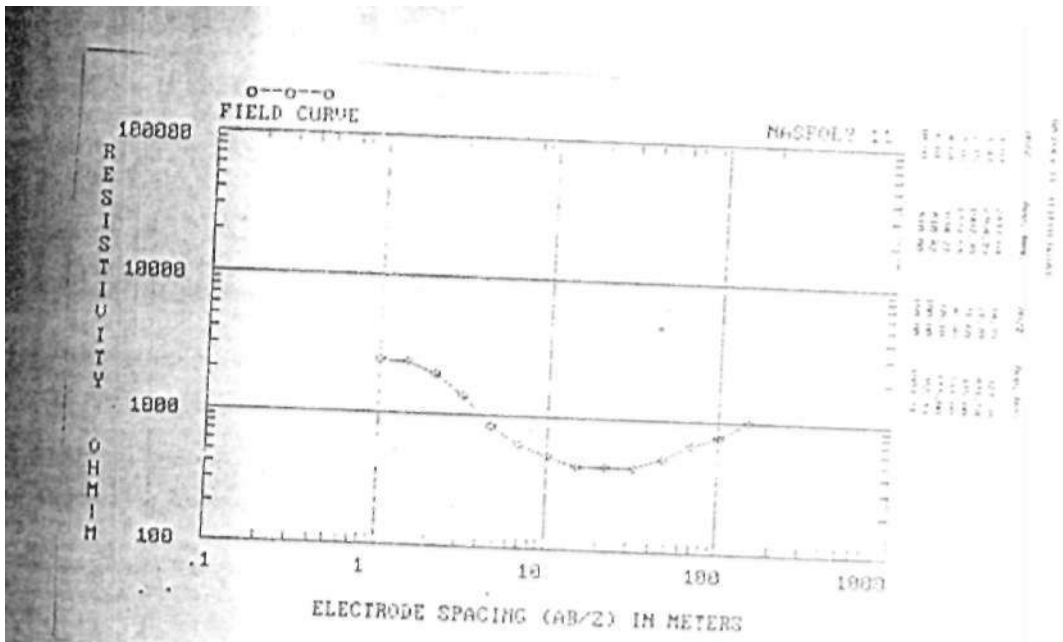

o--o--o
FIELD CURVE
RESISTIVITY OHMIM
10000
1000
100
10
.1
1
10
100
ELECTRODE SPACING (AB/2) IN METERS
o o o
DIGITIZED
CALCULATED
RESISTIVITY OHMIM
10000
1000
100
10
.1
1
10
100

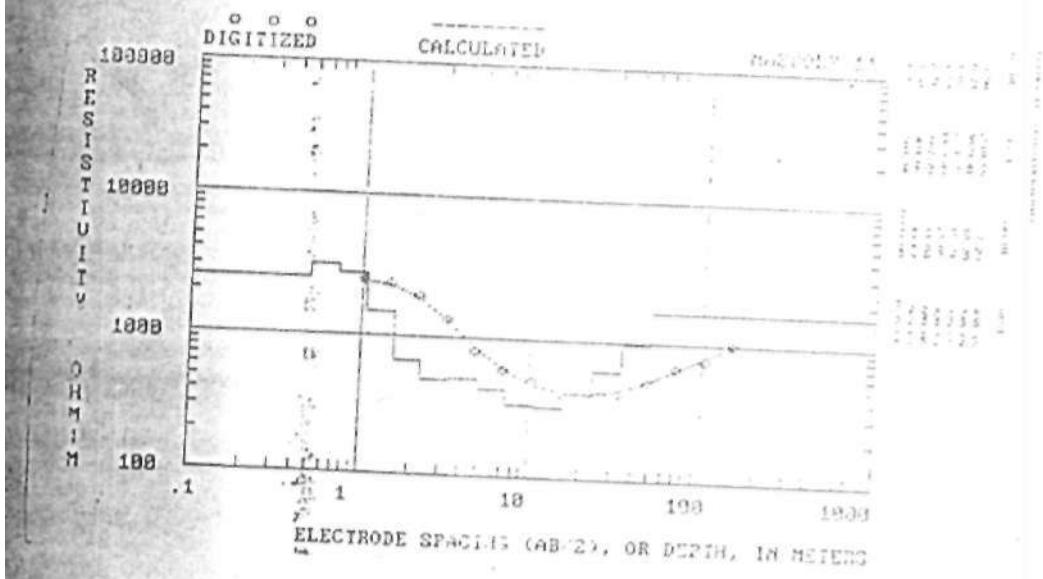


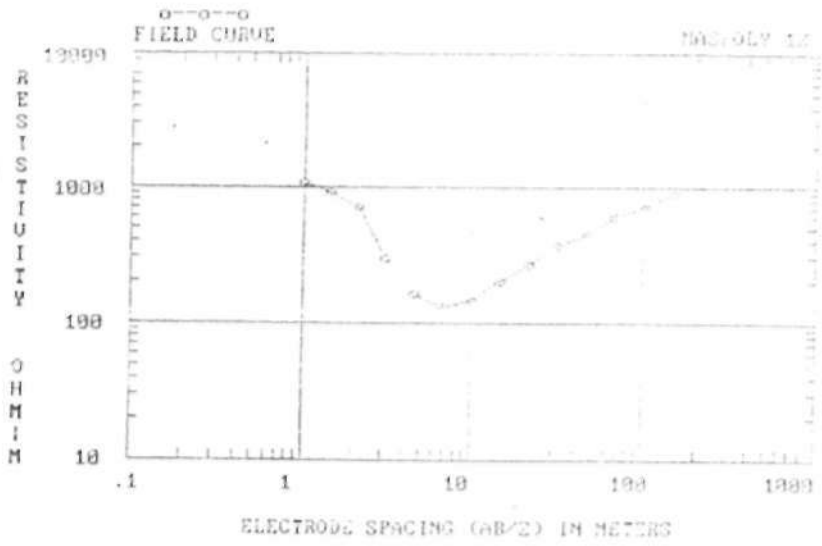


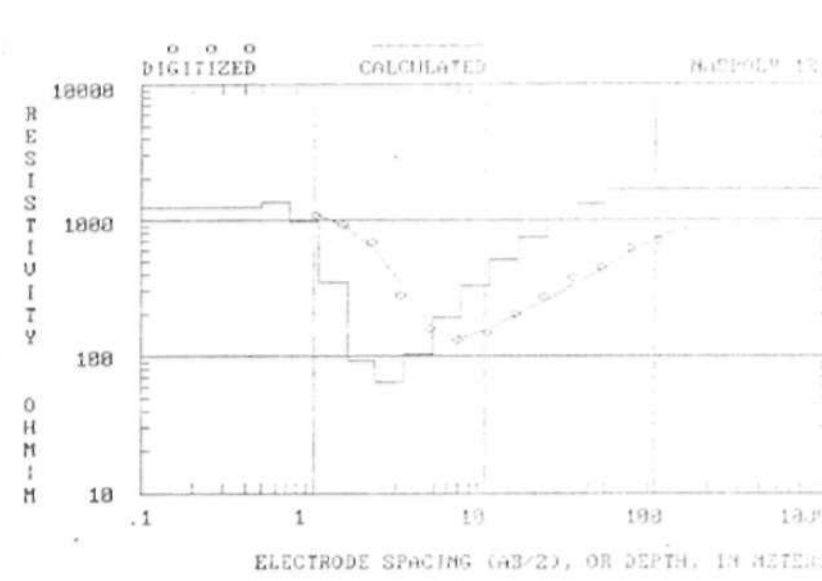
VASHIM IBRAHIM LIBRARY

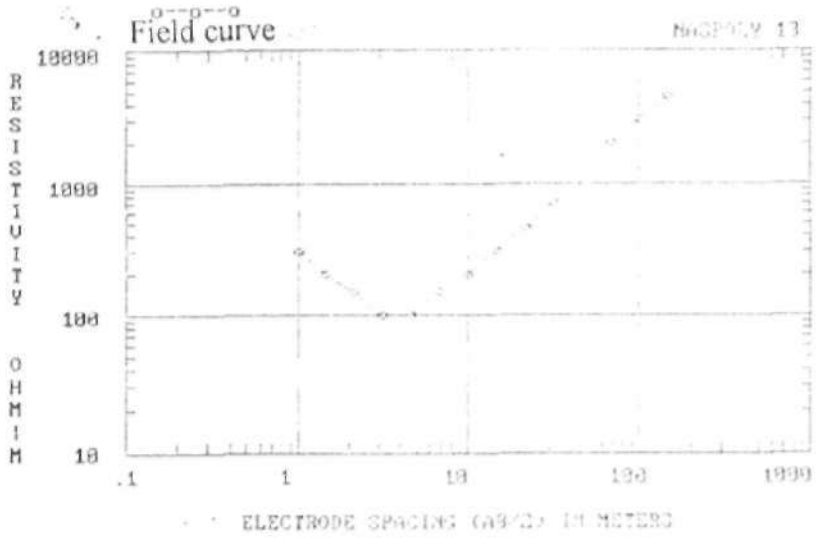

FIELD CURVE
MASPOLY 11
RESISTIVITY OHMIM
100000
10000
1000
100
.1
1
10
100
1000
ELECTRODE SPACING (AB/2) IN METERS
DIGITIZED
CALCULATED
MASPOLY 11
RESISTIVITY OHMIM
100000
10000
1000
100
.1
1
10
100
1000
ELECTRODE SPACING (AB/2), OR DEPTH, IN METERS

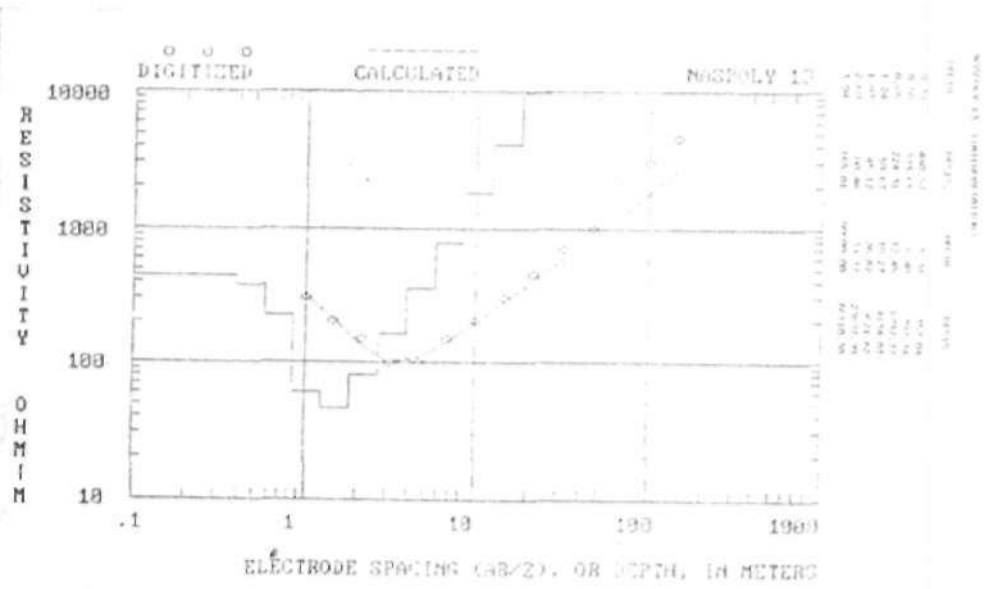

o--o--o
FIELD CURVE
100000
10000
1000
100
RESISTIVITY OHMIM
.1
1
10
100
1000
ELECTRODE SPACING (AB/2) IN METERS

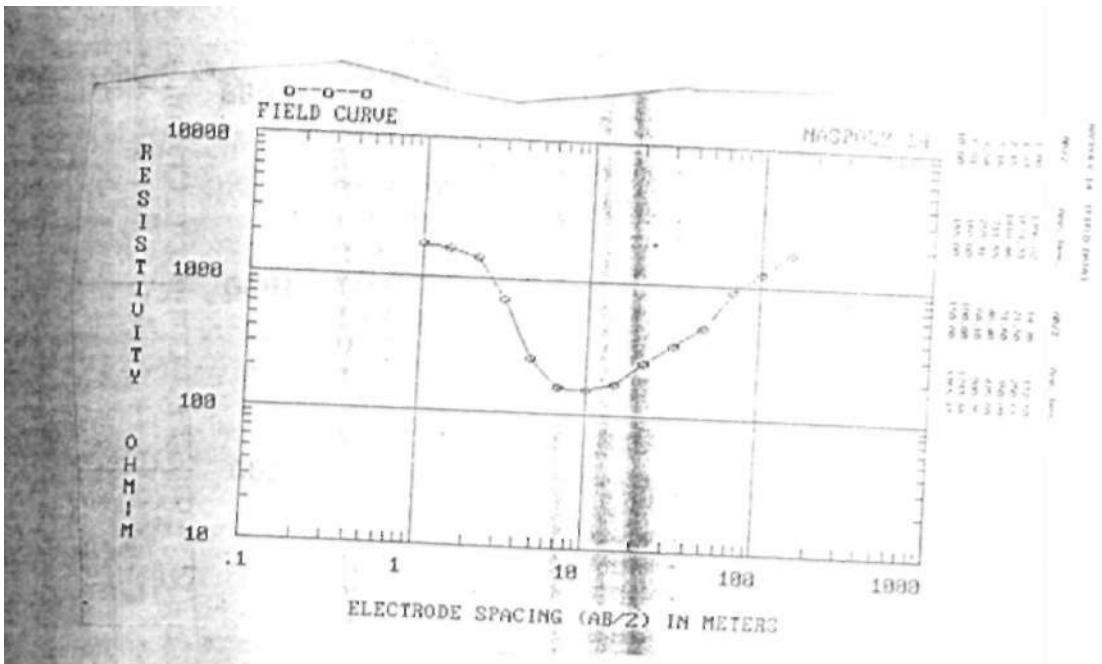

o o o
DIGITIZED
CALCULATED
100000
10000
1000
100
RESISTIVITY OHMIM
.1
1
10
100
1000
ELECTRODE SPACING (AB/2), OR DEPTH, IN METERS

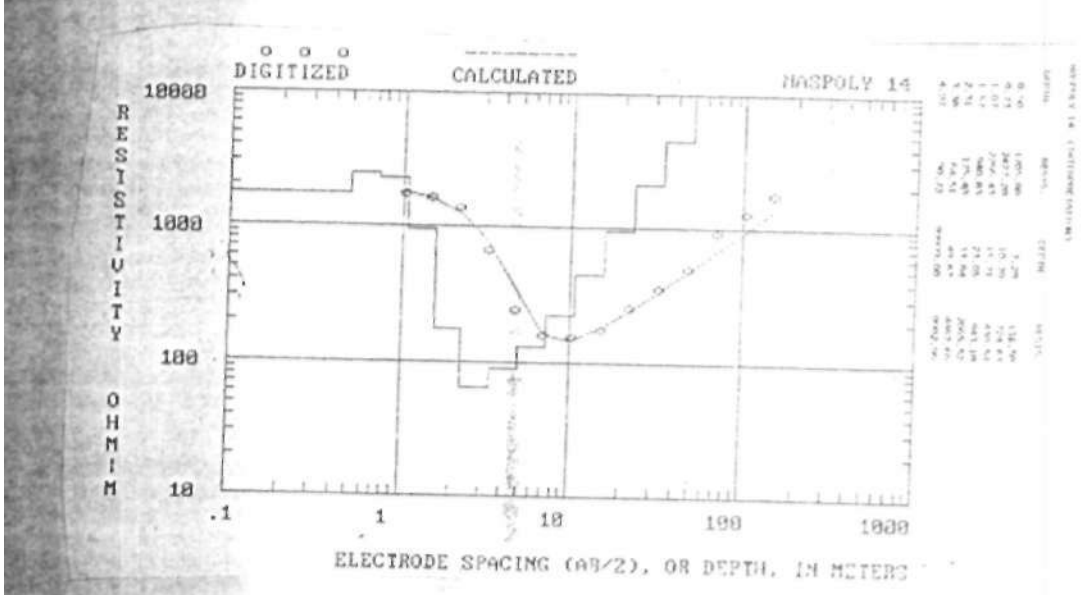

FIELD CURVE
10000
1000
100
10
RESISTIVITY OHMIM
.1
1
10
100
1000
ELECTRODE SPACING (AB/2) IN METERS

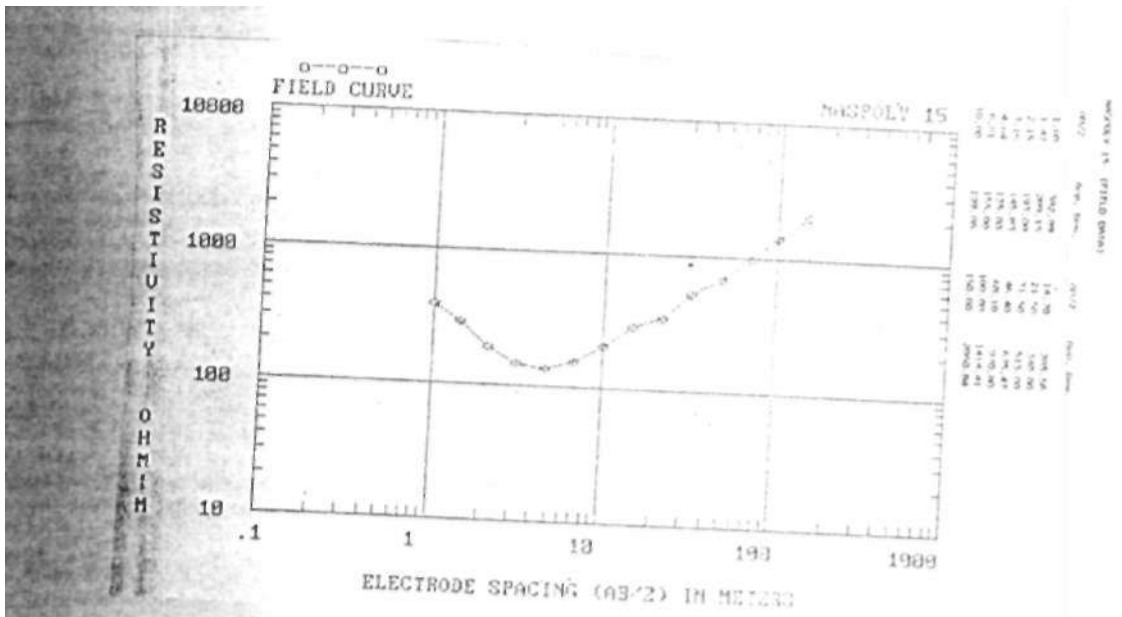

DIGITIZED
CALCULATED
10000
1000
100
10
RESISTIVITY OHMIM
.1
1
10
100
ELECTRODE SPACING (AB/2), OR DEPTH, IN METERS

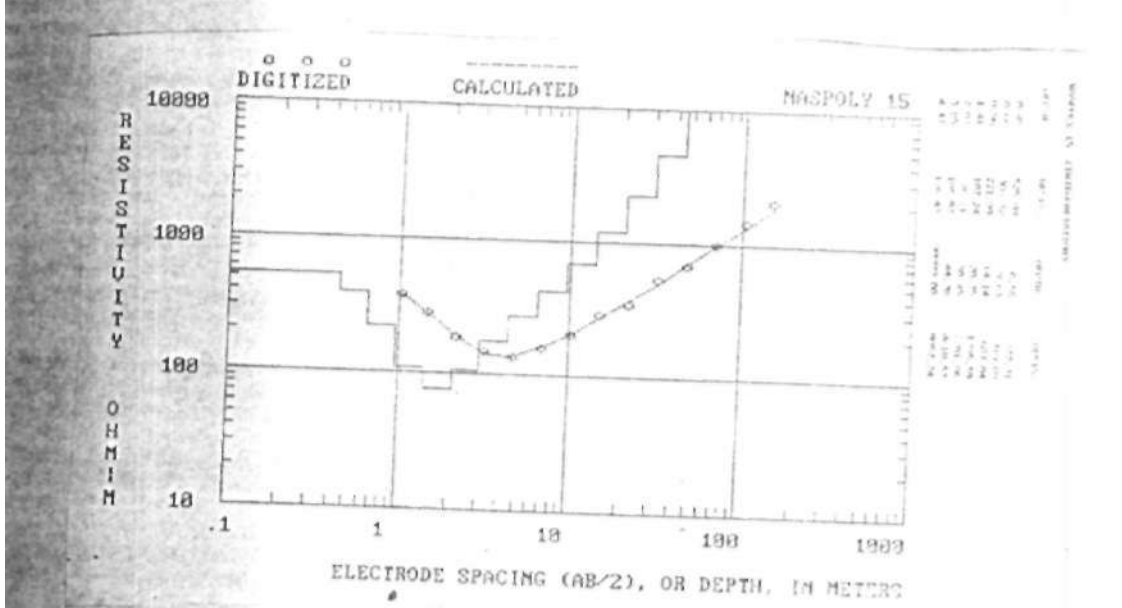

Field curve
RESISTIVITY OHMIM
10000
1000
100
10
.1
1
10
100
1000
ELECTRODE SPACING (AB/2) IN METERS

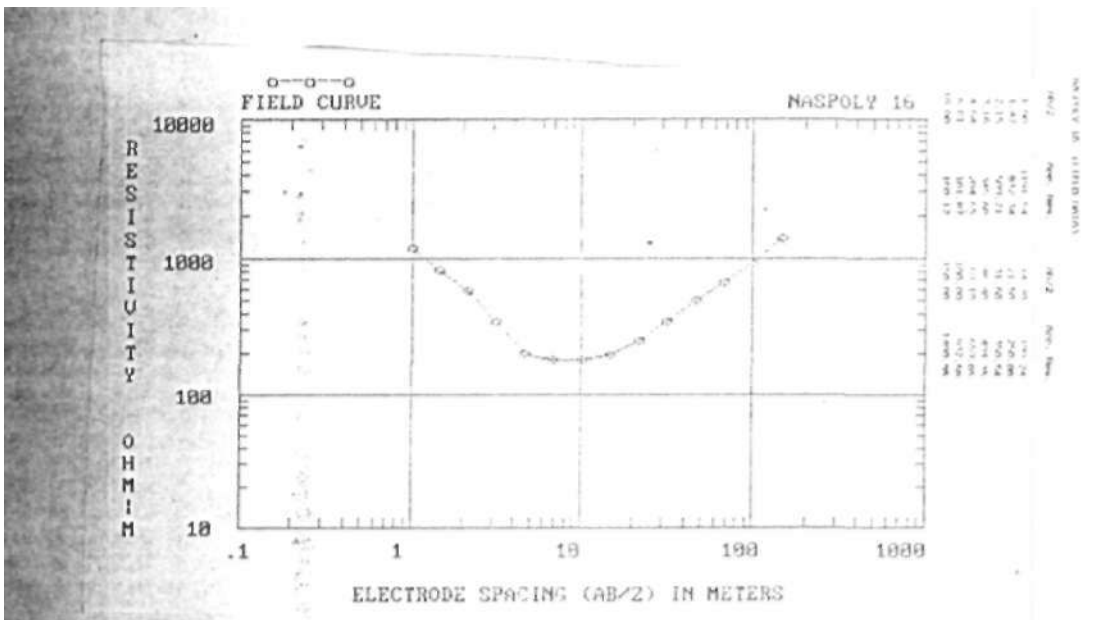

DIGITIZED
CALCULATED
RESISTIVITY OHMIM
10000
1000
100
10
.1
1
10
100
1000
ELECTRODE SPACING (AB/2), OR DCPTH, IN METERS

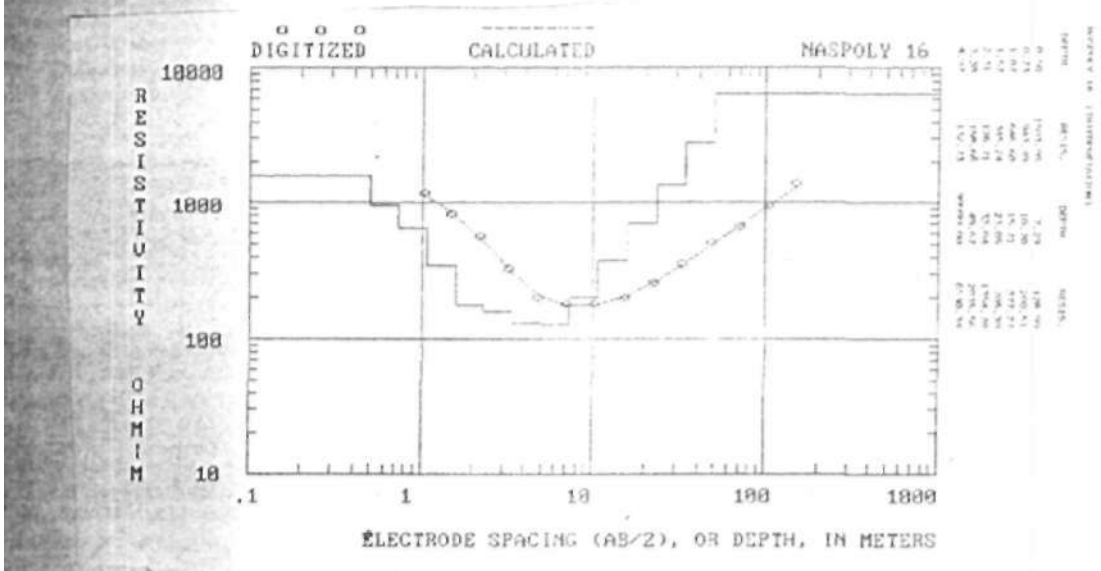

o--o--o
FIELD CURVE
RESISTIVITY OHMIM
10000
1000
100
10
.1
1
10
100
1000
ELECTRODE SPACING (AB/2) IN METERS


o o o
DIGITIZED
CALCULATED
RESISTIVITY OHMIM
10000
1000
100
10
.1
1
10
100
1000
ELECTRODE SPACING (AB/2), OR DEPTH, IN METERS

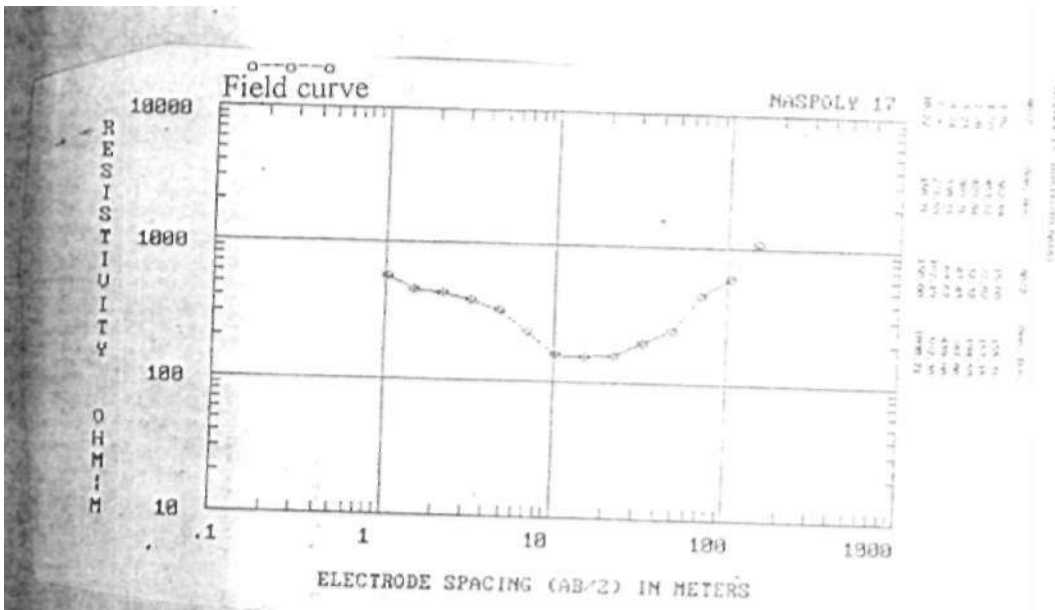

FIELD CURVE
MASPOLY 15
RESISTIVITY OHMIM
10000
1000
100
10
.1
1
10
100
1000
ELECTRODE SPACING (AB/2) IN METERS

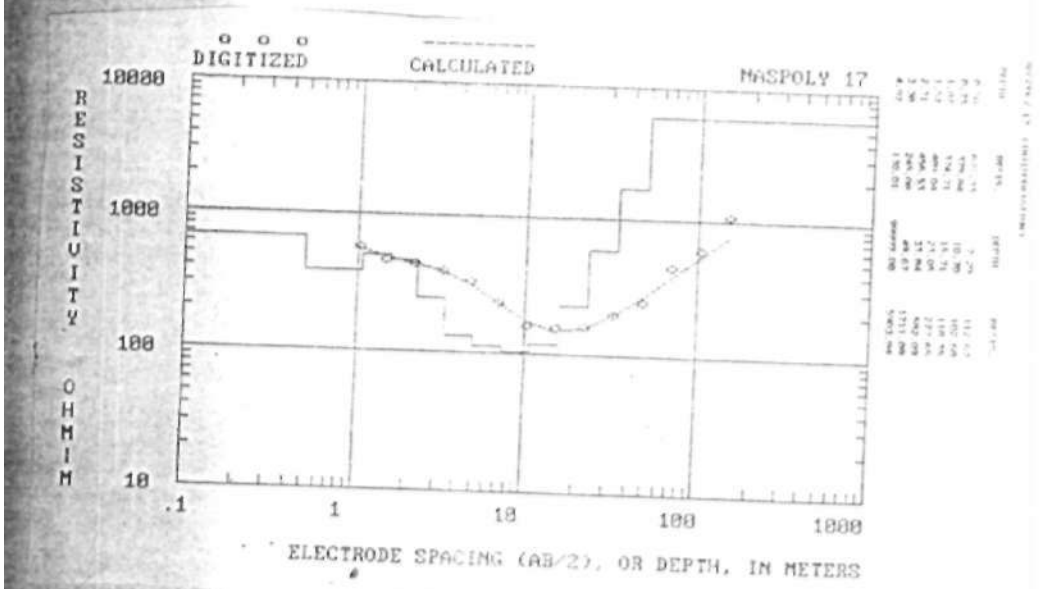

DIGITIZED
CALCULATED
MASPOLY 15
RESISTIVITY OHMIM
10000
1000
100
10
.1
1
10
100
1000
ELECTRODE SPACING (AB/2), OR DEPTH, IN METERS

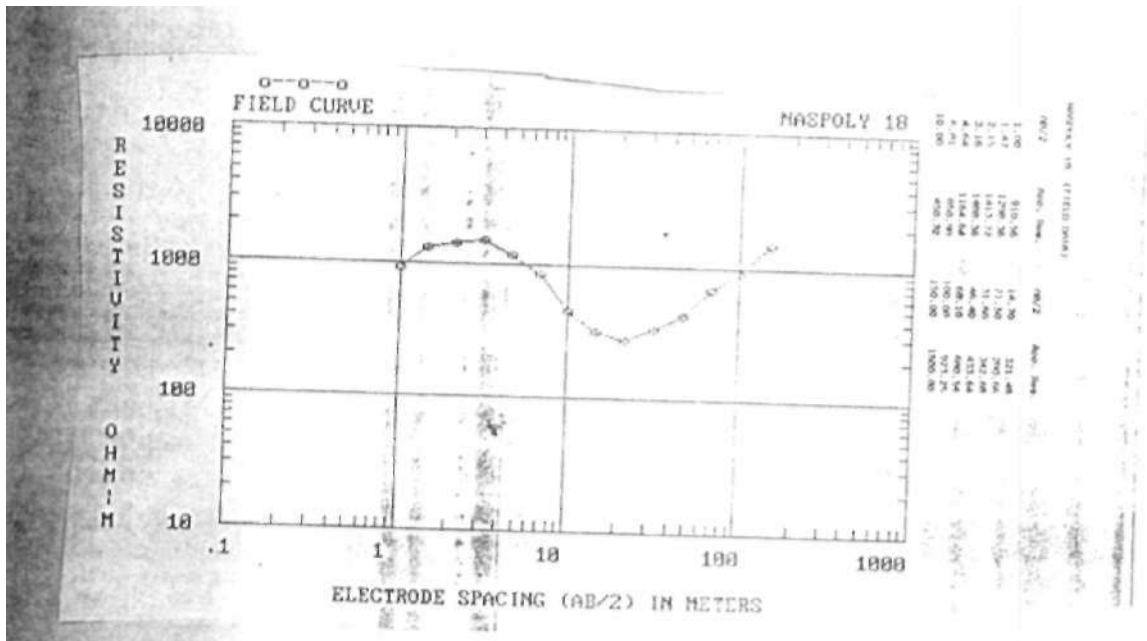


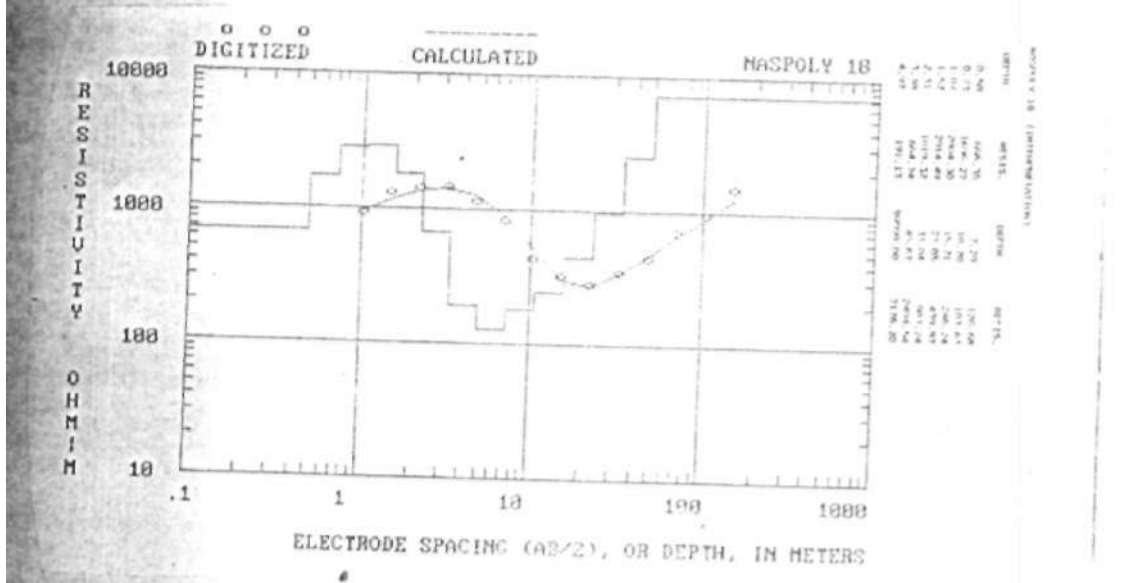


KASHIM IBRAHIM LIBRARY

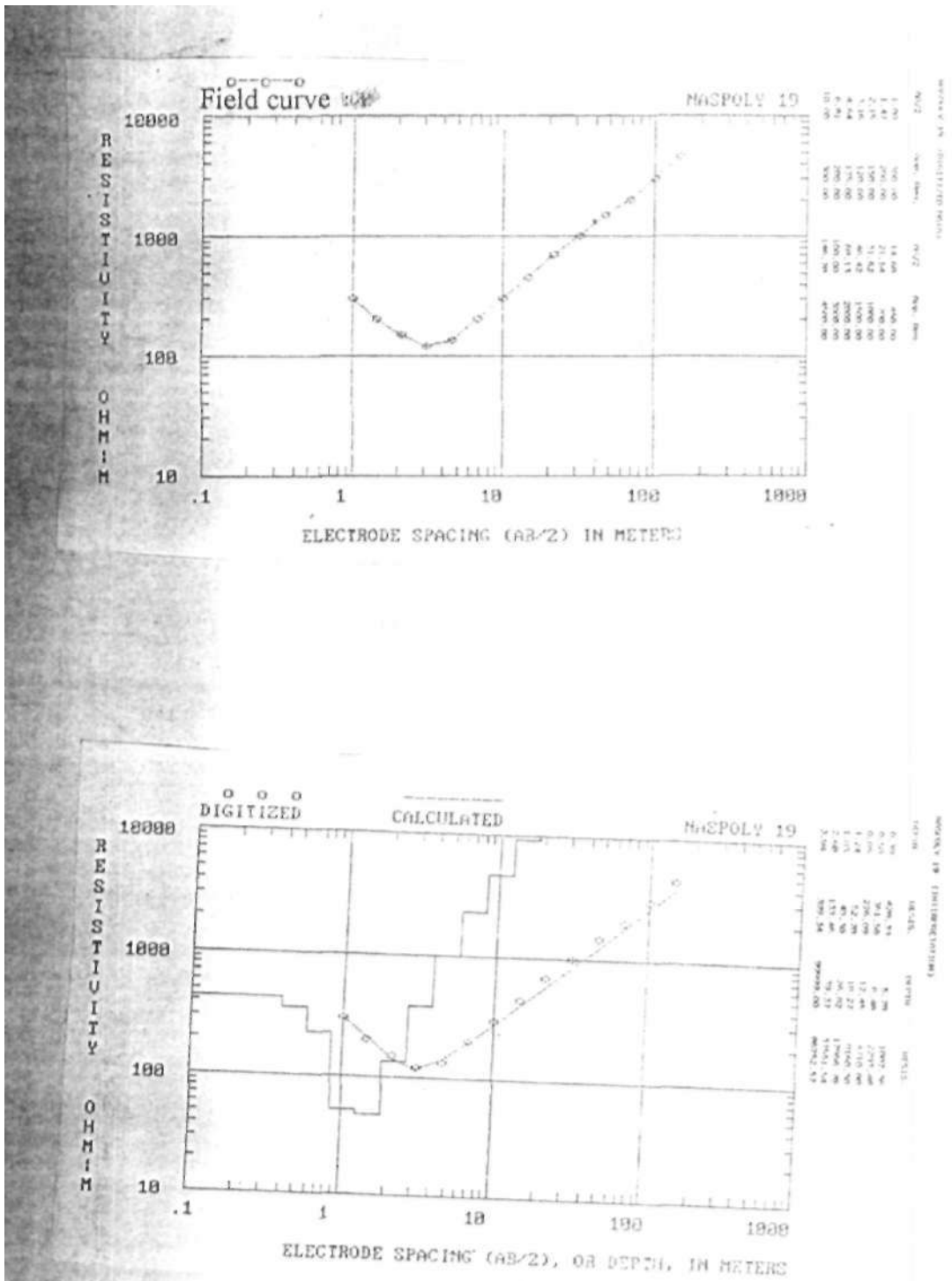

Field curve
NASPOLY 17
RESISTIVITY OHMIM
10000
1000
100
10
.1
1
10
100
1000
ELECTRODE SPACING (AB/2) IN METERS

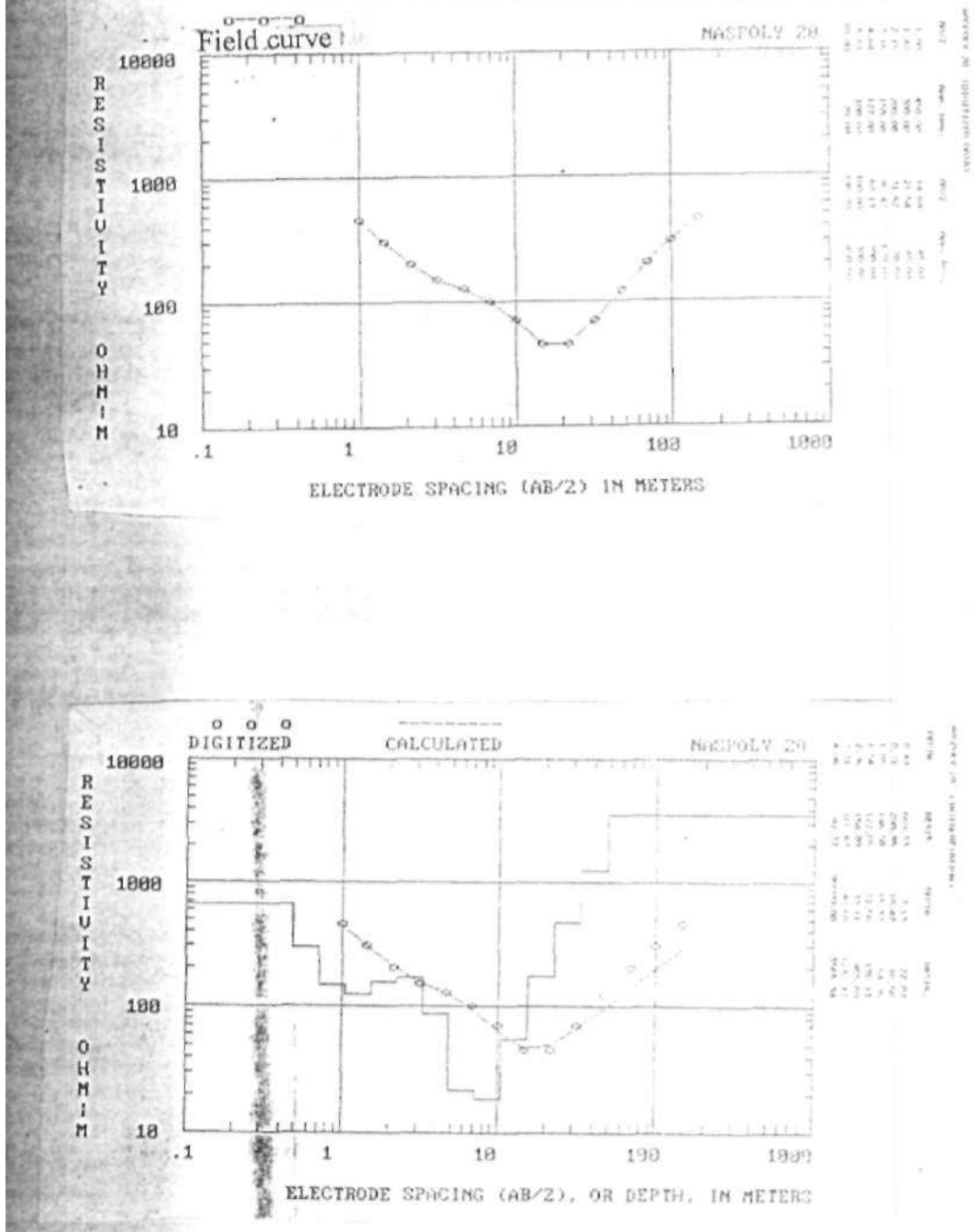

DIGITIZED
CALCULATED
NASPOLY 17
RESISTIVITY OHMIM
10000
1000
100
10
.1
1
10
100
1000
ELECTRODE SPACING (AB/2), OR DEPTH, IN METERS

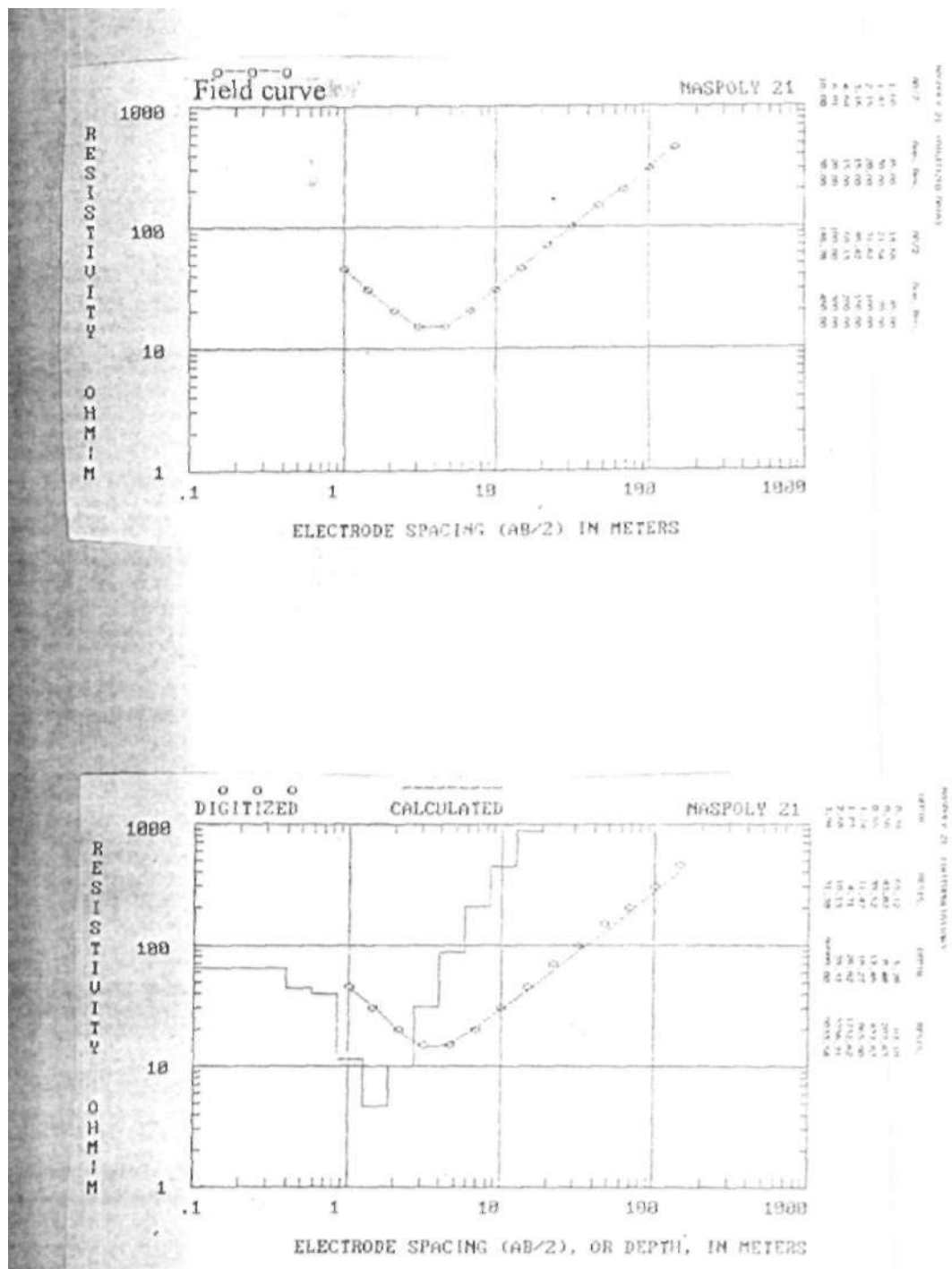




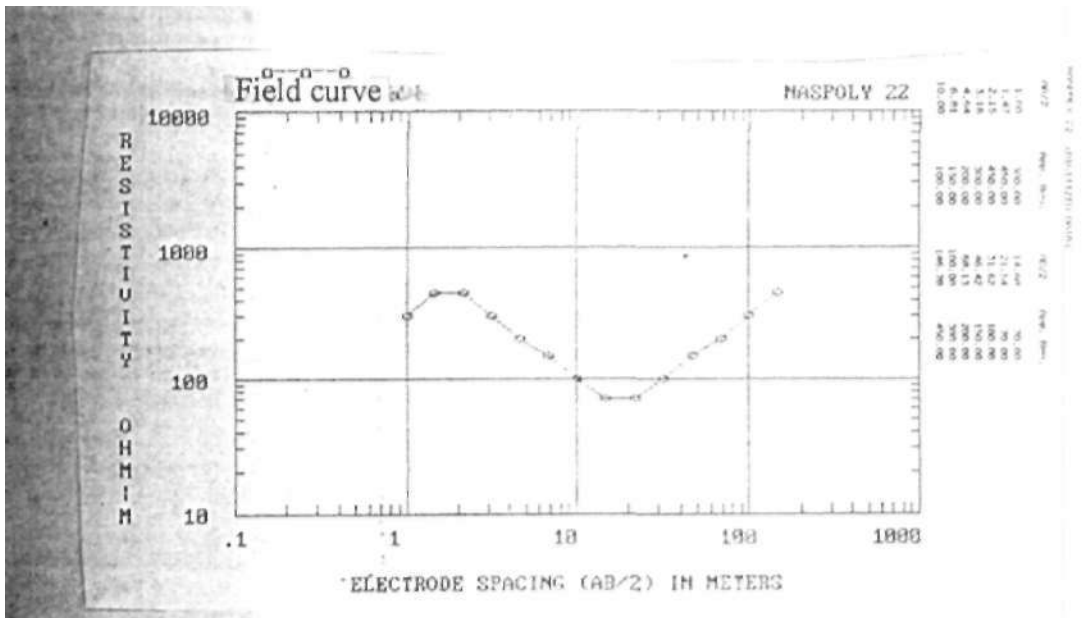
KASHIM IBRAHIM LIBRARY

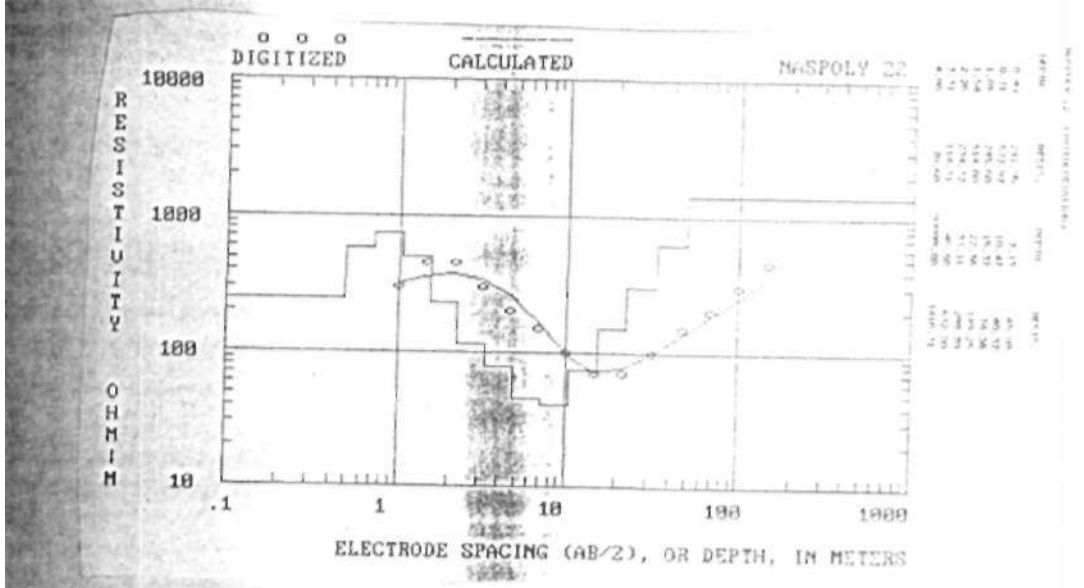

Field curve
MAGPOLY 19
RESISTIVITY OHMIM
10000
1000
100
10
.1
1
10
100
1000
ELECTRODE SPACING (AB/2) IN METERS
DIGITIZED
CALCULATED
MAGPOLY 19
RESISTIVITY OHMIM
10000
1000
100
10
.1
1
10
100
1000
ELECTRODE SPACING (AB/2), OR DEPTH, IN METERS

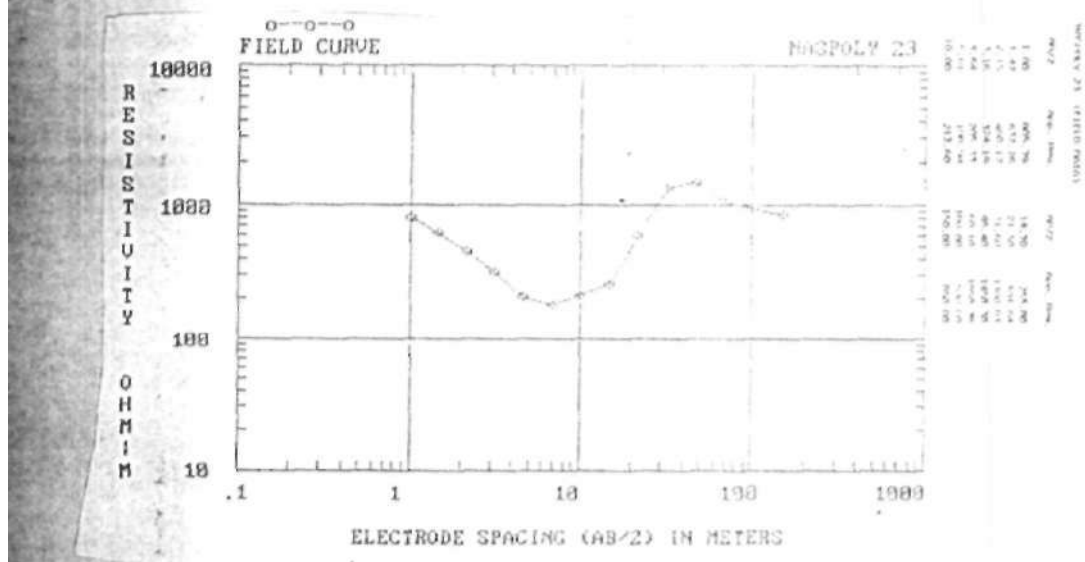

Field curve
MASPOLY 20
RESISTIVITY OHMIM
10000
1000
100
10
.1
1
10
100
1000
ELECTRODE SPACING (AB/2) IN METERS
DIGITIZED
CALCULATED
MASPOLY 20
RESISTIVITY OHMIM
10000
1000
100
10
.1
1
10
100
1000
ELECTRODE SPACING (AB/2), OR DEPTH, IN METERS

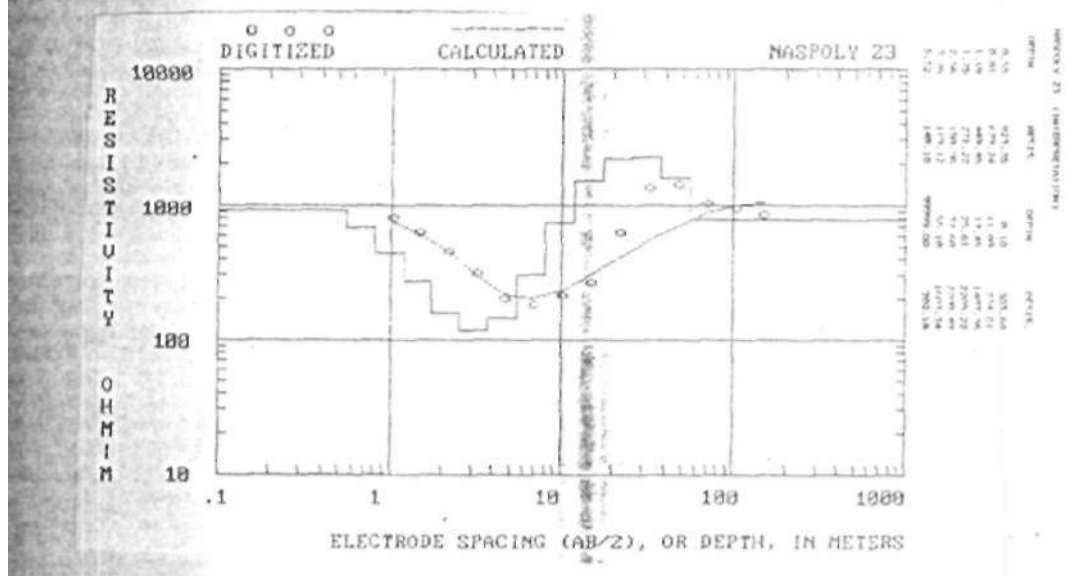


KASHIM IBRAHIM LIBRARY

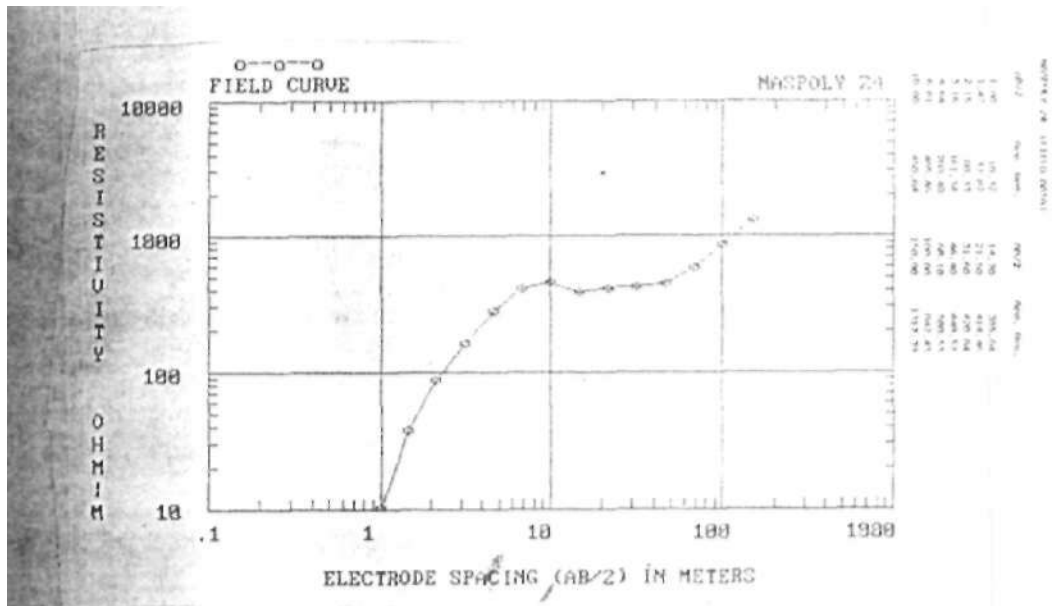

Field curve
NASPOLY 22
RESISTIVITY OHMIM
10000
1000
100
10
.1
1
10
100
1000
ELECTRODE SPACING (AB/2) IN METERS

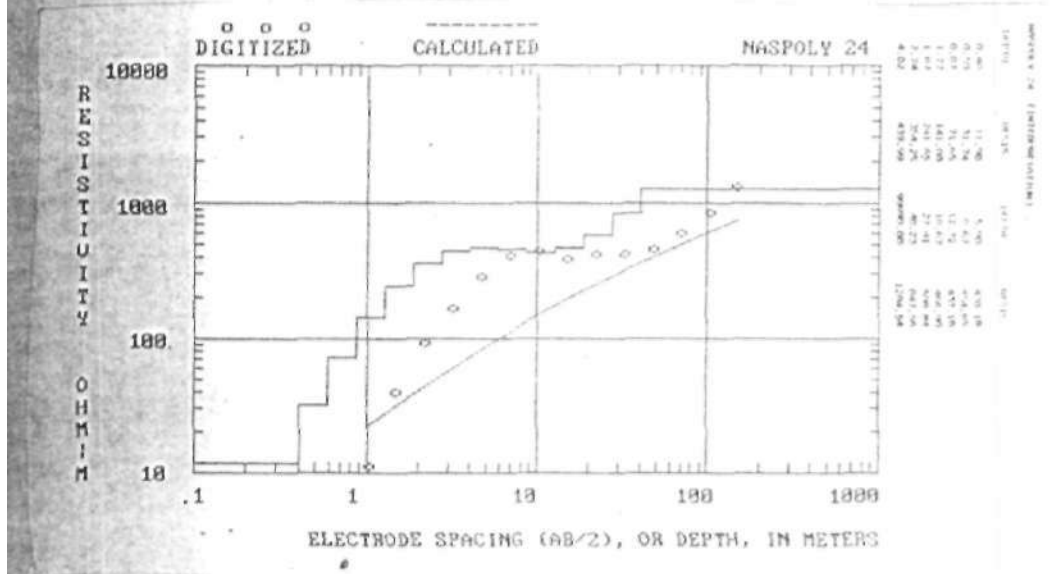

DIGITIZED
CALCULATED
NASPOLY 22
RESISTIVITY OHMIM
10000
1000
100
10
.1
1
10
100
1000
ELECTRODE SPACING (AB/2), OR DEPTH, IN METERS



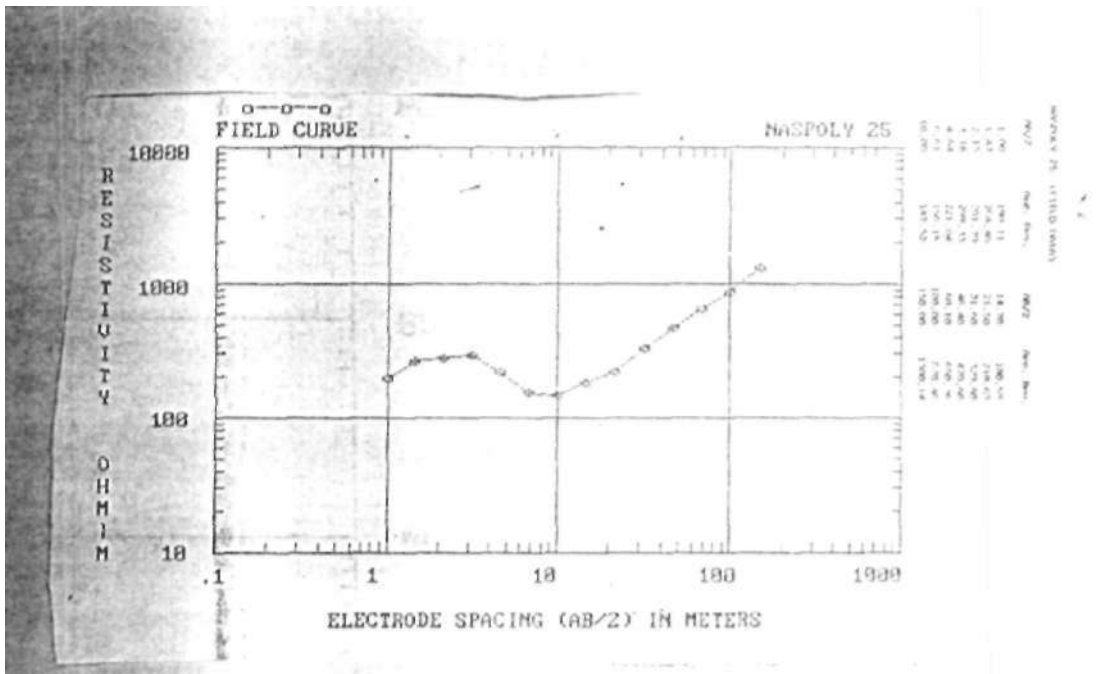


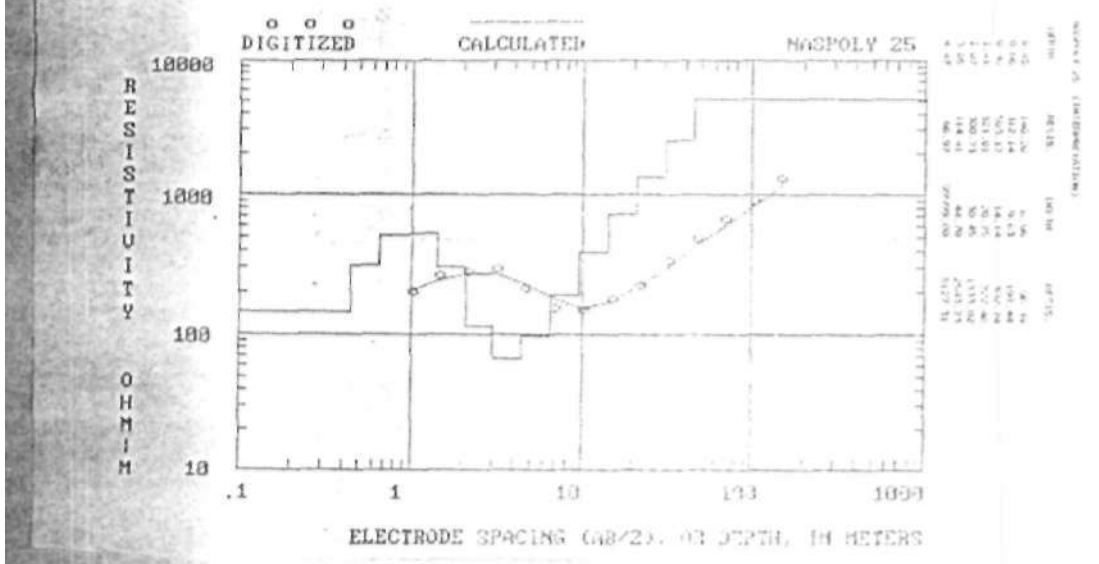
KASHIM IBRAHIM LIB



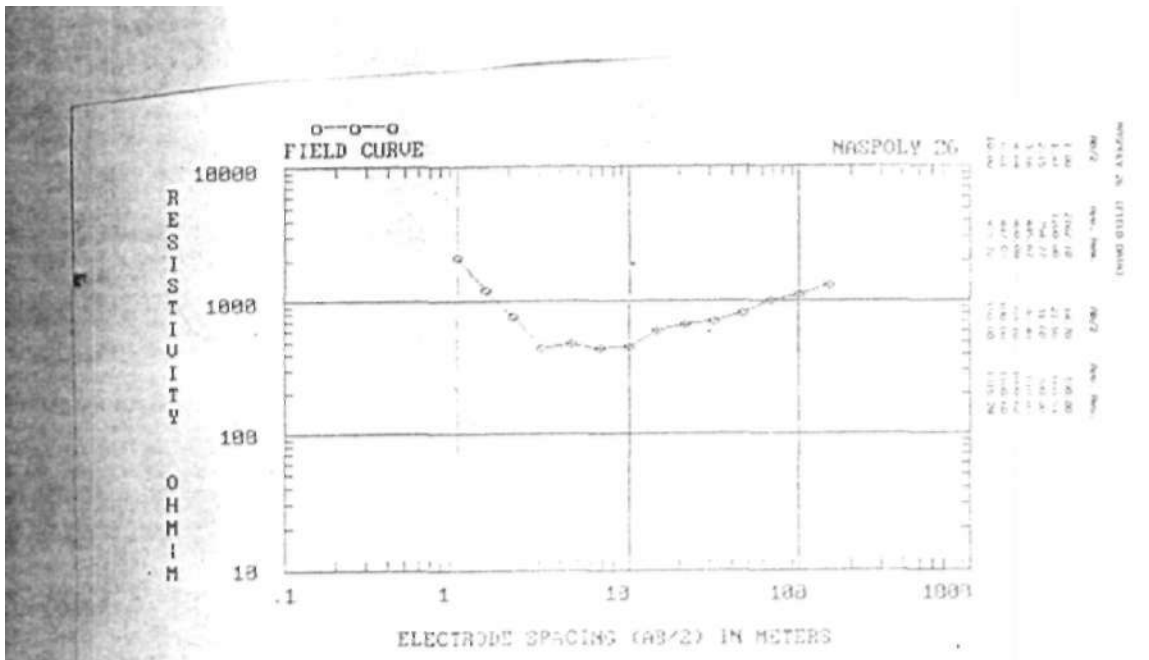


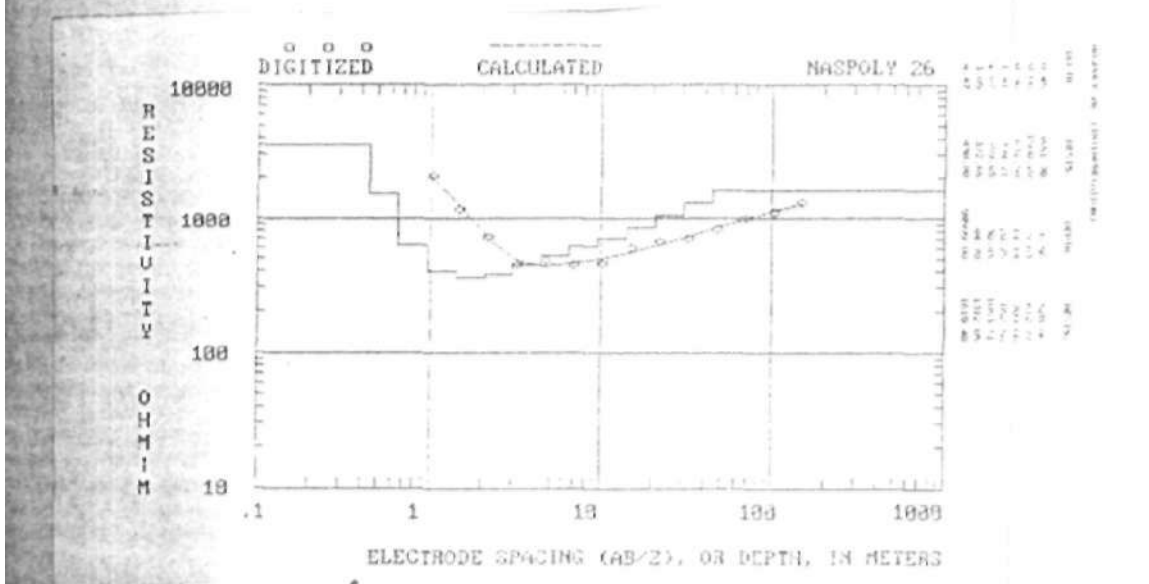
KASHIM IBRAHIM LIBRARY

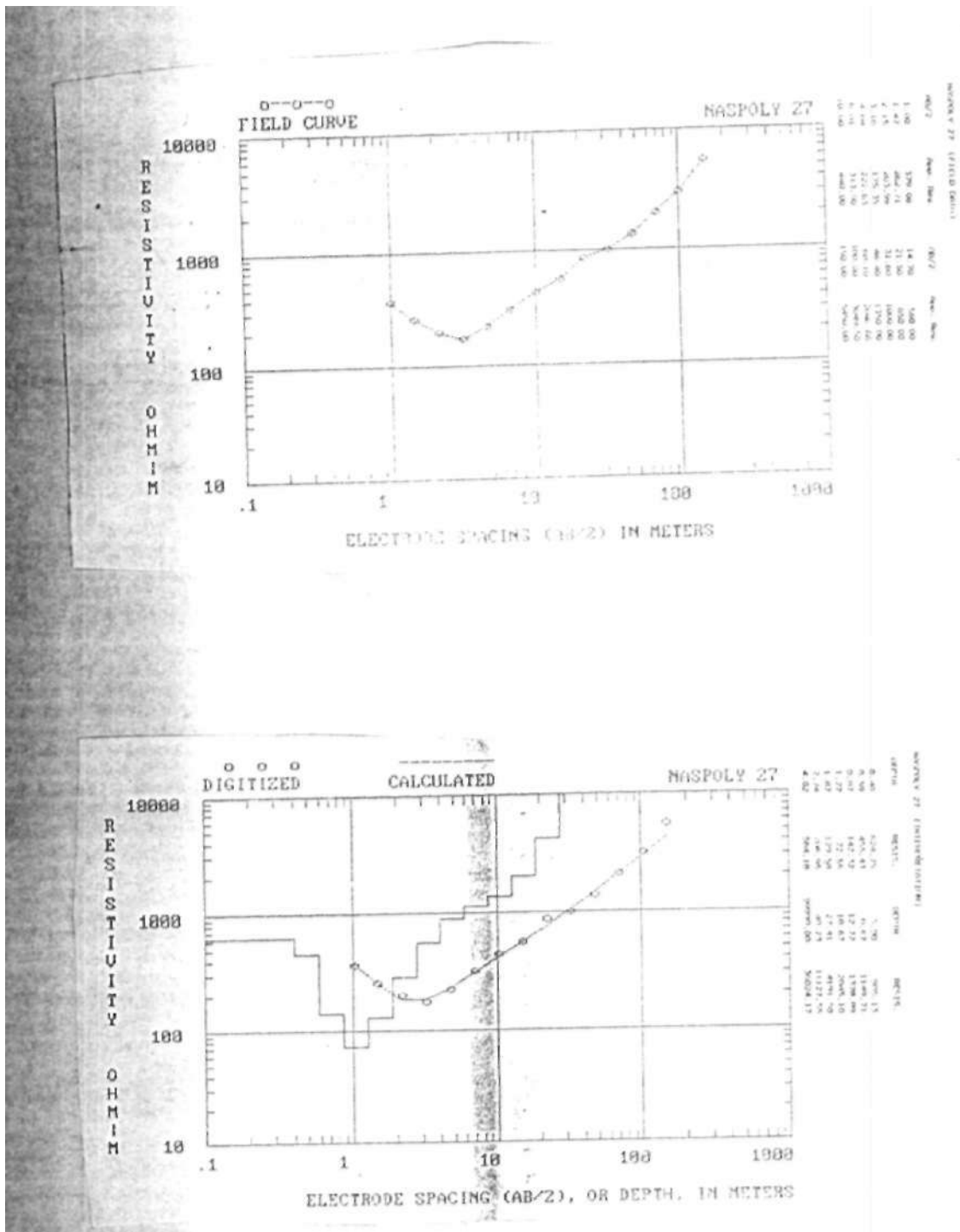


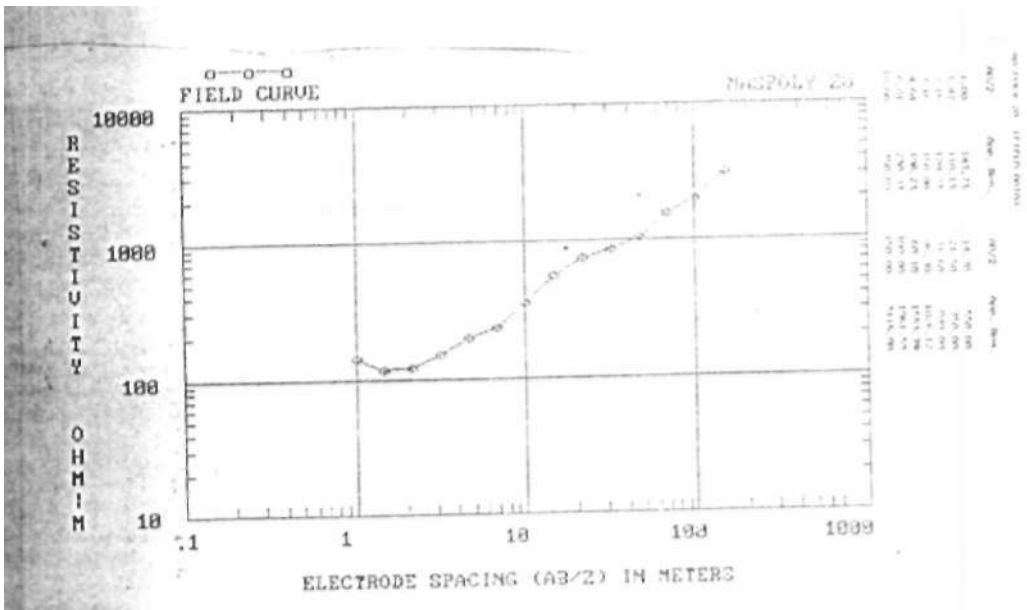


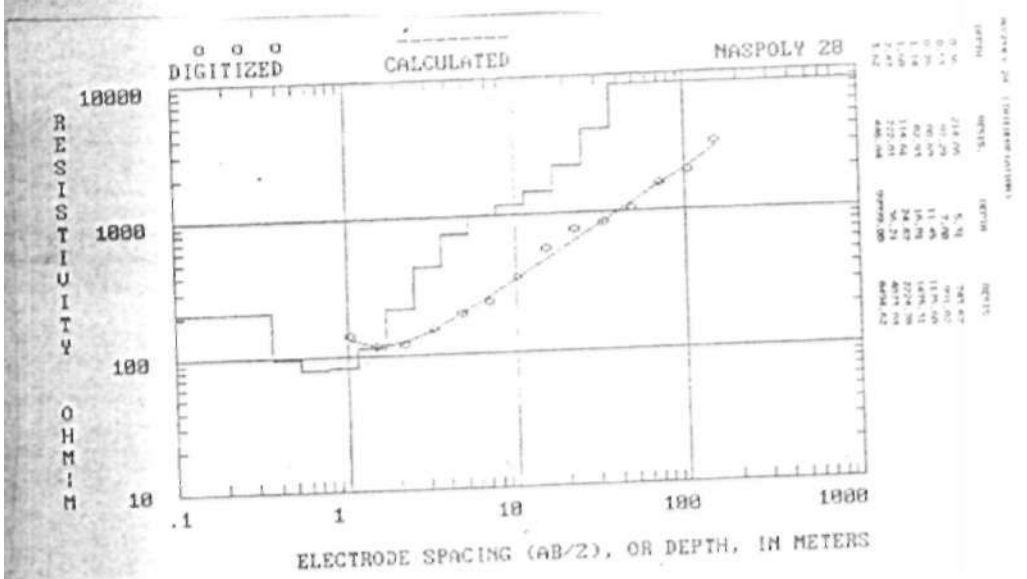
KASHIM IBRAHIM LIBRARY


o—o—o
FIELD CURVE
NASPOLY 26
RESISTIVITY OHMIM
10000
1000
100
10
.1
1
10
100
1000
ELECTRODE SPACING (AB/2) IN METERS

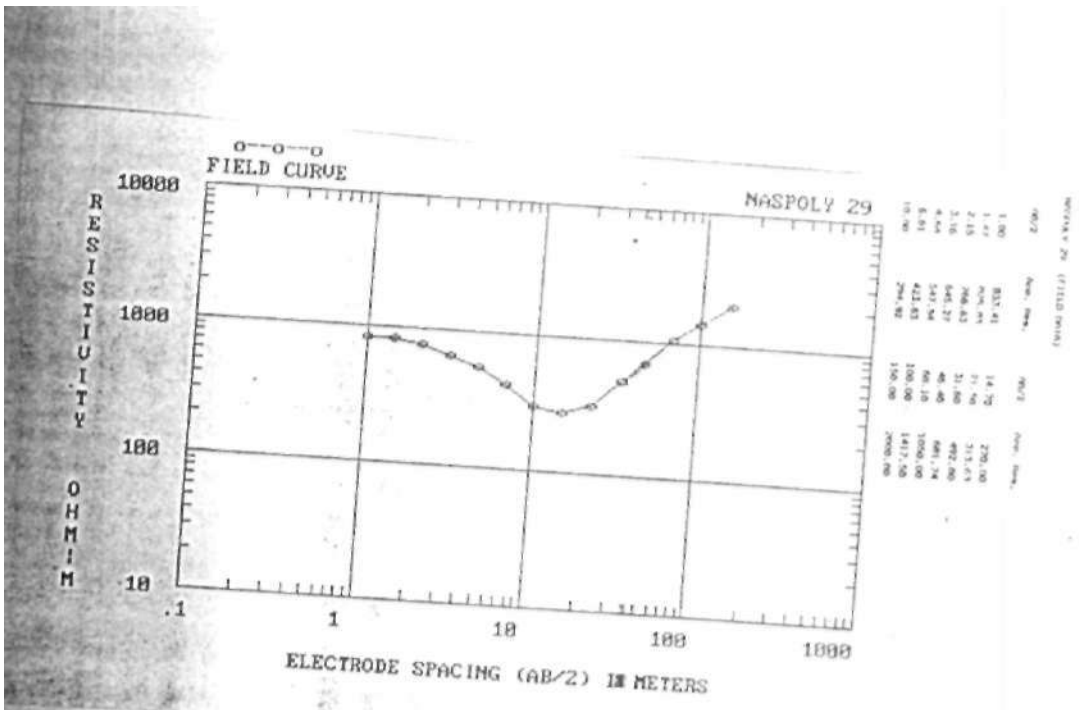

o o o
DIGITIZED
CALCULATED
NASPOLY 26
RESISTIVITY OHMIM
10000
1000
100
10
.1
1
10
100
1000
ELECTRODE SPACING (AB/2), OR DEPTH, IN METERS

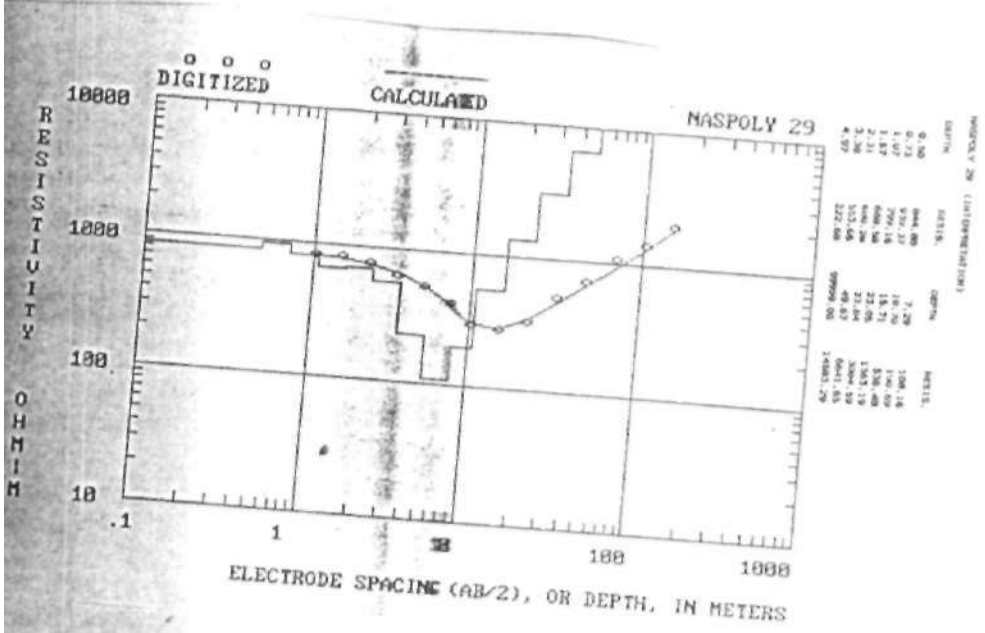

o--o--o
FIELD CURVE
NASPOLY 27
RESISTIVITY OHMIM
10000
1000
100
10
.1
1
10
100
1000
ELECTRODE SPACING (AB/2) IN METERS
o o o
DIGITIZED
CALCULATED
NASPOLY 27
RESISTIVITY OHMIM
10000
1000
100
10
.1
1
10
100
1000
ELECTRODE SPACING (AB/2), OR DEPTH, IN METERS

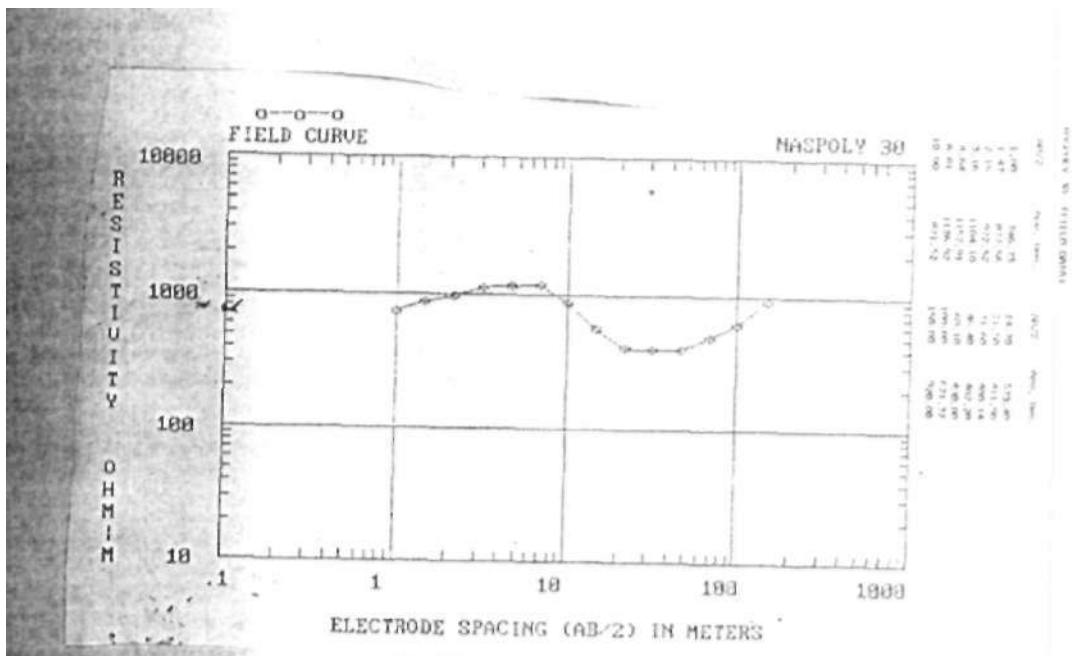


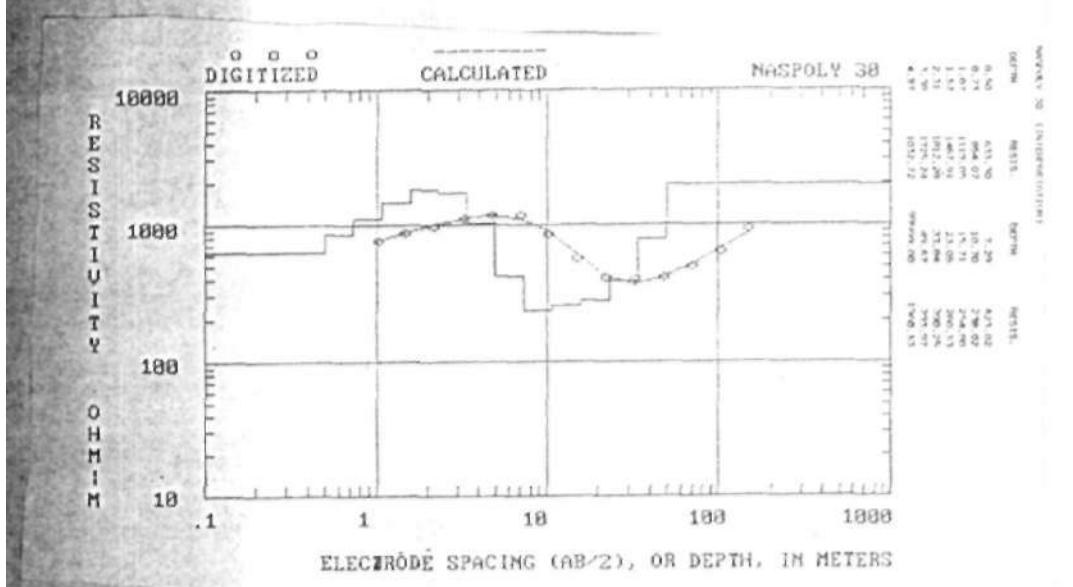


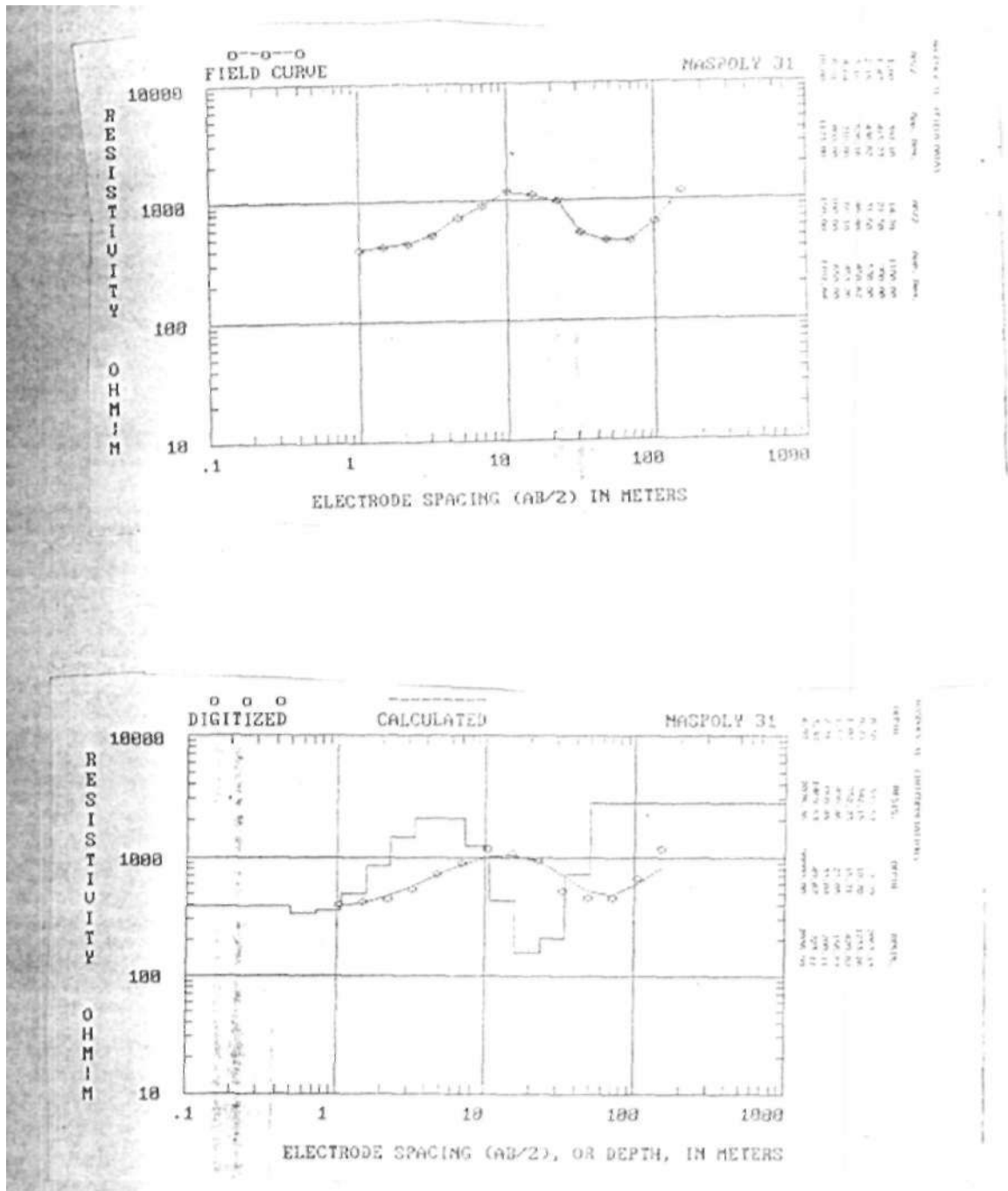
KASHITI IBRAHIM EBRARY


FIELD CURVE
NASPOLY 29
RESISTIVITY OHMIM
10000
1000
100
10
.1
1
10
100
1000
ELECTRODE SPACING (AB/2) IN METERS

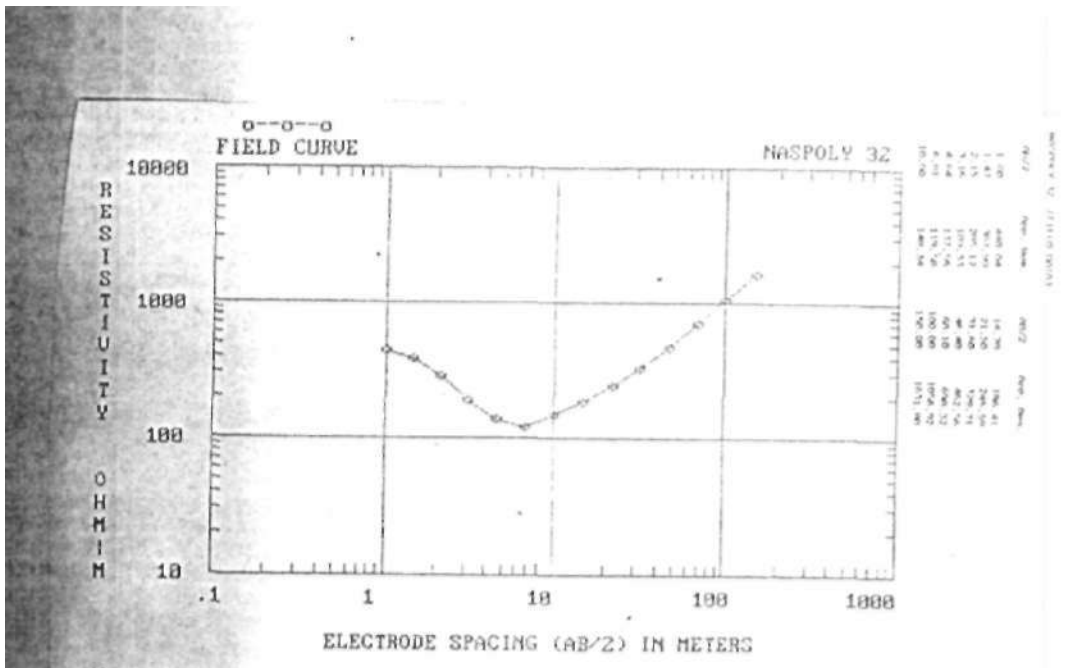

DIGITIZED
CALCULATED
NASPOLY 29
RESISTIVITY OHMIM
10000
1000
100
10
.1
1
100
1000
ELECTRODE SPACING (AB/2), OR DEPTH, IN METERS

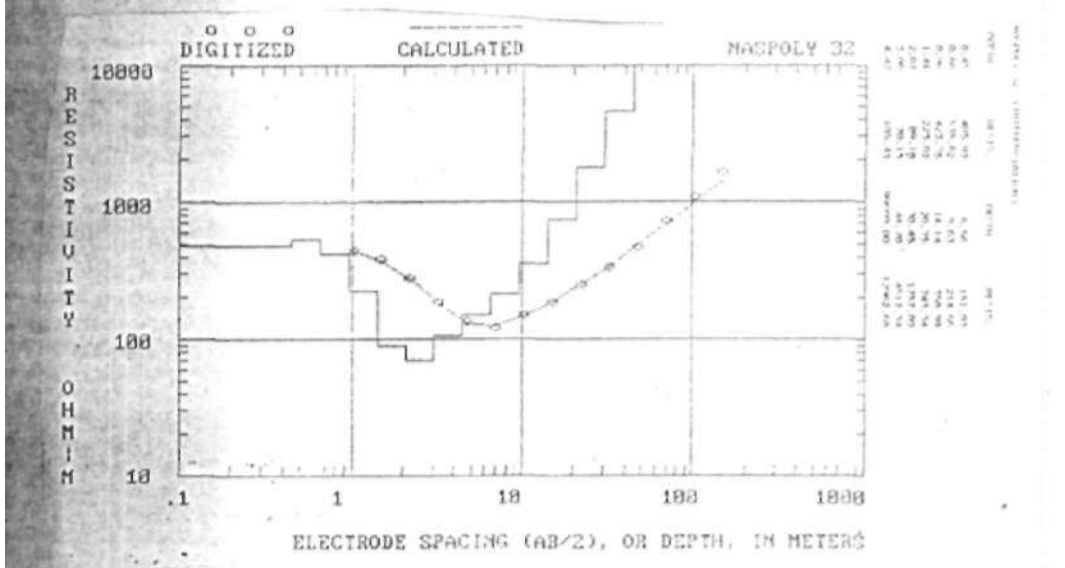

o—o—o
FIELD CURVE
NASPOLY 30
RESISTIVITY OHMIM
10000
1000
100
10
.1
1
10
100
1000
ELECTRODE SPACING (AB/2) IN METERS

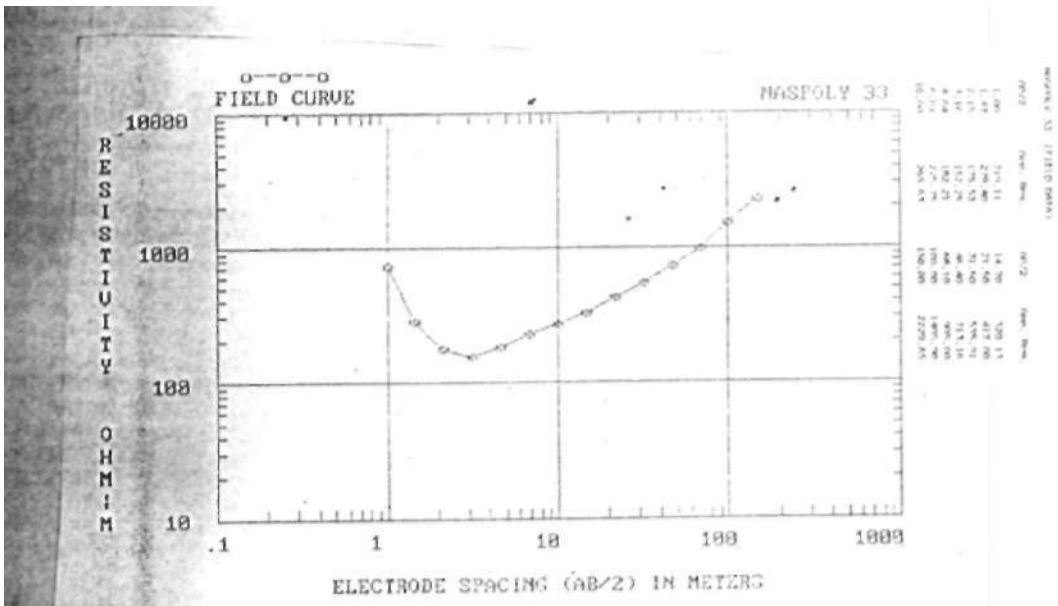

o o o
DIGITIZED
CALCULATED
NASPOLY 38
RESISTIVITY OHMIM
10000
1000
100
10
.1
1
10
100
1000
ELECTRODE SPACING (AB/2), OR DEPTH, IN METERS

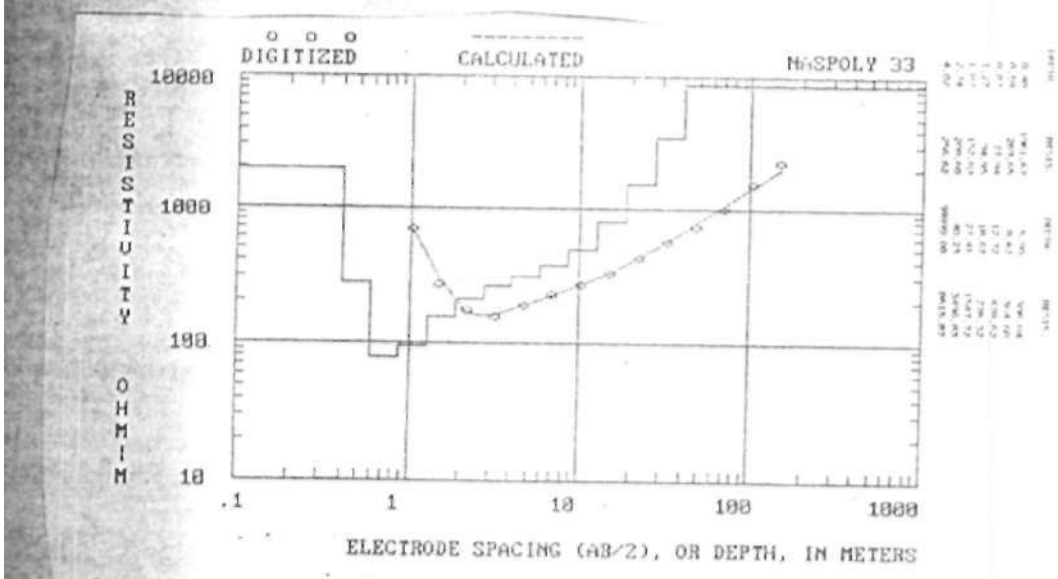


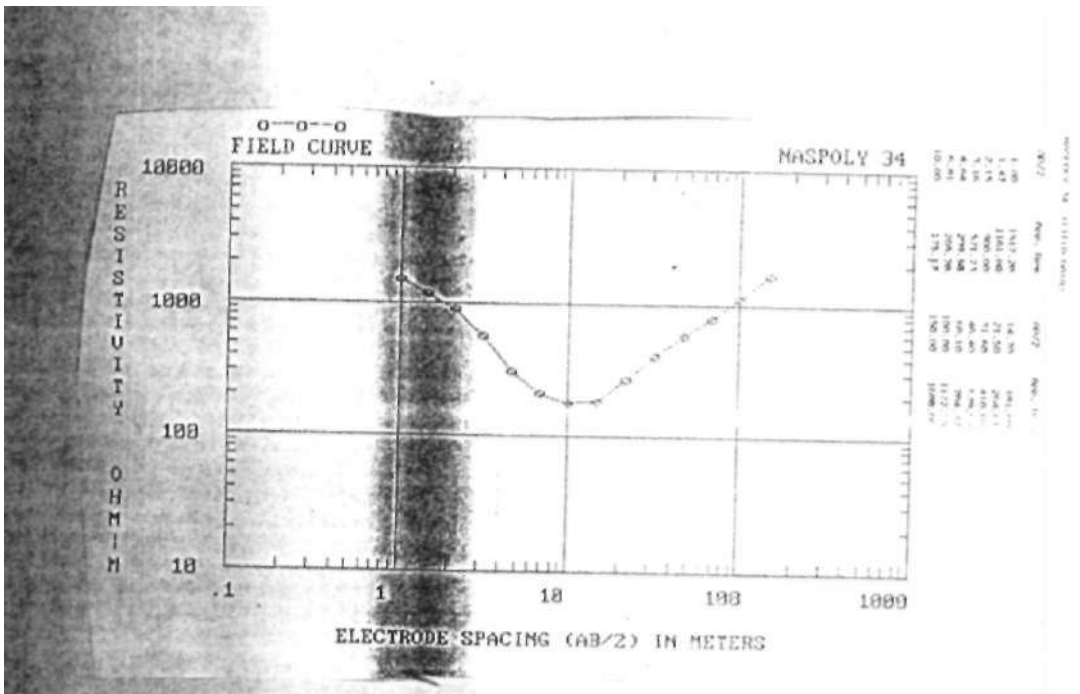
KASHIM IBRAHIM LIBRARY

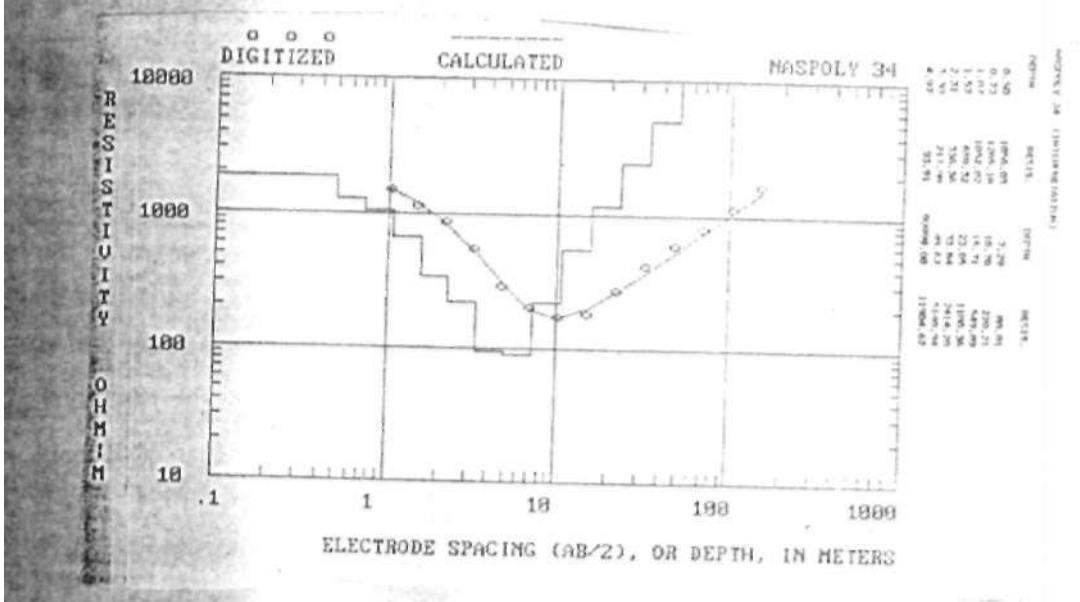

o--o--o
FIELD CURVE
NASPOLY 32
10000
1000
100
10
RESISTIVITY
OHMIM
.1
1
10
100
1000
ELECTRODE SPACING (AB/2) IN METERS


o o o
DIGITIZED
CALCULATED
NASPOLY 32
10000
1000
100
10
RESISTIVITY
OHMIM
.1
1
10
100
1000
ELECTRODE SPACING (AB/2), OR DEPTH, IN METERS

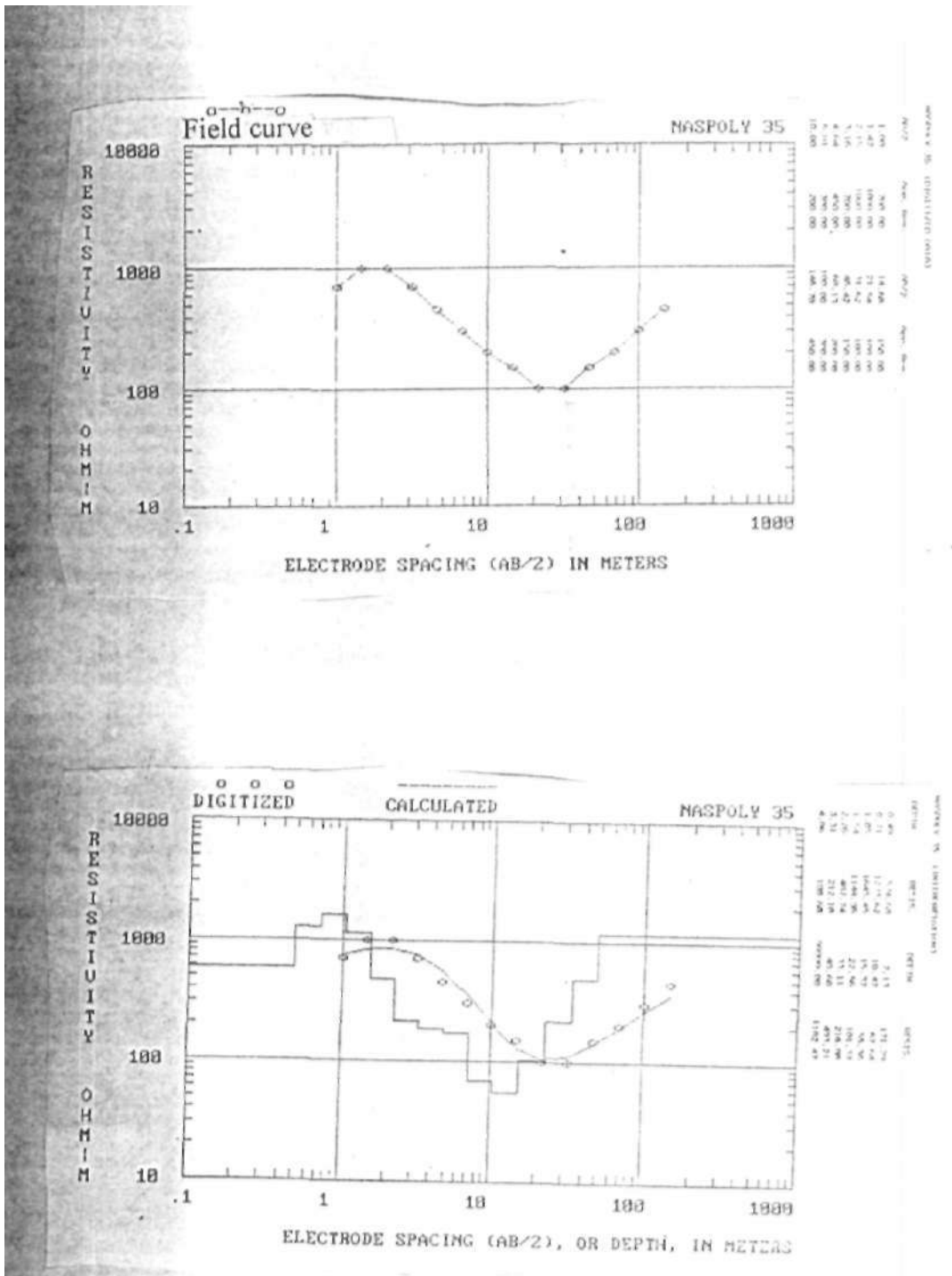

o--o--o
FIELD CURVE
NASPOLY 33
RESISTIVITY OHM-M
10000
1000
100
10
.1
1
10
100
1000
ELECTRODE SPACING (AB/2) IN METERS

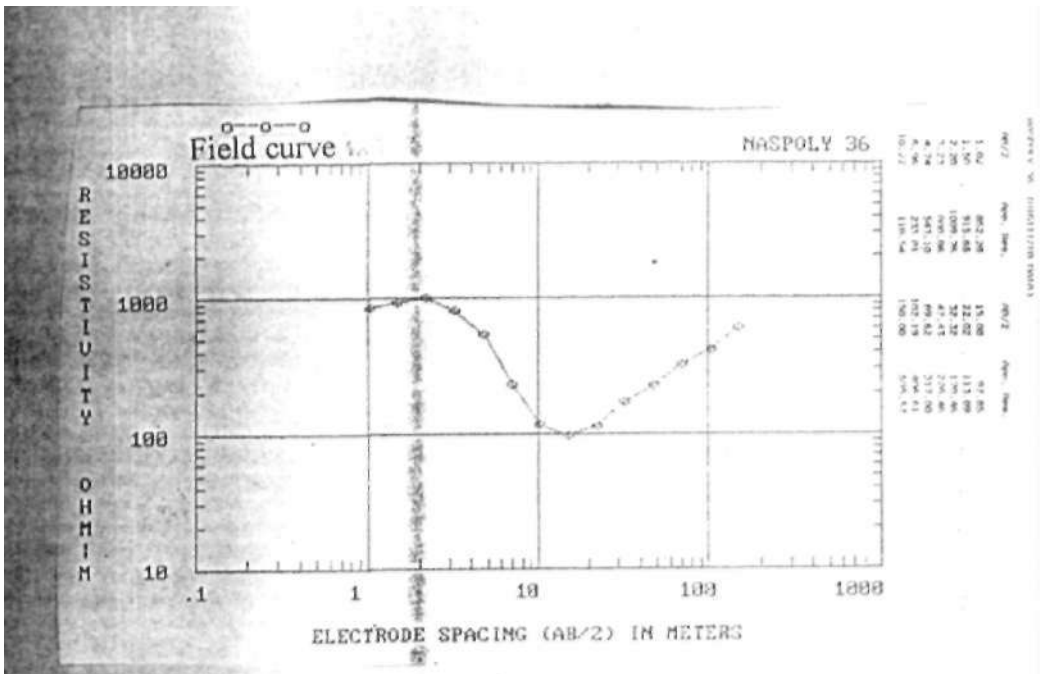

o o o
DIGITIZED
CALCULATED
NASPOLY 33
RESISTIVITY OHM-M
10000
1000
100
10
.1
1
10
100
1000
ELECTRODE SPACING (AB/2), OR DEPTH, IN METERS

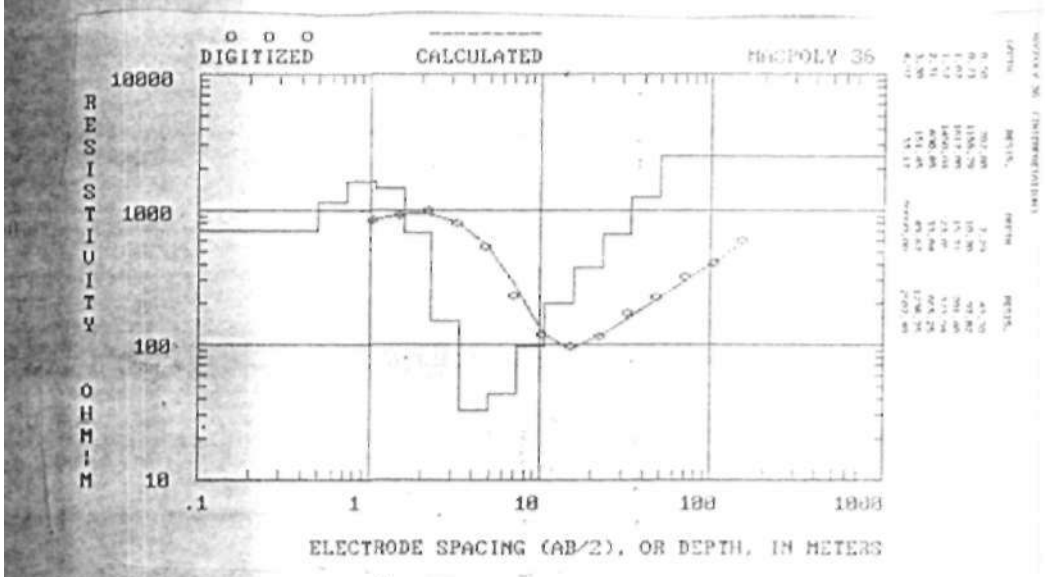




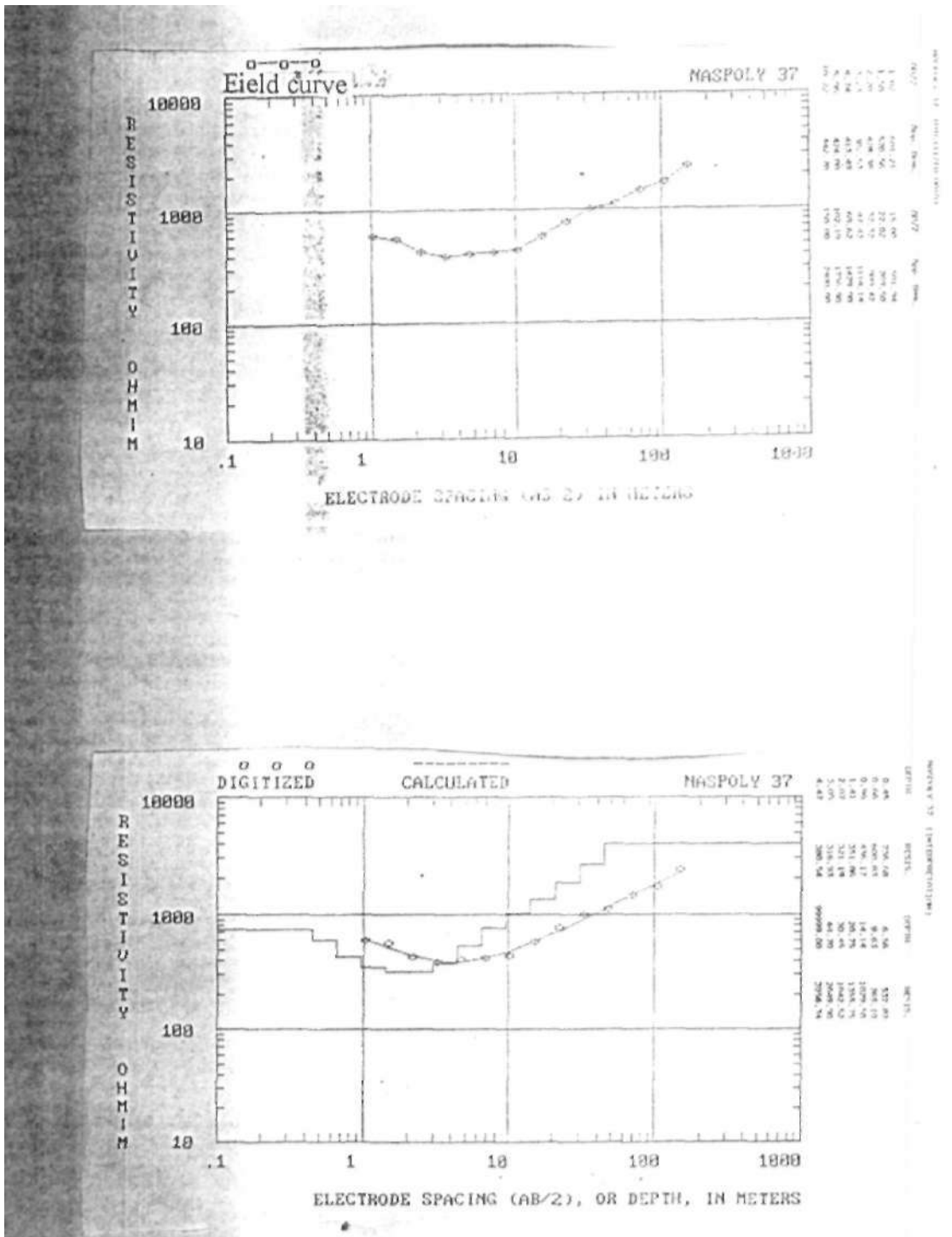
KASHIM IBRAHIM LIBRARY


Field curve
NASPOLY 35
RESISTIVITY OHMIM
10000
1000
100
10
.1
1
10
100
1000
ELECTRODE SPACING (AB/2) IN METERS
DIGITIZED
CALCULATED
NASPOLY 35
RESISTIVITY OHMIM
10000
1000
100
10
.1
1
10
100
1000
ELECTRODE SPACING (AB/2), OR DEPTH, IN METERS

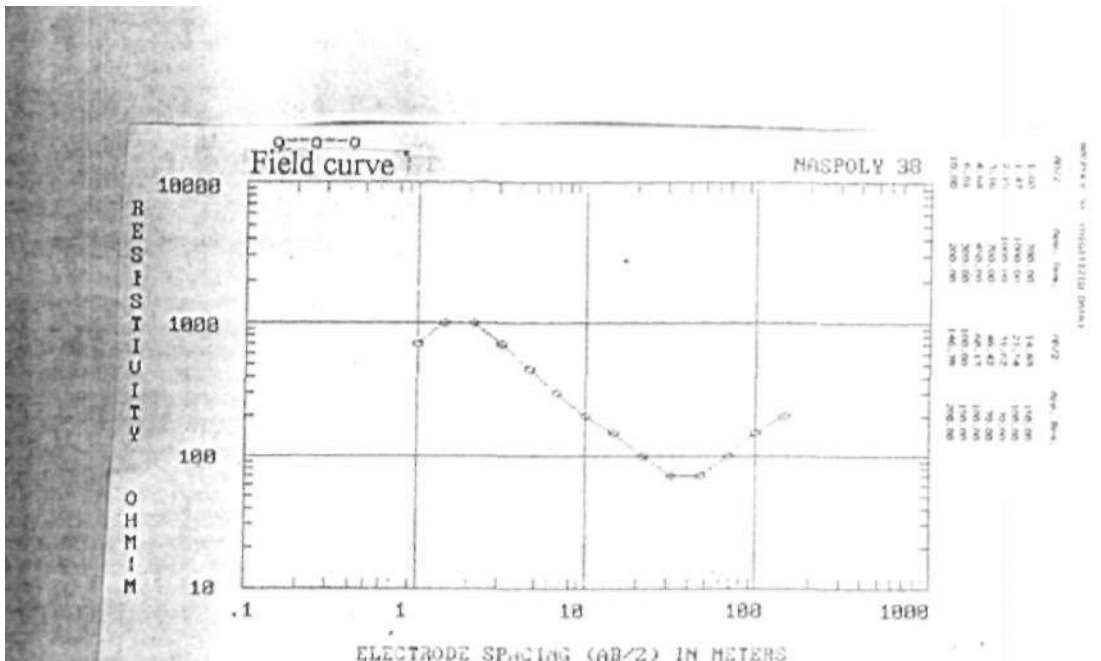


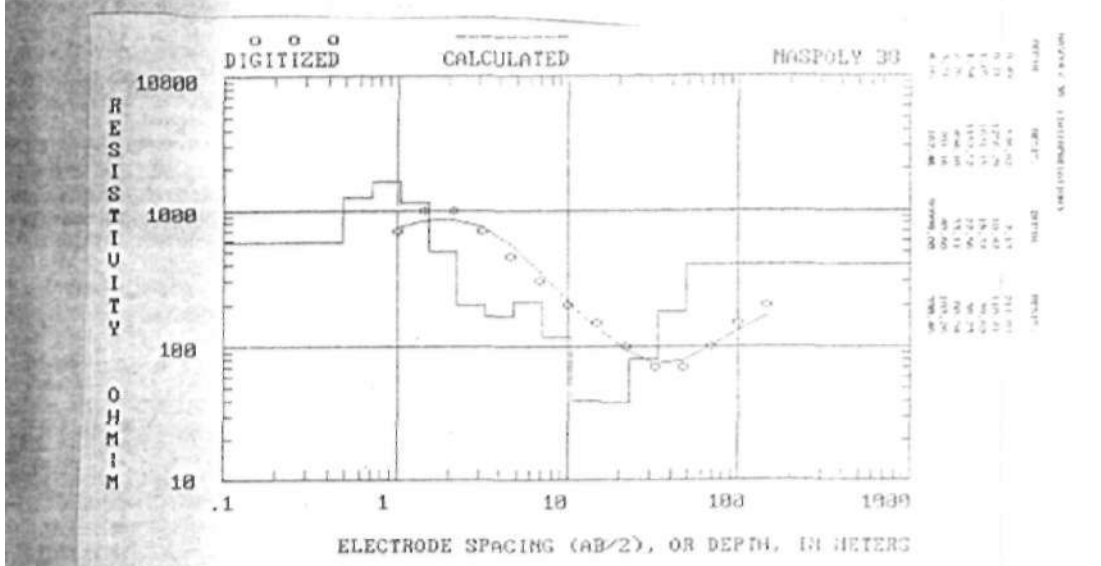


KASHIM IBRAHIM LIBRARY

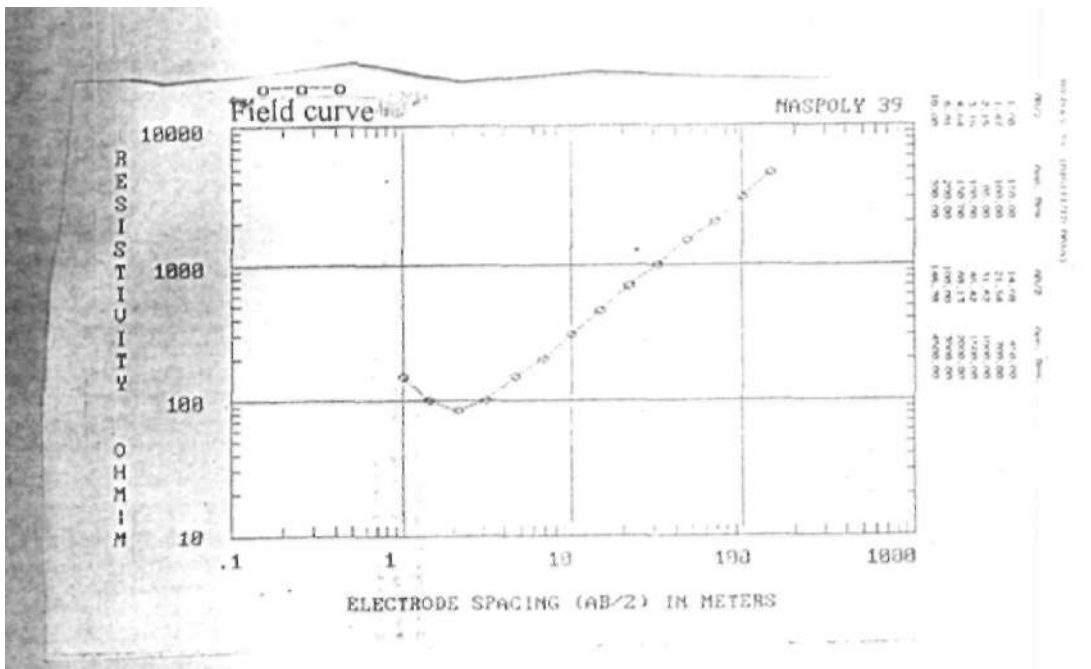


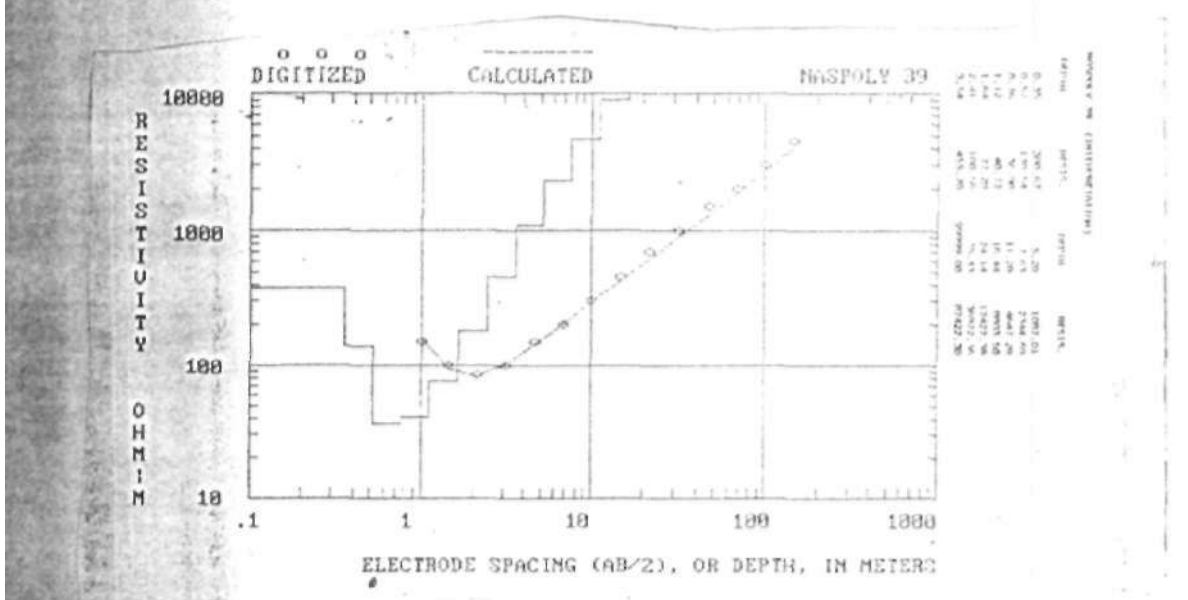
KASHIM IBRAHIM LIBRARY

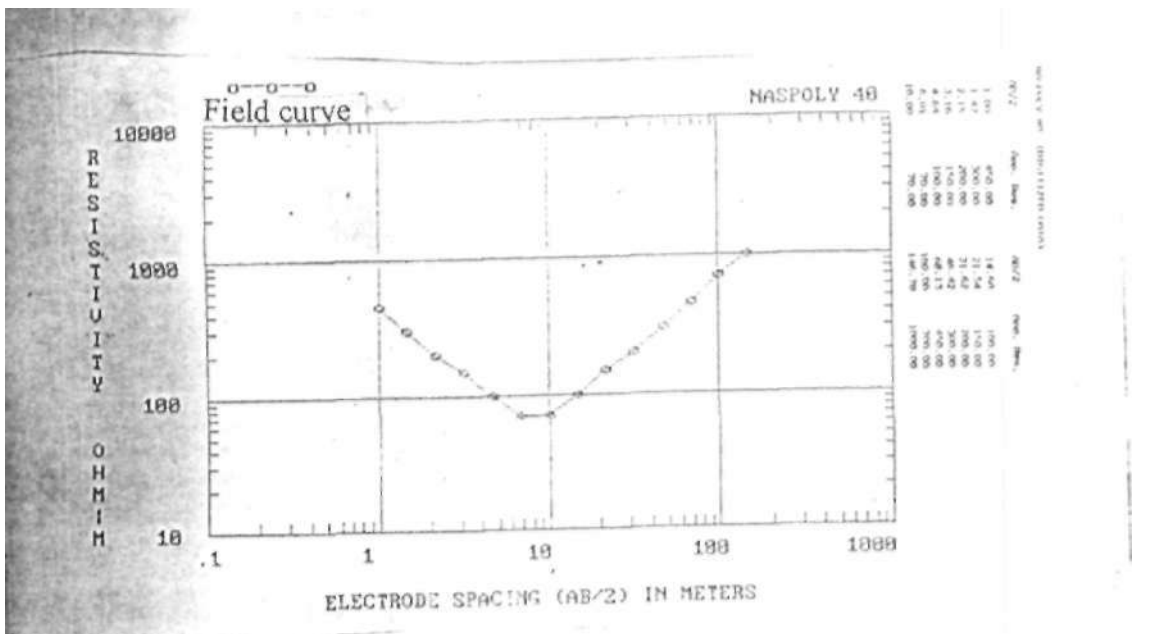


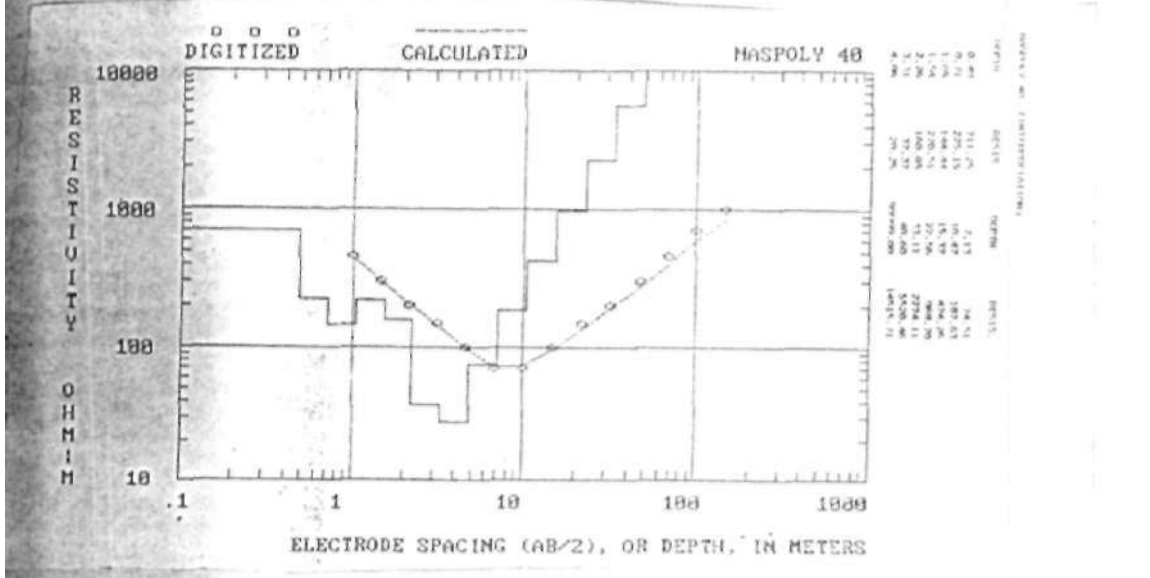


VASCHIM IRRAWIM LIBRARY


Field curve
NASPOLY 39
RESISTIVITY OHM-M
10000
1000
100
10
.1
1
10
100
1000
ELECTRODE SPACING (AB/2) IN METERS


DIGITIZED
CALCULATED
NASPOLY 39
RESISTIVITY OHM-M
10000
1000
100
10
.1
1
10
100
1000
ELECTRODE SPACING (AB/2), OR DEPTH, IN METERS


Field curve
NASPOLY 40
RESISTIVITY OHMIM
10000
1000
100
10
.1
1
10
100
1000
ELECTRODE SPACING (AB/2) IN METERS


DIGITIZED
CALCULATED
NASPOLY 40
RESISTIVITY OHMIM
10000
1000
100
10
.1
1
10
100
1000
ELECTRODE SPACING (AB/2), OR DEPTH, IN METERS

Appendix B:

Iso - resistivity contour maps.

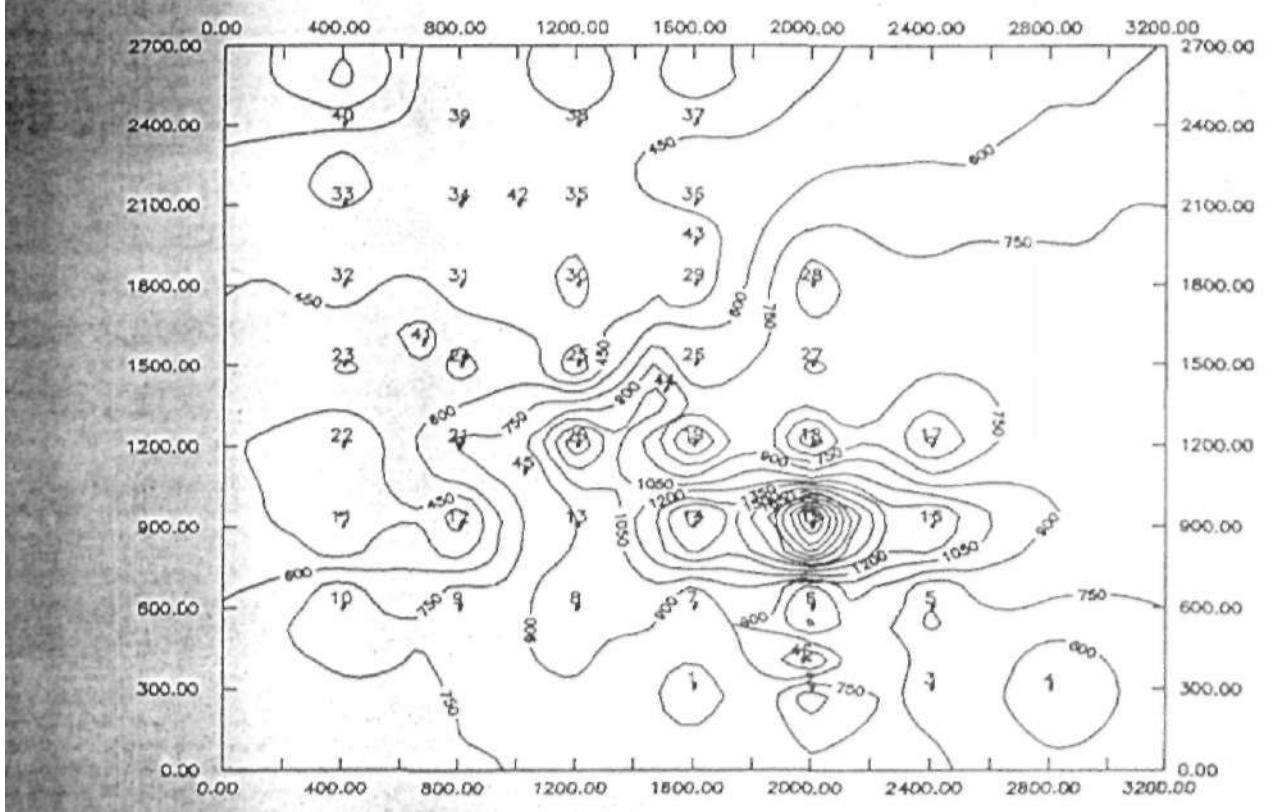


Fig. 5.8. Iso - resistivity contour map at 25m depth.

Contours at 150 Ωm interval

KASE

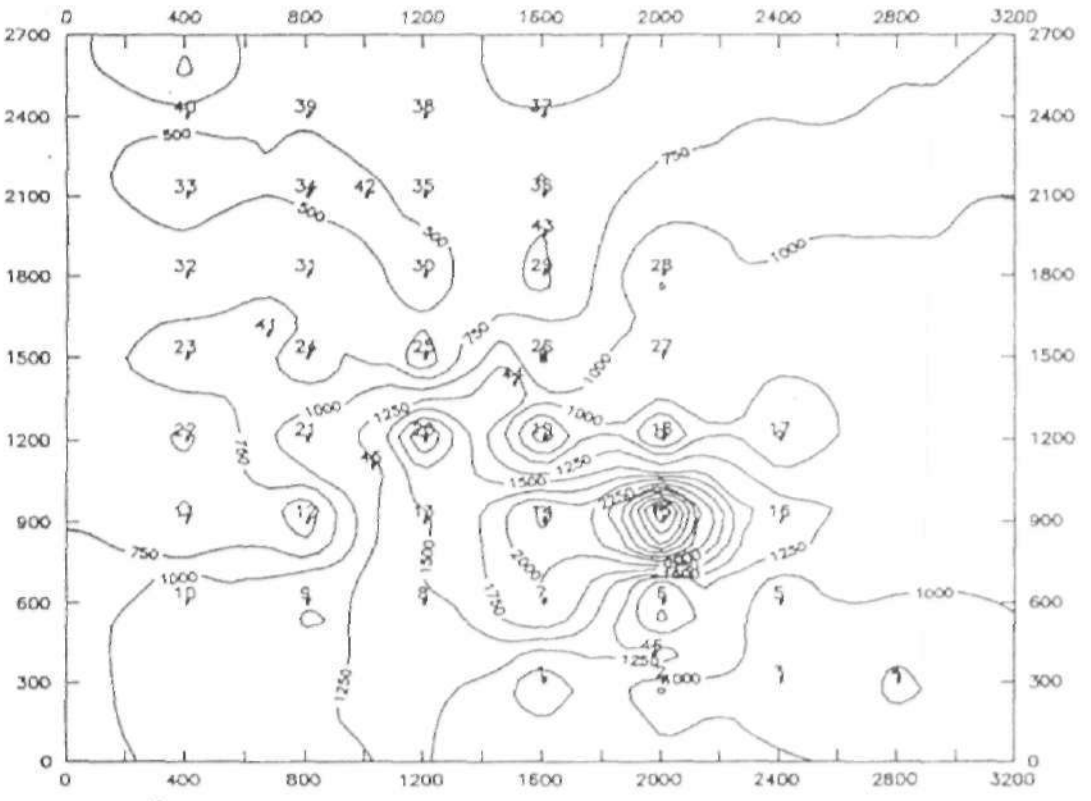


Fig. 5.9 Iso - resistivity contour map at 30m depth

Contours at 250 Ωm m interval

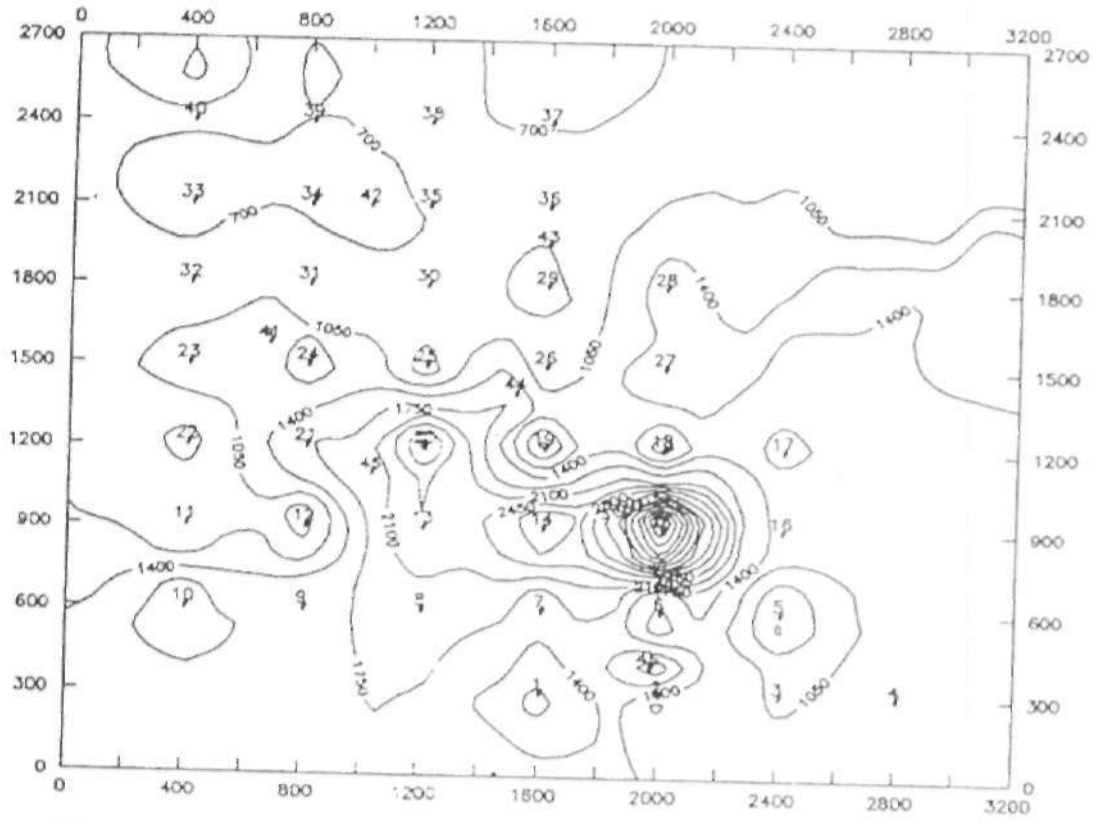


Fig. 5.10. Iso resistivity contour map at 35m depth.

Contours at 350 Ωm interval

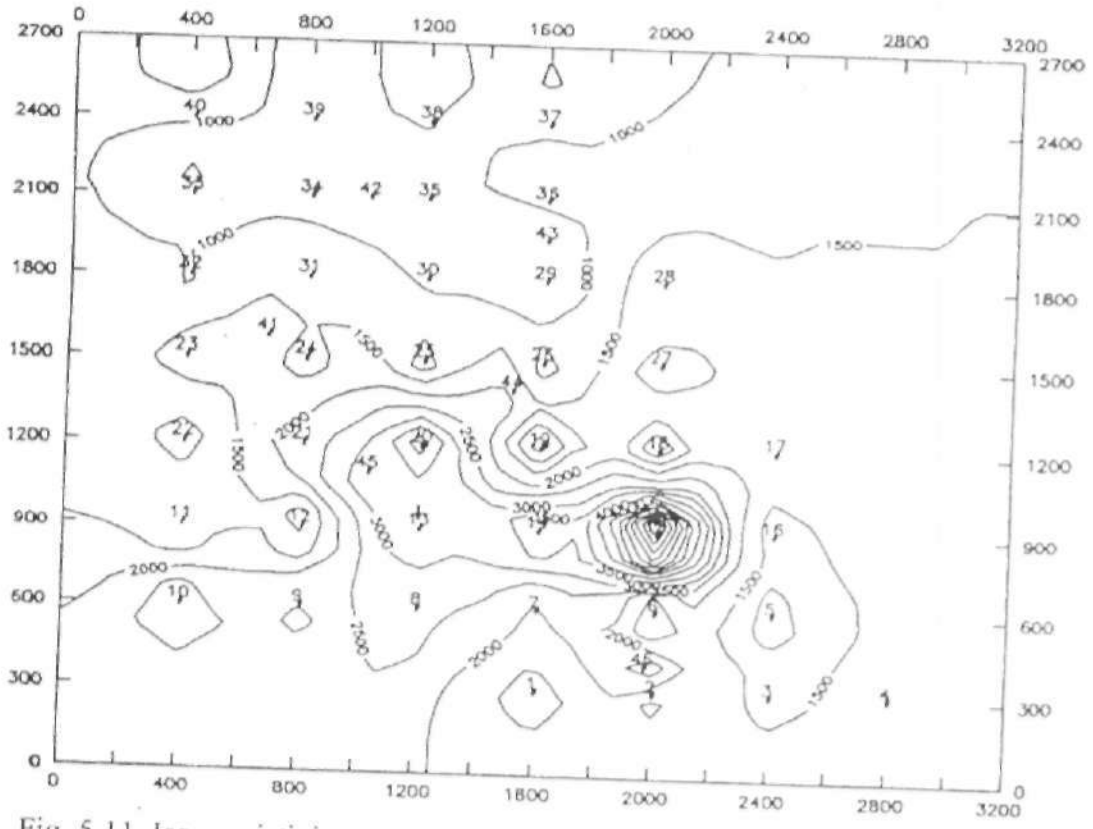


Fig. 5.11. Iso - resistivity contour map at 40m depth.

Contours at 500 Ωm m interval

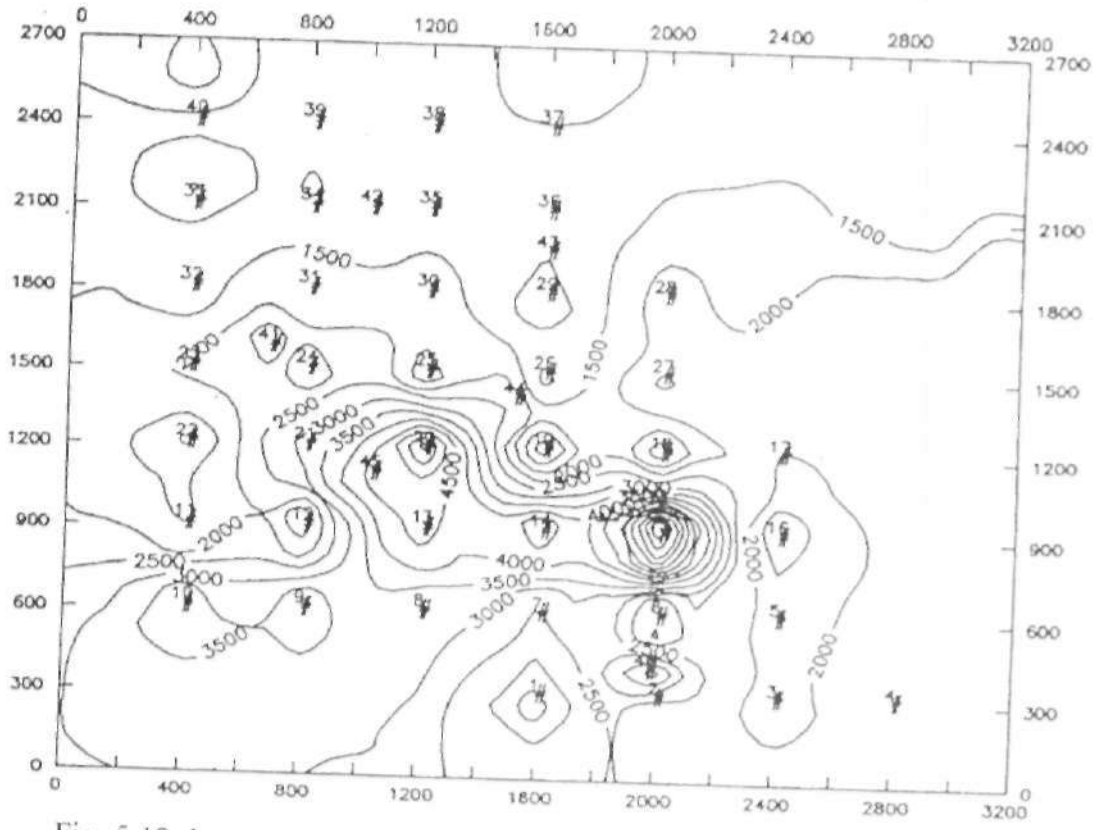


Fig. 5.12. Iso - resistivity contour map at 45m depth.
Contours at 500 Ωm interval

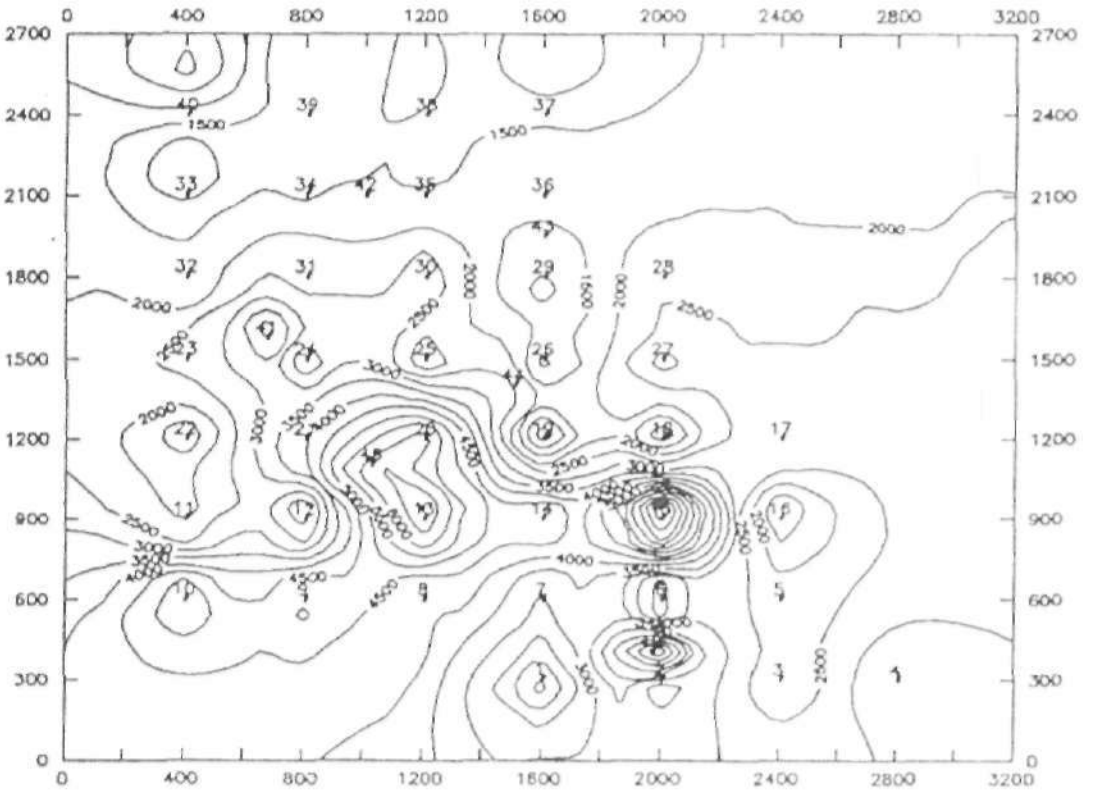


Fig. 5.13. Iso resistivity contour map at 50m depth.

Contours at 500 Ωm interval

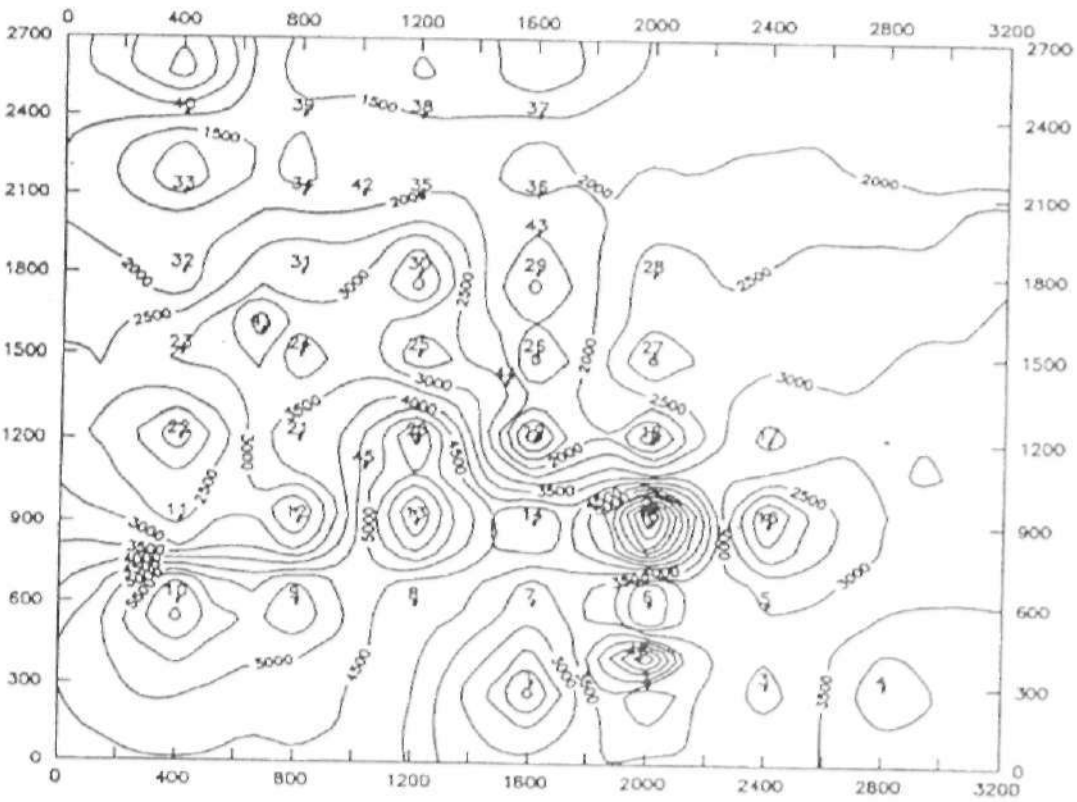


Fig. 5.14. Iso resistivity contour map at 55m depth

Contours at 500 Ωm interval

KASHIM IBRAHIM LIBRARY

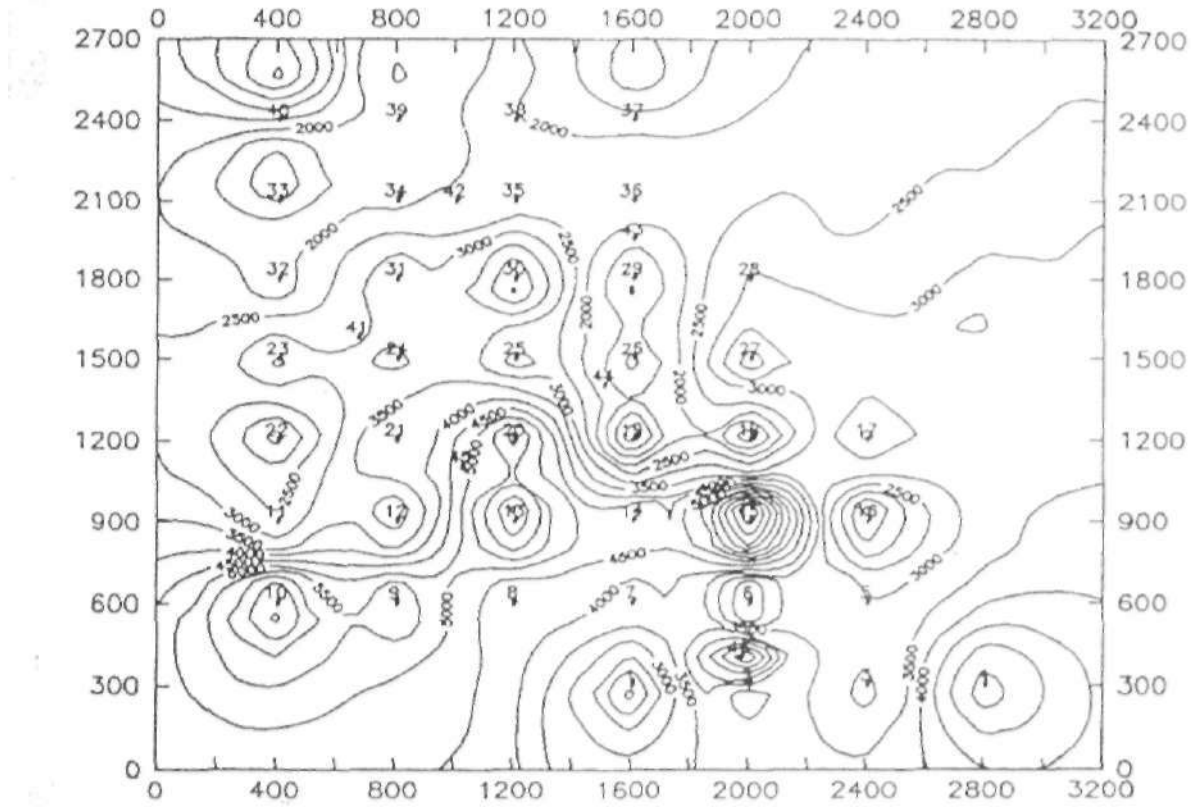


Fig. 5.15. Iso resistivity contour map at 60m depth

Contours at 500 Ωm interval

Ap◦◦endix: C

Iso - resistivity contour data

	Depth								
VES	Surface	5m	10m	15m	20m	25m	30m	35m	40m
				ρ(Ωm)					
1	305	801	448	450	510	600	1610	1050	917
2	450	224	250	315	400	750	930	450	2000
3	345	241	500	620	690	671	900	810	1100
4	1000	153	120	178	290	361	603	718	1764
5	545	56	100	220	380	600	782	410	840
6	645	184	305	340	345	450	1113	1050	1871
7	540	62	152	345	510	710	2013	1600	2000
8	40	247	200	390	660	1030	1300	1815	2360
9	168	100	148	250	500	650	967	1645	1500
10	120	76	148	295	690	72	1117	1810	2610
11	136	300	100	100	200	251	250	814	975
12	110	31	150	150	150	300	345	600	1000
13	350	104	150	295	600	900	1500	2450	2350
14	110	300	550	770	1200	1750	2250	2850	3800
15	275	300	400	700	1500	2750	3500	5460	8500
16	1030	163	320	705	850	163	1261	750	517
17	149	71	130	236	290	450	500	600	1000
18	350	190	236	260	291	450	2760	450	500
19	300	161	450	130	600	161	561	2032	3150
20	245	67	250	526	1000	1300	1115	1550	2120
21	135	65	110	260	450	750	481	551	890
22	352	76	150	200	170	200	901	1233	1210
23	450	64	100	230	328	300	545	316	1751
24	218	62	80	150	250	450	481	473	953
25	300	72	570	70	100	172	981	945	870
26	560	131	190	310	420	843	220	1540	2100
27	358	50	200	375	640	300	1161	1640	1763
28	1010	57	150	440	700	442	486	1440	1114
29	600	237	165	236	300	313	623	480	1200
30	1200	122	150	150	175	2171	350	813	1200
31	673	183	45	148	290	360	331	913	1780
32	3650	550	100	150	242	541	551	845	100
33	1540	285	150	150	280	450	523	415	871

34	500	143	150	148	265	351	473	465	735
35	600	58	145	250	350	544	561	841	931
36	750	376	110	75	180	260	544	700	967
37	600	67	130	170	185	315	533	781	1335
38	710	241	136	225	326	311	371	700	500
39	601	73	184	290	300	300	861	1213	783
40	900	237	190	328	490	323	541	388	1134
41	286	60	100	250	300	60	342	500	700
42	310	210	120	110	200	1110	250	1320	1205
43	546	60	100	170	285	815	1115	2000	1667
44	300	210	300	450	500	1110	350	1320	1205
45	150	300	300	375	550	815	1115	2000	1667
46	710	250	210	420	500	456	1113	450	2700

Depth

VES	45m	50m	55m	60m
		ρ(Ωm)		
1	1000	1600	4616	4000
2	3911	3500	2500	2915
3	1975	1145	400	5601
4	2415	3871	1731	3000
5	1800	1200	3200	2250
6	1755	2300	2100	3731
7	2500	3000	3335	4415
8	3350	4320	4325	5201
9	3916	4071	5710	6200
10	3710	5200	6305	3416
11	1500	2000	2500	3051
12	1500	2000	2400	7000
13	4000	6680	6730	4451
14	4700	4330	400	8000
15	8000	8000	8000	1633
16	1480	1131	1315	500
17	200	2700	3570	1500
18	500	1000	1000	500
19	500	500	501	500
20	5601	6000	6000	6000
21	3761	7000	3670	4210
22	1300	1630	1500	1500
23	1864	2650	3000	3500
24	1640	2880	3200	3647

25	943	1914	2320	2500
26	1750	1050	1000	1000
27	2500	3100	3500	4001
28	2345	2300	2650	3000
29	963	1050	1320	901
30	1454	2671	4000	4202
31	1750	2350	2210	3200
32	1225	1661	1700	1825
33	893	983	1000	1000
34	1345	1420	2001	2315
35	1100	1570	2000	1861
36	1328	1623	2000	2430
37	1000	1345	1500	1603
38	1320	781	1500	2000
39	681	1700	1761	1600
40	1350	1120	2000	1500
41	1124	8000	8000	2910
42	1200	1700	1900	1932
43	4520	1400	1500	2250
44	1200	2550	2401	1000
45	4520	6000	4600	5000
46	3600	2300	8000	6000

KASHIM IBRAHIM LIB

Appendix: D Aquifer depth contour data

VES No.	Depth (m)
1	5.3
2	6.2
3	4.4
4	14.3
5	12.0
6	10.2
7	9.0
8	9.3
9	6.5
10	14.0
11	19.0
12	19.0
13	10.0
14	3.5
15	3.5
16	10.1
17	12.4
18	12.4
19	9.0
20	5.0
21	7.0
22	11.0
23	11.0
24	13.0
25	23.0
26	10.0
27	10.4
28	8.3
29	13.8
30	13.7
31	3.0
32	7.0
33	13.0
34	10.4
35	10.6
36	11.0
37	11.8
38	10.6

39	10.5
40	13.6
41	11.0
42	10.3
43	11.3
44	10.5
45	9.0
46	7.0

KASHIM IBRAHIM LIBRARY

Appendix: E Aquifer thickness data

VES No.	Thickness (m)
1	8
2	6
3	4
4	14
5	4
6	6
7	8
8	10
9	6
10	14
11	14
12	19
13	10
14	4
15	4
16	6
17	12
18	12
19	9
20	5
21	6
22	16
23	10
24	13
25	23
26	10
27	10
28	18
29	14
30	14
31	3
32	7
33	14
34	12
35	12
36	10
37	12
38	12
39	12

40	14
41	11
42	12
43	12
44	10
45	12
46	12

Appendix: F Depth to Basement contour data

VES No.	DEPTH (meters)
1	35.5
2	29.5
3	33.6
4	35.0
5	57.3
6	30.3
7	26.2
8	27.3
9	26.4
10	39.8
11	48.9
12	26.6
13	18.2
14	17.3
15	26.8
16	34.1
17	50.1
18	30.6
19	20.0
20	28.6
21	47.3
22	32.0
23	38.4
24	44.2
25	50.3
26	26.6
27	24.8
28	53.9
29	38.5
30	36.0
31	42.2
32	50.3
33	48.1
34	39.5
35	40.2
36	41.9
37	38.8
38	45.1
39	29.2

KASHIM IBRAHIM LIBRARY

40	31.0
41	36.0
42	43.0
43	39.0
44	25.0
45	27.0
46	49.0